Source of Acquisition
CASI Acquired

NATIONAL ADVISORY COMMITTEE FOR AERONAUTICS

ADVANCE RESTRICTED REPORT

NEW RESEARCH ON THE COWLING AND COOLING OF RADIAL ENGINES

By Richard C. Molloy and James H. Brewster, III

SUMMARY

An extensive series of wind-tunnel tests on a half-scale conventional nacelle model were made by the United Aircraft Corporation to determine and correlate the effects of many variables on cooling air flow and nacelle drag. The primary investigation was concerned with the reaction of these factors to varying conditions ahead of, across, and behind the engine. In the light of this investigation, common misconceptions and factors which are frequently overlooked in the cooling and cowling of radial engines are considered in some detail.

Data are presented to support certain design recommendations and conclusions which should lead toward the improvement of present engine installations. Several charts are included to facilitate the estimation of cooling drag, available cooling pressure, and cowl exit area.

INTRODUCTION

Improvements in the cowling and cooling of radial aircraft engines have resulted from the study of the fundamentals of air flow, their general application to the problems to be solved, and detailed wind-tunnel and flight testing to determine optimum designs. In spite of the effort expended on cooling problems over the past decade, cooling difficulties still exist. In some cases they are due to a failure to grasp the underlying principles; in others they can be traced to a lack of appreciation of cooling work already accomplished, and a failure to apply these results in practice. The most important cause is, perhaps, that many quantitative cooling data are still wanting.

This need for more quantitative information led United Aircraft about 2 years ago to continue the cowling and

cooling investigation which had been begun several years previously and which had resulted in the development of pressure baffles and cowl flaps for radial aircraft engines. (See references 1 and 2.) Although the present research can be considered an extension of that previously conducted, it is basically new. Improved wind-tunnel models have been tested, and many drag and cooling variables have been investigated in considerable detail.

As in the case of past wind-tunnel investigations, it was found convenient to establish a standard test nacelle, so that the effectiveness of subsequent modifications in design could be compared with the standard nacelle. (See references 3, 4, 5, and 6.) This basic nacelle was developed from a streamline body (see fig. 6), but was provided with an NACA nose C cowl, which had previously proved (reference 7) to be excellent from the drag standpoint. No attempt was made to investigate the variables of cowl nose form, air heating, or amount of cowl periphery flapped. In addition, the nacelle was tested without a wing in order to eliminate other variables and because it was felt that wing-nacelle interference data were being adequately supplied by the NACA (references 8, 9, and 10).

With a body of constant cowl nose and afterbody form there seemed to be three major variables to be investigated:

1. Shape and size of the propeller hub and engine reduction-gear housing, or fairings over them, including spinners.

2. Restriction to cooling air flow offered by the engine, that is, engine conductivity; also the restriction offered by the entry to the engine and by the engine accessory compartment. (The term "conductivity" is defined in references 2 and 7.)

3. Size and location of exit for cooling air.

That item 1 affected the cooling air flow and drag was discovered by previous research.* However, it was then believed that nose shape had little effect on either nacelle drag or cooling. Since then it has gradually been recognized that the shape of nose configurations ahead of the engine must have a profound influence on the air-flow direction and the amount of turbulence created, and thus

*See reference 2.

on the pressure recovery under the cowl, the cooling drag, and the form drag of the nacelle. (See reference 11.) This present paper attempts to point out the importance of these features, and recommends how pressure recovery can be increased and drag reduced by improving air-flow conditions. These data should prove particularly useful in design.

Item 2 was known to have an important effect on both nacelle drag and pressure drop available, assuming any given flap length, but extensive quantitative data were not available. Except in a very few cases several conductivities have not been investigated on any one model in detail. Consequently, it was felt worth while to make tests using three conductivities, and in some cases five, to cover the entire range of "orifice coefficients" that might be expected with a radial engine. With this range of conductivities it would thus be possible to obtain the change in drag coefficient, pressure recovery, or mass flow for any modification in the physical arrangement of the nacelle at the exact conductivity desired. But, most important, it would be possible to compare the effect of conductivity on drag coefficient at the same mass flow so that the cooling drags obtained would be the same and any drag differences could be traced directly to a change in form drag. The restriction to cooling flow at the front of the engine has been herein considered on the basis of pressure recovery, while the additional restriction offered by the accessory compartment has been considered in terms of its conductivity.

Considerable effort has been expended on item 3, particularly as to the best form of exit control. Many arrangements were tried some years ago by United Aircraft and the results reported in reference 1. It is now almost universally agreed that cowl flaps are much better than shortened skirts or any other flight-induced flow arrangement to obtain the maximum mass air flow or pressure drop across the engine. (See reference 12.) The commonly used term "shortened skirts," refers to the successive shortening of the trailing edge of the cowl at the air exit from the nacelle, in order to achieve increased air flow through the engine. In this case the authors were interested in the shortened-skirt data not only to compare them with the cowl-flap data but in order to obtain the same mass flow when the conductivity was changed at zero flap angle, as discussed in the previous paragraph. Although there are some data available (reference 1) on the effect of flap

position on drag and maximum pressure drop obtainable, it was thought worth while to investigate three flap positions in more detail. The chord of all the flaps tested in the two conventional positions was 12.5 percent of the engine diameter.

TUNNEL SET-UP AND DESCRIPTION

With the test program formulated in this manner, the models were designed for testing in the Wright Brothers wind tunnel, which has been well described in reference 13. In brief, the variable-density M.I.T. Wright Brothers wind tunnel is of the closed-return, closed-throat type; a $7\frac{1}{2}$- by 10-foot elliptical section forms the throat. For normal running, as in these tests, tunnel dynamic pressure corresponds to an airspeed of 150 miles per hour under standard atmospheric conditions at sea level. This speed corresponds to an effective Reynolds number of 3,000,000, based on maximum body diameter. Although airspeeds up to 240 miles per hour are obtainable, these higher speeds are primarily required for extrapolation of data to full-scale Reynolds numbers.

As shown in figures 1 and 2, models are set up in the tunnel on a three-support system which offers comparatively little tare and interference drag. Actually, the total tare, interference, and buoyancy correction for low drag bodies is only about 40 percent of the measured drag as read from the balances, which is a low figure for any system.

Tunnel speed is referred to four static orifices located in the tunnel wall in the plane of the maximum cross section of the body. As far as the body is concerned, then, the test speed occurs under conditions more nearly simulating those of free-stream flight than if the tunnel speed were measured well in front of the body, which method requires the use of the so-called "blocking effect" correction.

Assuming that the tare and interference effects of the support system can be quite accurately obtained by duplication of all the parts necessary, the remaining correction is that offered by the losses in the tunnel throat, which manifest themselves as a static-pressure drop along its length. Suffice it to say that this static-pressure gradient has been measured at frequent intervals and has

resulted in a buoyancy correction that has been as accurately determined as possible. The importance of establishing all these corrections cannot be overemphasized when small drag differences, occurring from minor model changes, must be accounted for.

As mentioned previously, if drag differences of various nacelle configurations are desired, the drags must be compared at the same internal flow. Therefore the method of measuring the flow must be accurate and consistent. In addition, care must be taken to allow for any seeming change in engine conductivity that may occur from changes made in front of the engine. The apparent change in conductivity is due to the inability of pressure-measuring devices to read consistently with variation in air-flow direction.

Reference to figure 3, showing the basic nacelle in cross section, will be of assistance in describing the model itself and the methods employed for measuring flow. The nacelle here shown represents an approximate half-scale model of a Pratt & Whitney R-1830 or R-2800 installation. The front and rear screens by which the double-row engine is simulated are located at positions corresponding to planes at the forward edge of the front-row fins and the rear edge of the rear-row fins. In this manner the cooling flow is at least subject to a cycle of deceleration and acceleration in roughly the same manner as in an actual radial engine, although the tortuous path of flow existent in the engine is, of course, not present in the model. It was felt, however, that a better simulation was achieved than if a single perforated plate had been inserted at some arbitrary location within the nacelle. After a series of extensive calibration tests in a duct using the exact configurations to be tested in the tunnel, screen combinations were selected that gave orifice coefficients, or engine conductivities, covering a range sufficient to include present-day and future air-cooled engines. Each of the screen combinations was retested for widely varying nacelle configurations with and without propeller, to take into account any changes in conductivity. Actually, for the majority of tests, the change in conductivity for a given set of screens was so slight as to be negligible.

Several methods of pressure measurement were employed. Four integrating total-pressure rakes were placed in front of and four behind the "engine." As can be seen in figure 3, each total-pressure rake consists of five forward-facing

tubes spaced radially and joined to an averaging chamber, from which a single tube is connected to a manometer. The readings of these devices were checked by the area-averaged readings of a rake consisting of several individual Kiel shielded total-head tubes (reference 14) of Boeing company design (fig. 4) and were found to be accurate, even at angles of attack of the model other than zero. The excellent agreement between the readings of the integrating and non-integrating total pressure rakes is illustrated in figure 17.

In addition, a large piezometer ring, the diameter of which was 0.98 that of the "engine" diameter, was located in front of and behind each set of screens. A smaller piezometer ring of 0.625 diameter ratio was placed directly ahead of the front screens and behind the rear screens. According to standard flight-test procedure, the holes in the rings faced forward. Under certain conditions of reverse flow within the cowl, it is conceivable that static pressure might be measured with such a device. Under most conditions, however, the ring would attempt to measure total pressure, although the design is very unsatisfactory as a total-head tube. The measurements will be misleading, not only because of this, but because total-pressure distribution in front of a typical engine-nacelle combination is quite likely to appear as shown in figure 5. It so happens that front station 3 or rear station 2, at which the total pressure is highest, is just about where the holes in a piezometer ring with a diameter ratio of 0.625 would be located. Pressure head in front of an engine-cowl unit measured with such a ring would then appear entirely too optimistic, as would the cooling flow based on that measurement.

It is apparent from figure 5 that only radial rakes will give a true average of the pressure in front of the engine, while piezometer rings or other devices that measure one radial pressure will give readings greatly in error. The circumferential variation in pressure which occurs at angles of attack or yaw, as shown in figure 17, cannot, of course, be indicated by a piezometer ring. Therefore, piezometer rings should not be used under those conditions, and it is recommended that they be discontinued for pressure measurement.

Owing to the unreliability of the piezometer rings, it was decided to rely on the integrating rakes, which would give an average reading across a plane directly in

front of the engine disk. Throughout all the testing, however, pressure measurements were also taken by the piezometer rings, and check runs were later made with the shielded total-head tubes. In all cases the rings gave readings, especially at angles of attack, which were considerably less conservative and less consistent than the readings obtained by the rakes.

TRANSITION FROM STREAMLINE BODY TO NACELLE WITH AIR FLOW

As mentioned in a previous section, a streamline body of fineness ratio 3.25 was tested as a basis of comparison with the nacelle with air flow. These results are given in figure 6. For further comparison with the nacelle, a blunt streamline body was tested, which represents a fairing of the nose C cowled nacelle into a solid body. The drag coefficient of 0.0354 for this blunt body may possibly be slightly high relative to the other bodies, since it was found afterward that part of the nose contour was not properly faired.

It is desirable to have the drag coefficients obtained from wind-tunnel tests capable of being easily extrapolated to full-scale Reynolds numbers. In flight at these high Reynolds numbers, the transition from laminar to turbulent flow occurs at, or nearly at, the point of peak negative pressure on the body. Consequently, it is necessary to cause artificial transition to occur on the wind-tunnel models at the position of peak negative pressure if it is desired to extrapolate from model scale to full scale by the usual methods. Artificial transition can be caused either by introducing turbulence into the tunnel by a screen or by using "trippers" (threads placed around the periphery of the body at the position of the peak negative pressure). The tripper method was adopted for these tests, and by the use of different size trippers it was possible to determine the drag added by the tripper. This drag was subtracted from the gross drag of the body to find the effect of the tripper on the net drag, which did not include the tripper drag. Although trippers were also used on the cowled nacelles, as well as on the streamline bodies, it was found that in the cowled nacelles the transition point was always ahead of or at the tripper, so that no correction to the drag coefficients had to be made for this factor.

It is obvious from figure 6 that considerable improvement can still be realized in the drag coefficients of nacelles with air flow when compared with a good streamline body. Future research will undoubtedly show how further improvements can be obtained.

EFFECT OF SEVERAL VARIABLES ON NACELLE DRAG COEFFICIENT

Mass flow and engine conductivity.- Flow through a nacelle can be augmented by increasing the flap angle or successively shortening the cowl skirt to increase the exit gap. The volume flow Q is determined primarily by the pressure drop across the engine Δp and the engine conductivity or "orifice coefficient" K_q. (The term "conductivity" is explained in detail in references 2 and 7.) Thus:

$$Q = K_q S \sqrt{\frac{\Delta p}{\rho/2}} \tag{1}$$

where

Q volume flow, cubic feet per second

K_q nondimensional engine conductivity based on maximum nacelle cross-sectional area

S maximum nacelle cross-sectional area, square feet

Δp pressure drop across engine, pounds per square foot

ρ air density, slugs per cubic foot

The authors of reference 2 proposed that the flow be shown in coefficient form written in terms of airplane speed V, as follows:

$$Q = K_q C_Q SV \tag{2}$$

$$C_Q = \left(\frac{\Delta p}{\frac{1}{2}\rho V^2}\right)^{\frac{1}{2}} = \left(\frac{\Delta p}{q}\right)^{\frac{1}{2}} \text{ (nondimensional)} \tag{3}$$

It is to be noted that all conductivities in the present paper are based on maximum nacelle cross-sectional

area, and not on engine disk area, to eliminate confusion between them. Consequently, it is necessary to change conductivities based on engine disk area downward by the ratio of the two areas, when use is made of those figures or charts in this paper that have conductivity as one of the parameters. The authors have also preferred to present some of the data in terms of mass flow (strictly speaking, weight flow) rather than volume flow, since it is mass flow that cools the engine. Consequently, equation (1) can be rewritten in terms of mass flow, W:

$$W = Q\rho g = K_q g S \sqrt{2\rho\Delta p} \tag{4}$$

where g is the acceleration of gravity, 32.2 feet per second^2. In this paper, the mass flow W is given in pounds per hour, so that, on this basis, equation (4) becomes:

$$W \text{ (lb per hr)} = 116{,}000\ K_q S \sqrt{2\rho\Delta p} \tag{5}$$

Equation (5) states that mass flow is a direct function of conductivity and the area on which that conductivity is based and is also proportional to the square root of the air density and pressure drop across the engine. From this fact it might be concluded that it is more important to change the conductivity than the pressure drop; that is, it would seem important to keep the conductivity low.

That the reverse is actually the case, however, is illustrated in figure 7 by a plot of mass flow against nacelle drag coefficient for several conductivities, where for a given mass flow the highest conductivity produces the least drag. As the mass flow required increases, the high conductivities show up more and more to advantage. For instance, if the conductivities shown are compared at 12,000 pounds per hour, the increases in drag coefficient over the nacelle without air flow expressed in percent are quite astounding.

Conductivity	Increase in drag coefficient over basic nacelle without air flow, percent
0.315	27
.21	30
.12	48
.07	317

The penalty incurred by using low conductivities for large mass flows therefore becomes clear. It is also at once apparent that, conversely, the saving in cooling drag at a given mass flow by increasing the conductivity is substantial. The lower the original conductivity the greater the ultimate saving in drag.

The subject of reducing cooling drag by changing engine conductivity is very important and deserves at least a brief discussion here. With the possible exception of increasing allowable cylinder temperatures, this factor is the most important to be reckoned with and investigated. The problem of decreasing cooling drag by increasing conductivity is, quite obviously, directly related to the flow and the pressure drop required to cool. Since a certain mass of air must be kept in contact with the fins to cool the engine at all times, it follows that air is wasted if the baffles are not kept as tight as possible. Tightening the baffles lowers the conductivity but still leaves the pressure drop required unchanged for a given engine, although, of course, the over-all flow through the engine is reduced. Next, the optimum fin spacing is sought. For present-day engines this optimum spacing will serve to further reduce the conductivity. However, because of increased fin efficiency it will reduce the required flow, and hence the corresponding pressure drop required is <u>also</u> decreased. Thus far, reduction in cooling drag has been accomplished by decreasing both flow and pressure drop. This result has been achieved, however, only at the expense of lowering the conductivity. The conductivity can now be increased by lengthening the fins. By so doing, the required flow and pressure drop are still further reduced. This accomplishment means that the minimum flow and pressure drop required to cool are being obtained as efficiently as possible dragwise, that is, by the highest useful conductivity that can be built into a radial engine of present-day design.

Again, however, the drag picture does not tell the whole story. Although it is important to increase the conductivity under the conditions set forth, it is more important to have a low pressure drop. While the drag varies directly as the pressure drop, the cooling power varies as the 3/2 power of the pressure drop, but the drag and the cooling power both vary directly as the conductivity. In equation form, using the same symbols and units as before, the horsepower due to cooling the engine is

$$(hp)_c = \frac{\Delta p\ Q}{550}$$

$$= \frac{K_q\ (\Delta p)^{3/2}\ S}{550\ (\rho/2)^{1/2}} \qquad (6)$$

The expression for total cooling horsepower due to flow through the entire nacelle is also $\frac{\Delta p\ Q}{550}$, but in this case Δp is the higher pressure drop across the nacelle. The cooling flow Q remains the same. Equation (6) thus illustrates the importance of keeping the pressure drop required to cool the engine as low as possible in order to attain minimum cooling horsepower. The advantages drag-wise of liquid-cooled radiators having conductivities about 0.45 and low pressure drops required become only too obvious and should serve as an inspiration to air-cooled engine designers.

For purposes of comparison two other conductivities have been drawn on figure 7. The data for $K_q = 0.085$ have been taken from reference 5, except that the drag coefficients have been reduced to allow for the difference between the basic drag coefficients of the NACA and the United Aircraft models without air flow. From previously unpublished wind-tunnel data, obtained at M.I.T. some years ago by the former Chance Vought Division, a point for $K_q = 0.14$ has been located on the plot. These data, when adjusted, agree remarkably well with the more recent wind-tunnel test data.

It should be pointed out that in figure 7 and all subsequent figures in which mass flows are quoted, these mass flows are based on an area of 3.14 square feet and a tunnel dynamic pressure corresponding to an airspeed of 150 miles per hour under standard atmospheric conditions at sea level. In order to obtain mass flows for a nacelle of different cross-sectional area, the given mass flows must be multiplied by the ratio of the areas, as well as by the ratio of the velocities and densities.

Flaps compared with shortened skirts.- The ordinary increase in pressure drop induced by flaps is illustrated in figure 8, where an increase in flap angle up to about 25° results in an increase in pressure drop, and thus in

mass flow. This result is true at all three conductivities shown except, of course, that the lower the conductivity the higher the pressure drop.

Cowl flaps and shortened skirts can be conveniently compared on the same basis by using the nondimensional quantity K_2, which is taken as the ratio of minimum nacelle exit area to the maximum nacelle disk area. The quantity K_2 is usually referred to as the "exit gill area ratio." Figure 9 shows that to obtain the same pressure drop or mass flow it is necessary to have a much greater exit gill area for the shortened skirts than for the cowl flaps. This figure shows that much higher maximum pressure drops, or mass flows, are obtainable with cowl flaps.

Without air flow it would appear from figure 10 that shortened skirts are much to be preferred dragwise. This figure shows that with no flow the flaps are merely adding form drag. It is well known, however, that shortened skirts give approximately the same nacelle drag coefficient as cowl flaps, for a given mass flow. (See reference 5.) This result is illustrated in figure 11. The indication is that there is no increase in form drag due to cowl flaps up to flap angles corresponding to the maximum exit gill area ratio tested with shortened skirts. The subject of increase in form drag as affected by flap angle is discussed in more detail in the section - ESTIMATION OF NACELLE COOLING DRAG FROM THEORY

In addition, figure 11 includes the effect of conductivity, demonstrating that the maximum mass flow obtained with cowl flaps is more nearly approached with shortened skirts at low than at high conductivities. It is also indicated that as the conductivity increases cowl flaps tend to have more drag than shortened skirts for a given flow. More than 50 different configurations with both cowl flaps and shortened skirts were compared, and the results indicated that sometimes lower drags at a given mass flow were shown by the cowl flaps and sometimes by the shortened skirts. It must be pointed out, however, that in about two-thirds of the cases investigated for conductivities around 0.12, cowl flaps showed only slightly higher drag coefficients. Figure 11 is typical of one of these cases.

Flap position.- Figure 12 illustrates the three flap positions tested. The first, or forward, position corresponds to one immediately to the rear of the engine cylinders; the second is similar to a fire wall flap installa-

tion; and the third, or tail exit type, is of interest because it has so often been proposed to exhaust the cooling air at the tail of the nacelle.

It is shown in figure 13 that the maximum pressure drop available with a given cowl exit area is progressively reduced as the flap is moved backward toward the tail of the nacelle. Consequently, it would seem that the best position from the point of view of maximum flow obtainable is immediately to the rear of the engine. This superiority of the forward flap position is also borne out in figure 14, where it is shown that the highest mass air flow is obtained with flaps in this position. At a given mass air flow the forward flaps need the smallest exit gill area ratio, while the tail exit flaps need the largest area. The firewall flaps lie in between the two.

As far as drag coefficient is concerned, it is evident from figure 15 that the order of excellence of the three positions is not so clearly definable as in the case of mass flow obtainable. At low pressure drops there is little choice between the forward position and the firewall-flap location, but the firewall-flap location becomes increasingly worse dragwise as the flow increases. As the conductivity is increased the forward flaps show to considerably more advantage.

The tail-exit flaps appear to have the most drag at very low pressure drops, are superior to the others at intermediate flows, but apparently become inferior again at the highest pressure drops. Unfortunately, test data are not available for comparable configurations at the higher conductivities, so that the effect of conductivity cannot be determined for the tail-exit type. In spite of this slight variation in the order of merit, it can be reasonably concluded that, in general, the forward flaps are to be preferred from the drag standpoint, as well as from the point of view of maximum mass flow obtainable.

EFFECT OF AIR FLOW, AIRSPEED, AND ANGLE OF ATTACK ON PRESSURE RECOVERY AHEAD OF ENGINE

It is interesting to observe from figure 16(a), which is for four different nose configurations at 150 miles per hour, that there is a change in pressure recovery ahead of

the engine with air flow. It is of particular interest to note from the uppermost curve, which indicates the method of obtaining points for all the curves shown, that this change in recovery is independent of how the mass air flow is obtained, whether by changing the cowl-skirt length or flap angle or, most important, by changing the engine conductivity.

A comparison of all four curves of figure 16(a) shows that the maximum recovery of each is not at the same flow or range of flow. The individual curves are for widely differing configurations (one includes an operating propeller) and, consequently, there is considerable variation in recovery. In other cases tested and not shown in this figure, where poor recovery exists because of too small an entrance area, the curves have a much more pronounced peak, and maximum recovery occurs over only a very narrow range of flow.

Figure 16(a) does not give the complete picture, however, since pressure recovery apparently changes with airspeed. That this change exists is indicated in figure 16(b) for three configurations where pressure recovery is plotted against flow ratio Q/SV for three airspeeds. The majority of configurations tested indicated a variation very similar to that shown for the uppermost configuration on this figure. Although the change in pressure recovery is presented as due to a change in airspeed (tunnel speed), it is undoubtedly a Reynolds number variation, which is somewhat difficult to evaluate. For practical purposes the airspeed change can be considered a Reynolds number variation based on some dimension of the body, say, the maximum nacelle diameter. The Reynolds number effect of speed on recovery is, of course, logarithmic - that is, the change in recovery becomes progressively smaller as the speed, or Reynolds number, is increased. As a matter of interest, Reynolds numbers corresponding to the test airspeeds are also given on figure 16(b).

The curves in the lower portion of figure 16(b) for two different configurations show that, in other cases, the change with airspeed, or Reynolds number, is not a simple one. The differences are, in general, small. The fact that these changes are related to the diffuser expansion ratio from the cowl entrance to the engine is discussed in a later section. Although in many respects this information is disquieting to the airplane designer, at least it is important to know the probable magnitude of

these changes and to gain some insight as to the number of cooling factors that must be taken into account.

The important fact to keep in mind is that for any given configuration, there is a flow, or range of flow, which will give optimum recovery. It is therefore very necessary to choose a design that will give high recovery at the mass flow required to give adequate cooling. Failure to realize this fact has caused considerable perplexity in the past, because arrangements shown to be desirable in wind-tunnel tests often proved to be disappointing in flight tests. The proposed designs must therefore be tested at the cooling air flows and Reynolds numbers relating to the critical cooling condition.

As the angle of attack of the nacelle is changed, the recovery ahead of the engine is generally reduced. This result is due to the fact that the air flow becomes asymmetrical within the cowl, creating turbulence and resulting in flow breakaway. A comparison of figures 16(b) and 16(c), which are for 0° and 4° angle of attack, respectively, shows that the recovery is, as a rule, reduced. Although the average loss in recovery is found to be small, the local loss may be considerable. This fact is illustrated in figure 17, which shows what occurs to the pressures as measured by the total-head rakes located at the top and bottom of the front screen simulating the engine resistance. The loss in pressure of the top total rakes, either of the integrating type or of the individual shielded design, is greatly in excess of that of the bottom rake, indicating greater loss in pressure recovery. The loss is probably due to the blanketing effect of the hub or spinner ahead of the cowl. This fact explains why the top engine cylinders are generally more difficult to cool in climb.

EFFECT OF PRESSURE RECOVERY AHEAD OF THE ENGINE ON DRAG

The rather startling effect of pressure recovery on nacelle drag is demonstrated in figure 18. The test points on the curve were obtained from a successive improvement at the nose of the nacelle, while retaining the same NACA nose C external cowl. The methods used to obtain the improvement will later be discussed but for the moment suffice it to say that changes in the design of hubs, spinners, and reduction-gear housing fairings will produce results much the same as shown here. It should be

noted that the drag differences from one recovery to another can be considered due almost entirely to the change in recovery and increase in form drag caused by high flap angles, since the mass flow is held constant. There is, of course, some change in basic drag between model configurations, but it is a very small percentage of the total. Obviously, in order to achieve a given flow, a configuration offering an inherently poor recovery will require a higher flap angle than would be required by a configuration offering greater pressure head in front of the engine. The curve shows that for the flow of 17,000 pounds per hour a reduction in pressure recovery from 100 to 55 percent effects a drag increase of some 210 percent. This increase is especially significant in view of the fact that recoveries ahead of the engine in present-day installations, are usually in the 60- to 70-percent range, <u>if measured according to the method prescribed in this paper</u>. In other words, at fairly high flows, over-all nacelle drag reductions of the order of 66 percent are possible simply by increasing the available cooling head to the free-stream value.

At low flows, drag reductions of the order of 35 percent could be attained. This effect is shown in figure 19. As the flow is increased, the progressively detrimental effect of poor recovery is clearly evident. Furthermore, if the mass flow is held constant, as in figure 20, poor recovery has an even more harmful effect on drag as the engine conductivity is decreased and the pressure drop through the engine is necessarily increased. It should be noted that the curves of figure 20 are plotted for 12,000 pounds per hour - a relatively low flow for this diameter nacelle. At higher flows the situation would be correspondingly detrimental to the low conductivity engine.

A false impression of the pressure-recovery effect on drag can be all too easily gained by considering the change in drag due to a change in recovery <u>at the same flap angle</u>, without at the same time considering the change in flow. Assuming, for example, that an engine of conductivity 0.12 will just cool at the critical condition with the flaps set at 40° and that, for this condition, the recovery is 60 percent, it is desired to know the decrease in nacelle drag attainable if the recovery could suddenly be boosted to 100 percent. If the flow change is disregarded the decrease in drag will be negligible. If, however, the engine will cool at the flow obtained with 60-percent recovery and a 40° flap angle, it is found from the test data that

for 100-percent recovery only a 10° flap angle is needed to produce the same required cooling flow. The drag has now been reduced almost 80 percent.

EFFECT OF NOSE DESIGN ON PRESSURE RECOVERY AND DRAG

A large number of configurations was tested in the tunnel to study the effect of nose design on pressure recovery and drag. Many of those tested without propeller are illustrated in the composite drawing (fig. 21), which shows cowl liners 1 and 2. These configurations include three lengths of cowl nose and various sizes and shapes of spinners, hubs, liners, and reduction-gear housing fairings.

Omitting for the moment propeller considerations, let it be assumed that there is under consideration the problem of designing a nose arrangement for a typical nacelle equipped with an NACA nose C cowl that will give the highest possible pressure recovery ahead of the engine and the lowest possible drag within a reasonable flow range. Let it be further assumed that an engine of conductivity 0.12 is already installed within the nacelle and that for use as a basic configuration the reduction-gear housing has been removed, leaving only the drive shaft protruding from the cowl entrance. This condition is represented by A of figure 22. At the specified flow of 17,000 pounds per hour, which in each case was obtained by varying the skirt length, a recovery of 97 percent and a drag coefficient of 0.120 was obtained. The effect of now adding the reduction-gear housing, as shown in B, leaves the situation unchanged but, as soon as a simplified or idealized hub is allowed to protrude from the cowl (C), the entrance flow has been altered and disturbed enough to decrease the recovery 16 percent, thus resulting in a drag increase of some 33 percent. Installing a representation of a conventional hub and dome (D) effected an <u>additional</u> loss in recovery of 24 percent, resulting in a further drag increase of 31 percent. From the basic nacelle, then, simply by installing a conventional propeller-drive assembly (less propeller, of course), the available cooling head has suffered a 40-percent loss, which loss has resulted in a drag increase of some 75 percent.

These are serious effects, especially serious because the high output aircraft engines of today demand all the cooling flow that it is possible to supply. A large num-

ber of wind-tunnel and flight tests might conceivably produce enough design information that the engine designer could always depend on the airplane and the propeller designer to furnish him optimum recovery ahead of the engine, and thus aid in the solution of the engine-cooling problem. Although this ideal might some day be achieved, at present it is only possible to make certain design recommendations based on the data available. How then, for instance, can a tractor installation be improved to give optimum recovery and minimum drag? The first and perhaps the most obvious step would be to reduce the size of the propeller hub and dome, thus increasing the cowl entrance area, but there is involved here a very definite limit, which has, in fact, already been reached. Propeller hubs are of necessity becoming larger, rather than smaller. The cowl entrance diameter itself can be increased, but many tests (references 3 and 7) have shown the drag characteristics become severe so rapidly that the change is not justified. The remaining choice is to decrease the cowl entrance area, attempting in this manner to approach a diffuser design within the cowl. The natural objection to this method is that the conventional cowl offers very little room in which to expand the entering air efficiently. The efficiency of the diffuser itself is, no doubt, poor, but its over-all effectiveness as a recovery device is excellent. The use and effectiveness of diffusers within the cowl is now being investigated in considerable detail by the NACA. (See references 15, 16, and 17.)

Retaining temporarily the conventional cowl-hub-dome arrangement (D of fig. 22) and introducing a cowl "liner" of the form shown dotted in the same sketch results in an improvement in recovery of 16 percent and a drag reduction of about 21 percent. The addition of a so-called "dish-pan," or reduction-gear housing fairing (E), effects a further recovery benefit of 9 percent and a drag improvement of 12 percent. This rather arbitrary approach to an at best inefficient diffuser has produced an improvement of 25 percent in recovery and 31 percent in drag, the mass flow being always held constant.

If higher recoveries are to be obtained, the use of spinners must be resorted to. Starting as in A of figure 23 with only a nose spinner, the successive introduction of the cowl liner and reduction-gear housing fairing (B) has resulted in the reattainment of almost full recovery, a drag improvement of 25 percent over A, and a drag increase over the basic nacelle (22A) of only 10 percent. If a larger

fairing over the reduction-gear housing is installed (C of fig. 23), the entrance area is reduced too extensively, and the pressure recovery falls off. The drag has consequently increased. The same effects are demonstrated in D through F of figure 23 for spinners which are too small or too large.

In climb attitudes the same relative differences apply to all of these nose arrangements, but the actual values of recovery are less, as explained earlier by the aid of figure 17.

The expansion ratios of the diffusers within the cowl, that is, the ratios of the annular entrance area at the front face of the engine to the minimum annular entrance area near the cowl lip, were calculated for a number of hub and spinner configurations which had a fairly consistent variation in shape. Although no regular variation of pressure recovery with expansion ratio could be found because of varying diffuser length, in all cases those configurations having expansion ratios of about 3 or less were best, while those having expansion ratios over 4 were definitely inferior. Expansion ratios as high as 3 were still effective even when the diffuser length ratio was as low as 1.5. The diffuser length ratio is defined as the ratio of the diffuser length to height of throat as viewed in a cross section through the diffuser. It would seem advisable then not to exceed expansion ratios of 3, or preferably 2.5, to obtain reasonably high pressure recoveries. Of course, the greater the diffuser length ratio the better, but it must be borne in mind that it is not desirable to decrease the entrance area so much that the flow quantity is actually reduced below the value required to cool the engine. In this connection two points should be borne in mind. The test data definitely indicated that the diffuser-throat velocity should be about 50 to 60 percent of the free-stream velocity, where throat velocity is determined from the required flow divided by the throat area. Furthermore, the diffuser in cross section should, of course, be as symmetrical as possible.

It is, therefore, apparent that in many cases where design conditions permit, it would be of advantage to develop a semistandardized installation for a given engine - such that the cowl diameter, distance of cowl leading edge from the front of the cylinders, shape of cowl liner, reduction-gear housing fairing, and so forth, would be clearly specified so that optimum recovery will be realized.

It would also appear beneficial to have the front of the engine kept clear of accessories, such as magnetos, distributors, and propeller governors, unless the forward location is absolutely necessary because of mechanical or other important reasons.

Of the cowl liners tested (liners 1 and 2 shown in fig. 21), liner 1 was in all cases superior to liner 2, simply because the diffuser expansion ratios were low enough to warrant its use. If attempts are made to improve the recovery of a given installation by a cowl liner and fairing over the reduction-gear housing, it is entirely possible that a diffuser of too small a length ratio or too large an expansion ratio will result. In cases like these, liner 2 would probably be more beneficial, although a redesign of the cowling itself in order to use liner 1 should produce better ultimate results. If a diffuser is to be used within a short-nose cowl, the cowl leading edge should not, as in many cases, be unnecessarily far back of the propeller blades but should be as close to the propeller in the fully feathered position as possible.

EFFECT OF INCREASING COWL LENGTH ON PRESSURE RECOVERY AND DRAG

The assumption that a gain in pressure recovery is attained by increasing the cowl length alone is apt to be misleading (fig. 24), in that the recovery improvement may not be so much due to an increase in cowl length as to a reduction in the amount of hub and dome protrusion from the cowl entrance. It is evident from the sketches that practically full recovery can be obtained for any cowl length simply by avoiding any protrusion from the cowl entrance. Furthermore, the drag of the short cowl is actually less than the drag of the longest cowl at any specified flow through the engine, eliminating protrusion in both cases. It seems hardly necessary to point out that these "long" cowls being referred to here are in actuality "hollow spinners," the forward section of which must rotate with the propeller or, if stationary, would necessitate an extension drive shaft for the propeller. Serious problems of design and maintenance are inevitable with hollow spinners, but if a large decrease in recovery and drag over a large range of flow were obtainable, their use would presumably be justified. At the arbitrary and average condi-

tions of 150 miles per hour flight speed and 17,000 pounds per hour cooling flow, the most efficient long nose cowl, or hollow spinner, tested yielded a 4-percent increase in pressure recovery and a 3.5-percent decrease in drag over the optimum short nose cowl (fig. 23, B).

EFFECT OF AN UNCUFFED TRACTOR PROPELLER ON PRESSURE RECOVERY

Up to the present time, propeller considerations have been purposely omitted from this paper in an effort to avoid seemingly unnecessary complications. It should be pointed out that no attempt has been made to isolate propeller thrust and drag, the difficulties involved being considered too severe to warrant the extra time required for the tests. The propeller blades used were scale models of the Hamilton Standard 6105-A design, although the tips were cut off to avoid excessive interference effects with the tunnel wall. A typical set-up in the tunnel is shown in figure 25.

Perhaps the best way of visualizing propeller effects at various flows obtained by cowl flaps is by reference to figure 26. Here the loss in percentage recovery realized by the addition of a propeller is plotted against air flow for several configurations. The curves are numbered according to the sketches shown in figure 27. It is evident that the loss in recovery due to the presence of the propeller is dependent on air flow for different configurations, but one factor is especially noticeable. In each case where the cowl liner was used, the decrement in recovery reaches a peak at a certain flow and then starts to fall off toward zero as the flow is increased, while for the cases in which no liner was employed, the decrement becomes larger at such a rapid rate as the flow is increased that the chances of finally becoming smaller seem very remote. Several blade angles were tested, and the effects of blade angle on internal flow were not noticeable in a range between 15° and 28°. This result is reasonable since the blade shanks are very nearly round within the entrance diameter of the cowl. It is fairly evident that at low cooling flows, the propeller will account for about 10-percent loss in recovery, that at medium flows the loss may be as much as 15 percent, and that at high flows the loss <u>may</u> be negligible, depending purely on how favorable

is the entrance design of a particular installation. One thing, at least, is certain - the engine would prefer not to have an uncuffed propeller operating ahead of it.

THE EFFECT OF PROPELLER CUFFS ON PRESSURE RECOVERY

Owing to unavoidable limitations in test data up to the present, no attempt will be made to generalize on the effects of propeller cuffs on pressure recovery. Several rather specific results were obtained, however, and from figure 27 the indications are that under certain flow conditions the cuffs employed on a three-blade propeller operating at a blade angle of 25° at 0.75R and a V/nD of 0.95 are quite beneficial for nose assemblies using conventional hubs and domes. The recovery with propeller and cuffs for the configuration employing a hub, dome, cowl liner, and dishpan (B of fig. 27) is actually higher than for the case when no propeller was present. This result represents a considerable gain over the recoveries realized with an uncuffed propeller.

When a cuffed propeller was tried on the optimum short-nose cowl arrangement which had attained nearly 100 percent recovery <u>without</u> a propeller, the value dropped to 83 percent - a 6.5-percent loss from the case with an uncuffed propeller. This result perhaps indicates that for this particular set of conditions the cuffs were stalled. It seems reasonable to suppose that with redesigned cuffs the recovery could be at least as good, if not beter, than the value obtained with the uncuffed propeller.

Yes, 100-percent pressure head in front of the engine, or nearly that, should be possible for tractor installations utilizing either long-nose or short-nose cowls, but it will probably be attained <u>only under certain conditions of cooling flow, airplane speed, and attitude of flight</u>, for which conditions the spinners, cowl liners, and reduction-gear fairings must be carefully designed to give the proper entrance velocity and diffuser expansion ratio. Considering all the difficulties of achieving and maintaining full recovery for tractor installations under varying flight conditions, in the long run the simplest solution may be what seems at the moment to be the most drastic and, perhaps to some, more or less defeatist - and that is to remove the source of the trouble itself. Artificial improvement can be employed, but the solution is still far

short of the ideal. On the basis of these tests it has been demonstrated that full recovery can be obtained under practically all conditions of flight if the cowl entrance is clear of encumbering assemblies. If nacelles are of the pusher type, the nose of the cowl can be made as long as desired for optimum diffuser efficiency and, moreover, the cowl will, of course, be stationary. Full recovery should be achieved under all flight conditions, and if fans or blowers are required, they could presumably be mounted within the diffuser to give good operating efficiency. The added weight and the new design problem is a consideration to be reckoned with, but at least the engine is being placed in a location favorable for maximum pressure recovery and low drag.

EFFECT OF INTAKE AND EXHAUST PIPES AND ACCESSORIES AT REAR OF ENGINE ON COOLING FLOW

Strictly speaking, as has been pointed out so often before by other writers, there are other "conductivities" to be considered besides engine conductivity when the engine is installed within a cowl. There are two other major sources of pressure loss: the cowl entrance and the accessory section from the rear of the engine to the cowl exit gill. The cowl entrance has already been discussed in some detail, in terms of pressure recovery ahead of the engine, which is considered the most convenient method of presentation. However, if for the moment the pressure loss ahead of the engine is assumed as corresponding to some conductivity K_{q_a} and the loss to the rear of the engine corresponding to a conductivity K_{q_r}, the two together with engine conductivity K_q may be expressed in the equation:

$$\frac{1}{\left(K_{q_t}\right)^2} = \frac{1}{\left(K_{q_a}\right)^2} + \frac{1}{\left(K_q\right)^2} + \frac{1}{\left(K_{q_r}\right)^2} \qquad (7)$$

where K_{q_t} is the total conductivity of the cowl installation. It is obvious that it is desirable to keep the pressure losses ahead of and to the rear of the engine as low as possible, which means that K_{q_a} and K_{q_r} must be kept high. The desirable ideal is, of course, that K_{q_a}

and K_{q_r} equal infinity, indicating 100 percent recovery ahead of the engine and no losses to the rear of the engine.

In actual practice this ideal can be more closely attained ahead of the engine than at the rear because two-row engines require in the accessory section so many intake and exhaust pipes, wires, ducts, control rods and mechanisms, along with the other necessary paraphernalia which may include the carburetor, electrical equipment, and accessory drives. A rough approximation of this condition was made in the United Aircraft nacelle model, by including in it dummy intake and exhaust pipes which, along with pressure tubing that of necessity had to pass through the "accessory section," offered some restriction to air flow. The set-up with this equipment installed is illustrated in figure 28. It is to be noted that this arrangement was greatly simplified over an actual engine installation.

As shown in figure 29, there was a greater total-pressure loss from the rear of the engine to the exit gill with the dummy pipes in place. Based on the maximum nacelle area, the rear conductivity K_{q_r} was found to be of the order of 0.4 (fig. 30). It is highly possible that some installations might give values as low as 0.2. It is obvious that such installations have a very detrimental effect on cooling flow for a given cowl exit gap.

THE USE AND ADVANTAGE OF FANS

If cowl flaps in conjunction with the best possible nacelle entrance and exit conditions will not supply the pressure drop and flow required for cooling, the use of fans, or blowers, must be resorted to. Not only will fans provide an increase in flow, but by their use the exit velocity can be made to equal the free-stream velocity. In this case the cooling drag has been reduced to zero, since there has been no loss in momentum through the nacelle. Quite naturally, if the fan produces an exit velocity in excess of the free-stream value, a beneficial thrust will result.

The fans, or blowers, tested during this program were placed behind the "engine" (fig. 31) and, although the ac-

tual testing was very general and limited in scope, a few rather interesting results were brought to light. In the first place, it was demonstrated very conclusively that fans are a more "efficient" means of inducing cooling flow than flaps at high angles. "Efficiency," as used here, simply refers to the fact that the horsepower put into a fan to achieve a given flow is less than the horsepower (manifesting itself as drag) required when the cowl flaps are opened to obtain the same given flow without a fan. The better efficiency is most noticeable under conditions where high flap angles would be required without a fan. Under these conditions the saving in drag by use of a fan is really considerable (fig. 32). The curves in the figure are for the three different configurations tested. At low values of $\Delta p/q$ obtained by low flap angles, the fan is less efficient - as is shown by the negative values of drag coefficient. At the higher pressure drops, corresponding to high flap angles, the saving in drag by using a fan is represented by positive values of drag coefficient. In other words, any radial engine which requires a flap angle above 12° for cooling under the critical condition might profit by utilizing a fan instead of cowl flaps - or, in conjunction with cowl flaps, should they still be necessary for cooling requirements in climb at altitude. But at least the required flap angle to obtain the flow necessary in climb will be less than if a fan were not present, and thus considerable saving in drag should be realized. The high-speed condition would presumably be unaffected, with perhaps a slight loss realized due to the added installation weight of the blower, but climb performance should be materially improved, perticularly single-engine climb.

Ideally, of course, if the fan is designed to operate at peak efficiency at high speed and if the exit for cooling flow is a reasonable jet, the power input to the fan can be largely regained in thrust. With a very inefficient design of fan, propulsive efficiencies of more than 60 percent were obtained at the limiting flap angle of 12°. Above this angle, the thrust and the propulsive efficiency fall off rapidly and, while increased cooling flow can still be obtained, it is only at great cost in power input to the fan.

EFFECT OF SEVERAL VARIABLES ON NACELLE CRITICAL MACH NUMBER

It is more or less obvious that it might be possible to obtain a cowled nacelle which would be entirely satisfactory from all points of view as previously discussed but which would have high drag at high speeds because of the onset of compressibility effects. The fact that there is a rapid increase in cowl drag with speed, when this critical condition is reached, is no doubt familiar at all but, if not, typical curves are included in reference 7.

As is well known, it is possible to estimate critical speeds of cowled nacelles from low-speed pressure-distribution data obtained from wind-tunnel tests. Using the minimum pressure obtained along the body, the critical speed can be determined by a method proposed by Jacobs (reference 18), which is reasonably accurate. This determination has been made for several of the basic bodies, and the results are given in figures 33 and 34. Both the critical speeds at 30,000 feet and the corresponding critical Mach numbers are given. Critical Mach number is defined as the dimensionless ratio of the velocity at which compressibility takes effect V_c to the speed of sound in air c, both taken at a given altitude. That is,

$$M_c = \frac{V_c}{c} = \frac{V_c \text{ (mph)}}{33.5\sqrt{460 + t}} \tag{8}$$

where t is the temperature in $^{\circ}F$ at the altitude under consideration.

It is to be noted from figure 33 that the best streamline body has the highest critical speed, while the plain NACA cowled nacelle without air flow has the lowest. By the addition of a spinner to the NACA cowled nacelle the critical speed or Mach number has been improved almost to that of the blunt streamline body. Although pressure-distribution measurements were not made on the long-nose cowls, it is probable that their critical speeds would be higher than that of the short-nose cowl.

Figure 34 shows that the addition of air flow results in a change in critical speed, with the highest conductivity or mass air flow giving the highest speed. Although the critical Mach number appears to vary with conductivity,

the real criterion appears to be mass flow through the cowl. If the mass flow is held constant and the conductivity varied, within the limits of the data obtained, there is negligible change in M_c unless the cowl flaps have to be opened to obtain the specified flow. As can be seen in figure 35, the opening of the cowl flaps more than a few degrees begins to have a substantial effect on the critical speed, since the slope of the curve is fairly steep. This figure also shows that as the nacelle angle of attack is increased the critical Mach number is progressively decreased. The change in critical speed at 30,000 feet from 0° to 6° is from 397 to 335 miles per hour. It is important to bear this fact in mind, especially in connection with high-altitude airplanes which must, of necessity, fly at a considerable angle of attack of the wing and thus of the nacelle.

The effect of the propeller on critical Mach number could not be isolated by the small number of tests conducted on this phase of the problem. Several runs that were made with operating propeller on two different configurations indicated that the peak negative pressures on the nacelles were definitely reduced. For a typical case with a conductivity of 0.12 and a mass flow of 10,700 pounds per hour, the peak negative pressure coefficient was decreased from about -0.95 to -0.69. Whether this result indicates an increase in M_c over the no-propeller case is difficult to determine, since there is undoubtedly a pressure rise through the propeller, which effect is superimposed on the pressure field of the body. However, since it was found that the pressure rise alone cannot account for such a large change in peak negative pressure, the remainder may be attributed to a change in air-flow direction. With uncuffed propeller the round shanks may account for some actual slowing down of the air over the cowl nose, while with cuffed propellers the reverse may be true. In either case the propeller-operating conditions are necessarily important. At high speed, where M_c is of primary importance, the average slipstream velocity is only slightly higher than the flight velocity, from which it may be deduced that for a first approximation the critical Mach number for a comparable configuration without propeller may be close enough to the actual case with propeller. Although it may be argued that the passage of the propeller blade gives a momentary increase in velocity over the cowl, which is much higher than the average slipstream velocity, this factor is probably negligible at high speed.

ESTIMATION OF NACELLE COOLING DRAG FROM THEORY

Over-all nacelle, or fuselage, drag can be broken down into three parts, which in coefficient form are as follows:

(1) C_{D_o} the form drag coefficient of the body with no cooling flow

(2) C_{D_c} the cooling drag coefficient due to flow through the nacelle

(3) ΔC_{D_o} the additional form drag coefficient which under certain conditions manifests itself when cooling flow exists

C_{D_o} can be estimated from known values and is, of course, dependent on body characteristics such as fineness ratio and type of cowling.

C_{D_c}, the internal drag coefficient, can be calculated in a number of ways, but it has been found by comparison with innumerable wind-tunnel test data that the following equation will yield the most accurate and consistent results:

$$C_{D_c} = 2\,\frac{Q}{SV}\left[1 - \sqrt{\frac{PR}{q} - \left(\frac{Q}{S\ V\ K_q}\right)^2}\right] \qquad (9)$$

where

K_q engine conductivity based on nacelle frontal area

Q volume flow through the engine, cubic feet per second

S frontal area of nacelle, square feet

V flight speed, feet per second

$\frac{PR}{q}$ total pressure ahead of engine referred to free-stream dynamic pressure

The derivation of equation (9) from momentum considerations is included in an appendix to this paper.

ΔC_{D_0}, the increase in form drag, has been found to be, for all intents and purposes, negligible up to flap angles of about 12°. Beyond this value the increase in form drag is not only very abrupt and severe but apparently totally unpredictable from theoretical considerations. At these high flap angles, ΔC_{D_0} is known to be a function of the change in pressure drag when cooling flow exists, the change in skin friction back of the cowl flaps, and the drag of the flaps themselves. These are complicated effects and in an effort to find if ΔC_{D_0}, the change in form drag, was a function of any nondimensional parameter, it was plotted against quantities which represented:

1. The flow of air through the nacelle
2. The velocity of flow at the gill exit
3. The momentum of the air escaping through the gill
4. The kinetic energy of the air escaping through the gill
5. The pressure at the rear of the engine
6. The square of the total pressure drop through the engine
7. An empirical formula modifying the above
8. The change in pressure immediately behind the flap with the flap sealed and then open
9. The pressure drop from the accessory compartment to the region immediately behind the cowl flap
10. The pressure drop from the accessory compartment to the region immediately ahead of the cowl flap
11. A combination of 9 and 10

It was concluded that the increase in form drag which occurs above flap angles of about 12° is not a simple function of any one of the preceding quantities.

Returning once again to equation (9), it will be noted that the expression $\frac{PR}{q}-\left(\frac{Q}{S\ V\ K_2}\right)^2$, appearing under the square root sign, is merely a convenient way of representing the total pressure at the rear of the engine referred to free-stream dynamic pressure. It will be noted further that real theoretical values of cooling drag coefficient are possible only when the expression has positive values or is zero. In other words, when the pressure at the rear of the engine becomes negative (the condition realized at high flap angles), the theoretical cooling drags become imaginary. It has often been suggested that in cases like these, the negative sign be disregarded and that the square root of the expression then be <u>added</u> instead of subtracted from unity. In figure 36 cooling drag coefficients have been calculated from equation (9) by assuming different values of $\frac{Q}{SV}$ and $\frac{PR}{q}-\left(\frac{Q}{S\ V\ K_q}\right)^2$. Imaginary values of cooling drag coefficient are indicated by the broken portion of the curves which, due to their form, makes it almost needless to state that these values are imaginary in fact as well as in theory. The solid portions of the curves can presumably be used as a convenient chart for the calculation of cooling drag coefficients, although there is some error involved, as mentioned later. The assumption that there is no increase in form drag due to cooling flow for positive values of pressure at the rear of the engine can be easily checked by the use of the wind-tunnel test results. If the basic drag of the body be subtracted from the measured drag as corrected for tare and interference effects, the difference should be the cooling drag. In figure 37 the test points obtained in this way have been located on the plot appearing at the left. The curves have been replotted from figure 36. It should be pointed out that the test data are for cowled nacelles of two different fineness ratios. Although there is some scatter of the data, fairly good agreement is evident.

No correlation between theory and test can be expected for negative values of pressure at the rear of the engine, since the difference in basic and model drag mentioned is no longer solely cooling drag, but a combination of cooling and form drag, neither of which is easily estimated at high flap angles. As a matter of interest only, test points for this combination drag coefficient have been located for several values of Q/SV in figure 37. It is possible that the slopes of the curves serve as

a fair indication of how form and cooling drag vary with negative pressures at the rear of the engine, but it is suggested that extreme caution be exercised if attempts are made to estimate drags of other bodies from the right-hand group of curves.

CHARTS FOR THE ESTIMATION OF COWL EXIT GAP REQUIRED

From the mass of test data obtained, charts were developed which should aid in the determination of cowl exit gaps for varying flight conditions, or conversely, which should assist in estimating the flow obtainable with a given exit gap. The charts are presented in figures 38(a) through 42.

Figure 38(a) gives the pressure recovery to be expected from the use of various configurations with propeller. Figure 38(a) is for 0° angle of attack, while figure 38(b) indicates the pressure recovery for the same configurations at 6° angle of attack. Both conventional and optimum configurations are included, the designs of which can be seen by reference to the figure number given in the table on each figure. The values for pressure recovery should be increased or reduced by an amount depending on the variation in design (diffuser expansion and length ratio) or operating conditions (airplane speed, angle of attack) from the configuration under consideration. The change due to different operating conditions will be slight in most cases and can be estimated from figures 16(b), 16(c), and 38(b). If the diffuser is within the design limits prescribed in an earlier section of this paper, the effect on pressure recovery will also be slight.

It should be noted that in figures 38(a) and 38(b) the <u>square root</u> of the pressure recovery is plotted against the flow ratio, Q/SV. This method has been used to be in keeping with the design parameters appearing in the working charts. From the flow ratio, the exit gap for maximum speed can be determined once the product of conductivity and square root of pressure recovery are known (fig. 39). The quantity K_{q_c} is <u>not</u> the engine conductivity but is the combined conductivity of the engine and the accessories from the rear of the engine to the exit gap. K_{q_c} is obtained from the relation

$$\frac{1}{\left(K_{q_c}\right)^2} = \frac{1}{\left(K_q\right)^2} + \frac{1}{\left(K_{q_r}\right)^2} \qquad (10)$$

where

K_q engine conductivity (quoted by manufacturer but based on maximum nacelle cross-sectional area, not engine disk area)

K_{q_r} rear compartment conductivity (based on maximum nacelle cross-sectional area)

K_{q_r} has previously been mentioned as being of the order of 0.4, in the section - EFFECT OF INTAKE AND EXHAUST PIPES AND ACCESSORIES AT REAR OF ENGINE ON COOLING FLOW. The inclusion of both pressure recovery and the accessory-compartment conductivity in the preliminary calculations is essential in the practical use of the charts for design work. Attention is called to the fact that the product of $K_{q_c}\sqrt{\frac{PR}{q}}$ represents the conductivity of the entire nacelle, K_{q_t} (equation (7)), since $\sqrt{\frac{PR}{q}}$ corresponds to the conductivity ahead of the engine. It is K_{q_t} which determines the cooling flow that is to be attained for any given exit gap. Although it is sufficiently accurate for practical purposes to consider K_{q_t} as equal to $K_{q_c}\sqrt{\frac{PR}{q}}$, strictly speaking, the actual relationship is as follows:

$$K_{q_t} = K_{q_c}\sqrt{\frac{1}{1 + \frac{1 - \frac{PR}{q}}{\left(Q/SVK_{q_c}\right)^2}}} = K_{q_c}\sqrt{\frac{\frac{PR}{q} - \frac{P_{exit}}{q}}{1 - \frac{P_{exit}}{q}}} \qquad (11)$$

where P_{exit} is the pressure at the cowl exit gill. The percentage error involved in determining K_2 by using the less rigorous and far simpler expression for K_{q_t} should not exceed 5 percent within a pressure recovery range of 55 to 100 percent.

Assuming, then, that the high-speed exit gap has been obtained from figure 39, the low speed (or any intermediate speed) exit gap can be readily determined from figure 40. Here the parameter $K_{q_c}\sqrt{\frac{PR}{q}}$ determines the chart to be used. The broken curve in each chart is for shortened skirts and thus represents zero flap angle exit gaps for the high-speed condition. (See fig. 39.) At any point on the curve, then, there is an additional curve for flap angles which begins with that point as the origin. (See fig. 9.) Several of these cowl flap curves (solid lines) are included in each chart for specific values of zero flap angle exit gaps to facilitate interpolation. The intersection of the value of flow ratio Q/SV with the solid curve corresponding to the high-speed exit gap already calculated (from fig. 39), gives the K_2 for the low-speed case. Knowing the flap length and shoulder shape, it is then a simple matter to calculate the flap angle corresponding to that K_2.

Inasmuch as the limit of the induced flow ratio Q/SV is determined solely by $K_{q_c}\sqrt{\frac{PR}{q}}$ for cowled nacelles with continuous flaps, a plot of this limiting value is included (fig. 41). All values falling below this curve may be obtained by flight-induced flow, but those above the curve require forced flow by the use of blowers or other auxiliary means.

As an example of how the charts are used, assume that it is desired to find the exit gap for the following conditions:

Airplane maximum speed (true air speed)	= 350 mph
Nacelle (or fuselage) frontal area	= 16 sq ft
Operating altitude	= 20,000 ft
Engine conductivity (based on nacelle frontal area)	= 0.108
Flow required to cool (from engine manufacturer)	= 500 cu ft per sec

The airplane has a conventional nose assembly consisting of an NACA nose C cowl, hydromatic hub, and dome. The first step is the determination of the flow ratio.

$$\frac{Q}{SV} = \frac{500}{16 \times 350 \times 1.467} = 0.0609$$

The square root of the pressure recovery can then be estimated from curve 3 of figure 38. The value of $\sqrt{\frac{PR}{q}}$ at 150 miles per hour for a Q/SV of 0.061 is 0.775. For a speed of 350 miles per hour little increase can be expected, as seen from figure 16(b) (at bottom). Hence, the same value of $\sqrt{\frac{PR}{q}}$ will be used at 350 miles per hour. Assuming the rear compartment conductivity K_{q_r} to be 0.4, K_{q_c} is determined from equation (10).

$$\frac{1}{(K_{q_c})^2} = \frac{1}{(0.108)^2} + \frac{1}{(0.4)^2}$$

$$K_{q_c} = 0.104$$

Then $$K_{q_c}\sqrt{\frac{PR}{q}} = 0.104 \times 0.775 = 0.081$$

A high-speed exit gap ratio of 0.12 can now be found directly from figure 39 as indicated by the broken line.

The high-speed exit gap having been determined, it is desired to know the gap required for climb at sea level for the same airplane, assuming that:

Climbing speed	= 140 mph
Altitude	= sea level
Flow required to cool	= 290 cu ft per sec
Angle of attack	= 7°

then

$$\frac{Q}{SV} = \frac{290}{16 \times 140 \times 1.467} = 0.0885$$

From figures 38(b), 16(b), and 16(c), the $\sqrt{\frac{PR}{q}}$ is estimated to be about 0.77, giving a $K_{q_c}\sqrt{\frac{PR}{q}}$ of 0.080. Checking from figure 41 to find if a blower is necessary for these values of Q/SV and $K_{q_c}\sqrt{\frac{PR}{q}}$, it is seen that flaps will just provide the necessary flow. Turning to

chart B of figure 40(a), the broken line for Q/SV of 0.0885 can be followed across to point 2 and then down vertically, giving an exit gill area ratio of 0.33 for a maximum speed exit gap of 0.12.

The low-speed example just completed was chosen because it brings up several important points in connection with the use of the charts in figure 40. First, when Q/SV is near the limiting value obtainable by cowl flaps for a given value of $K_{q_c}\sqrt{\frac{PR}{q}}$, use of the charts to determine K_2 is actually, of course, unnecessary, since an arbitrary flap angle between 25° and 40° can be selected according to the discretion of the user. If the charts are used in a case like this, it should be remembered that a large increase in exit gill area ratio, or flap angle, produces little or no gain in flow but does produce high drag. Therefore, if the calculated value of Q/SV is near the limiting value, the intersection of the calculated value with the flap curve for a maximum speed value of K_2 equal to 0.05 will be conservative in determining the exit gap required. This intersection is labeled point 1 on chart B, the vertical projection of which point will give a K_2 of 0.22. For most purposes, however, the charts shown in figure 40 will be most valuable in estimating exit gill area ratios other than those required for maximum speed and critical climb conditions, for example, the cruising condition. Figure 39 will be used for maximum speed, while figure 41 will be used for the climb condition.

The second point to bear in mind is that for a given Q/SV the exit gill area ratio found from the charts must be maintained regardless of the percentage of the cowl periphery that is flapped. A cowl whose periphery is only 80 percent flapped requires at least the same K_2 to obtain a given Q/SV as a 100-percent flapped cowl. The difference will only appear in the flap angles required to maintain the same K_2 and thus the same flow. Since the test data, from which the charts were drawn, were based on a cowl whose periphery was 100 percent flapped, discretion should be used when estimating exit gill area ratios for cowls which have a considerably lower percentage of periphery flapped. It should be remembered that the lower the flap angle for a given flow the lower will be the drag. Therefore, it follows that continuous cowl flaps are best.

Obviously, if an engine of a given diameter is housed in an exceptionally large-diameter cowl, the values of K_2 taken from the charts may be misleading. The charts are based on the minimum ratio of cowl to engine diameter that can be maintained in an actual installation. If large ratios of cowl to engine diameter are to be used, it is suggested that all chart parameters be based on engine disk area, not nacelle area. This method will tend to keep values of pressure recovery more nearly in line.

In order to avoid confusion in the calculation of the few basic flow parameters and their use in estimating cooling drag coefficients and exit gill area ratios, everything in this paper relating thereto has been based on maximum nacelle cross-sectional area. It is recommended that this procedure be followed. However, with proper care, flow parameters and cooling drag coefficients can be based on engine disk area.

Although the charts given here should be of assistance in the estimation of pressure recovery and cowl exit gaps, they are still only approximate, and require their user to employ a great deal of judgment based on an understanding of the limitations of the charts. When additional tests are made and further information is available, it will undoubtedly be found beneficial to revise and extend these charts.

COMPARISON OF DATA ESTIMATED FROM WORKING CHARTS WITH FLIGHT-TEST RESULTS

In spite of the fact that figures 38 to 41 are based on wind-tunnel test data for a nacelle without a wing and have certain other previously mentioned limitations, it was thought desirable to determine how close one could come to the actual cooling flows and cowl exit gaps required by comparing the data estimated from working charts with flight-test results. The test points in figure 42 were obtained from six different flight-test runs on a multiengine airplane having noncontinuous cowl flaps but a more or less conventional nacelle installation with a hydromatic propeller and no internal cowl fairings. The flight-test data are fairly consistent at low exit gill area ratios. At high flap angles, angles above 20°, there was some scatter, which may have been due to a number of

reasons, including the inability of the particular pressure-measuring devices to measure the pressure accurately. It is believed, however, that the solid line represents a fair average of the data.

The broken line of figure 42 was determined from the working charts in this paper, using the known conductivity of the engine, the estimated pressure recovery ahead of the engine, and the estimated conductivity of the accessory section. Although good agreement with flight-test data exists at the high flow ratios, the agreement is only fair at the lower ratios. This lack of agreement can be explained to a large degree by the fact that the engines installed in this particular airplane were easily cooled under practically all flight conditions, thus indicating that the high-speed exit gap was too large. In other words, the engines could have been cooled at a lower mass air flow. In spite of some discrepancy between the curves, it is felt that they check reasonably well.

CONCLUSIONS

1. A typical cowled nacelle, without air flow, has a drag coefficient about 50 percent higher than that of a comparable streamline body.

2. For a given quantity of cooling flow, the higher the conductivity the lower the drag. As a corollary to this conclusion, the pressure drop required to cool should be kept as low as possible.

3. The optimum location of cowl flaps appears to be immediately behind the engine, both from the standpoint of low drag and maximum obtainable flow.

4. Test results show conclusively that piezometer rings should be discontinued for pressure measurement. All flow measurements through the engine installation require the use of total-head rakes for accurate and consistent results. These rakes may be of the radial integrating or nonintegrating type but should preferably be shielded.

5. For a given installation the pressure recovery ahead of the engine, referred to free-stream dynamic pressure, is dependent solely on quantity of flow and a Reynolds number effect of flight speed. The pressure recovery is independent of the various conductivities and pressure drops which may determine the flow.

6. For a given installation there is a range of flow which will give optimum pressure recovery ahead of the engine.

7. The use of a cowl liner and reduction-gear housing fairing to simulate a diffuser is essential for the attainment of high recoveries. This fact, combined with conclusion 6, means that the diffuser must be designed for the critical cooling condition.

8. For good recovery, the diffuser expansion ratio must be kept below 3.0 and preferably below 2.5. The velocity at the diffuser throat should be between 50 and 60 percent of the free-stream value.

9. Increase in angle of attack generally has an adverse effect on available cooling head. The loss is more pronounced for top engine cylinders than for bottom cylinders.

10. For a given cooling flow, poor recovery has a large detrimental effect on nacelle drag, especially at high flap angles.

11. If there are no objects protruding forward from the cowl entrance, optimum recovery can be attained under all conditions of flow, flight speed, and attitude of the nacelle.

12. The use of an uncuffed propeller may result in a loss of as much as 15 percent in pressure recovery from that attainable without a propeller. The addition of properly designed cuffs may considerably improve the recovery of poor installations.

13. The accessory compartment pressure losses, due to the presence of intake and exhaust pipes, cowl-flap mechanism, and so forth, are of considerable magnitude and must be accounted for in determining cowl exit requirements for a specified flow.

14. Provided the pressure at the rear of the engine remains positive, there is no apparent increase in nacelle form drag with cooling flow and the cooling drag can be calculated reasonably well from theory. Depending on conductivity, the limiting flap angle for zero increase in form drag is about 12°.

APPENDIX

The cooling-drag equation, given as equation (9) in the text, can be easily derived from momentum considerations. Only two simplifying assumptions are necessary:

(1) The density within the cowl is equal to free-stream density.

(2) The static pressure at the exit gill is equal to the free-stream static pressure.

The numerical subscripts given in the equations below refer to the stations indicated in figure 43.

Beginning with the momentum equation:

$$\text{Net drag} = M(V_1 - V_5)$$

$$= \rho\, Q(V_1 - V_5) \qquad (1)$$

But, from assumption 2, $V_4 = V_5$

thus, net drag $= \rho\, Q(V_1 - V_4)$ (2)

The losses from (1) to (2) and from (2) to (3) may be expressed by Bernoullian equations as follows:

$$\frac{\rho}{2} V_1^2 + P_1 = \frac{\rho}{2} V_2^2 + P_2 + \text{losses}_{1-2} \qquad (3)$$

$$\frac{\rho}{2} V_2^2 + P_2 = \frac{\rho}{2} V_3^3 + P_3 + \text{losses}_{2-3} \qquad (4)$$

Subtracting equation (4) from equation (3) gives:

$$\frac{\rho}{2} V_3^2 = \frac{\rho}{2} V_1^2 + P_1 - P_3 - \text{losses}_{1-2} - \text{losses}_{2-3} \qquad (5)$$

Assuming no losses from (3) to (4), in figure 43:

$$\frac{\rho}{2} V_3^2 + P_3 = P_4 + \frac{\rho}{2} V_4^2 \qquad (6)$$

Thus, solving equation (6) for V_4 after substituting for $\frac{\rho}{2} V_3^2$ (from equation (3)),

$$V_4 = \sqrt{\frac{P_1 - P_4 - \text{losses}_{1-2} - \text{losses}_{2-3}}{\rho/2} + V_1^2} \qquad (7)$$

Since $P_1 = P_4$ by assumption:

$$\text{Net drag} = \rho Q \left(V_1 - \sqrt{V_1^2 - \left(\frac{\text{losses}_{1-2} + \text{losses}_{2-3}}{\rho/2}\right)}\right)$$

$$= \rho Q\, V_1 \left(1 - \sqrt{1 - \frac{(\text{losses}_{1-2} + \text{losses}_{2-3})}{q}}\right) \qquad (8)$$

But $1 - \frac{\text{losses}_{1-2}}{q}$ is the front total-head reading, and losses represent the total losses across the engine, that is, the <u>total-head</u> pressure drop. Equation (8) can now be written as

$$\text{Net drag} = \rho Q V_1 \left(1 - \sqrt{\frac{PR}{q} - \frac{\Delta P\ \text{total}}{q}}\right) \qquad (9)$$

where $\frac{PR}{q}$ is the pressure recovery ahead of the engine referred to free-stream dynamic pressure. It is of interest to point out that equation (9) is of the same form as that given by Ellis in reference 11.

Substituting $\left(\frac{Q}{SVK_q}\right)^2$ for $\Delta P/q$, $K_q SV\left(\frac{\Delta P}{q}\right)^{\frac{1}{2}}$ for Q, and dividing equation (9) by Sq to change from drag to drag coefficient, there is obtained cooling-drag coefficient, $C_{D_c} = 2K_q \left(\frac{\Delta P}{q}\right)^{\frac{1}{2}} \left(1 - \sqrt{\frac{PR}{q} - \left(\frac{Q}{SVK_q}\right)^2}\right)$

$$= \frac{2Q}{SV}\left(1 - \sqrt{\frac{PR}{q} - \left(\frac{Q}{SVK_c}\right)^2}\right) \qquad (10)$$

REFERENCES

1. Beisel, Rex B., MacClain, A. Lewis, and Thomas, F. M.: The Cowling and Cooling of Radial Air-Cooled Aircraft Engines. SAE Jour., vol. 34, no. 5, May 1934, pp. 147-166.

2. Shoemaker, J. M., Rhines, T. B., and Sargent, H. H., Jr.: Further Progress in Controlled Cooling of Radial Aircraft Engines. SAE Jour., vol. 37, no. 4, Oct. 1935, pp. 349-360.

3. Theodorsen, Theodore, Brevoort, M. J., and Stickle, George W.: Full-Scale Tests of N.A.C.A. Cowlings. Rep. No. 592, NACA, 1937.

4. Brevoort, M. J., Stickle, George W., and Ellerbrock, Herman H., Jr.: Cooling Tests of a Single-Row Radial Engine with Several N.A.C.A. Cowlings. Rep. No. 596, NACA, 1937.

5. McHugh, James G., and Dorring, Eldridge, H.: The Effect of Nacelle-Propeller Diameter Ratio on Body Interference and on Propeller and Cooling Characteristics. Rep. No. 680, NACA, 1939.

6. Theodorsen, Theodore, Brevoort, M. J., and Stickle, George W.: Cooling of Airplane Engines at Low Air Speeds. Rep. No. 593, NACA, 1937.

7. Wood, Donald H.: Design of Cowlings for Air-Cooled Aircraft Engines. SAE Jour., vol. 41, no. 6, Dec. 1937, pp. 581-596.

8. Wood, Donald H.: Tests of Nacelle-Propeller Combinations in Various Positions with Reference to Wings. Part I. Thick Wing - N.A.C.A. Cowled Nacelle - Tractor Propeller. Rep. No. 415, NACA, 1932.

9. Wood, Donald H.: Tests of Nacelle-Propeller Combinations in Various Positions with Reference to Wings. II. Thick Wing - Various Radial-Engine Cowlings - Tractor Propeller. Rep. No. 436, NACA, 1932.

10. Wood, Donald H.: Tests of Nacelle-Propeller Combinations in Various Positions with Reference to Wings. III. Clark Y Wing - Various Radial-Engine Cowlings - Tractor Propeller. Rep. No. 462, NACA, 1933.

11. Ellis, D. L.: Cooling and Cowlings. The Aeroplane, vol. LIX, no. 1520, July 12, 1940, pp. 40-42 and vol. LIX, no. 1521, July 19, 1940, pp. 73-75.

12. Beisel, Rex B.: Why Use Cowl Flaps. Jour. Aero. Sci., vol. 4, no. 5, March 1937, pp. 185-191.

13. Markham, John R.: The M.I.T.-Wright Brothers Wind Tunnel and Its Operating Equipment. SAE Jour., vol. 49, no. 3, Sept. 1941, pp. 380-388.

14. Kiel, G.: Total-Head Meter with Small Sensitivity to Yaw. T.M. No. 775, NACA, 1935.

15. Silverstein, Abe, and Guryansky, Eugene R.: Development of Cowling for Long-Nose Air-Cooled Engine in the NACA Full-Scale Wind Tunnel. NACA A.R.R., Oct. 1941.

16. Valentine, E. Floyd: Preliminary Investigation Directed toward Improvement of the NACA Cowling. NACA A.R.R., April 1942.

17. Bailey, F. J., Jr., Johnston, J. Ford, Voglewede, T. J.: Flight Investigation of the Performance and Cooling Characteristics of a Long-Nose High-Inlet-Velocity Cowling on the XP-42 Airplane. NACA A.R.R., April 1942.

18. Jacobs, Eastman N.: Methods Employed in America for the Experimental Investigation of Aerodynamic Phenomena at High Speeds. Misc. Paper No. 42, NACA, 1936.

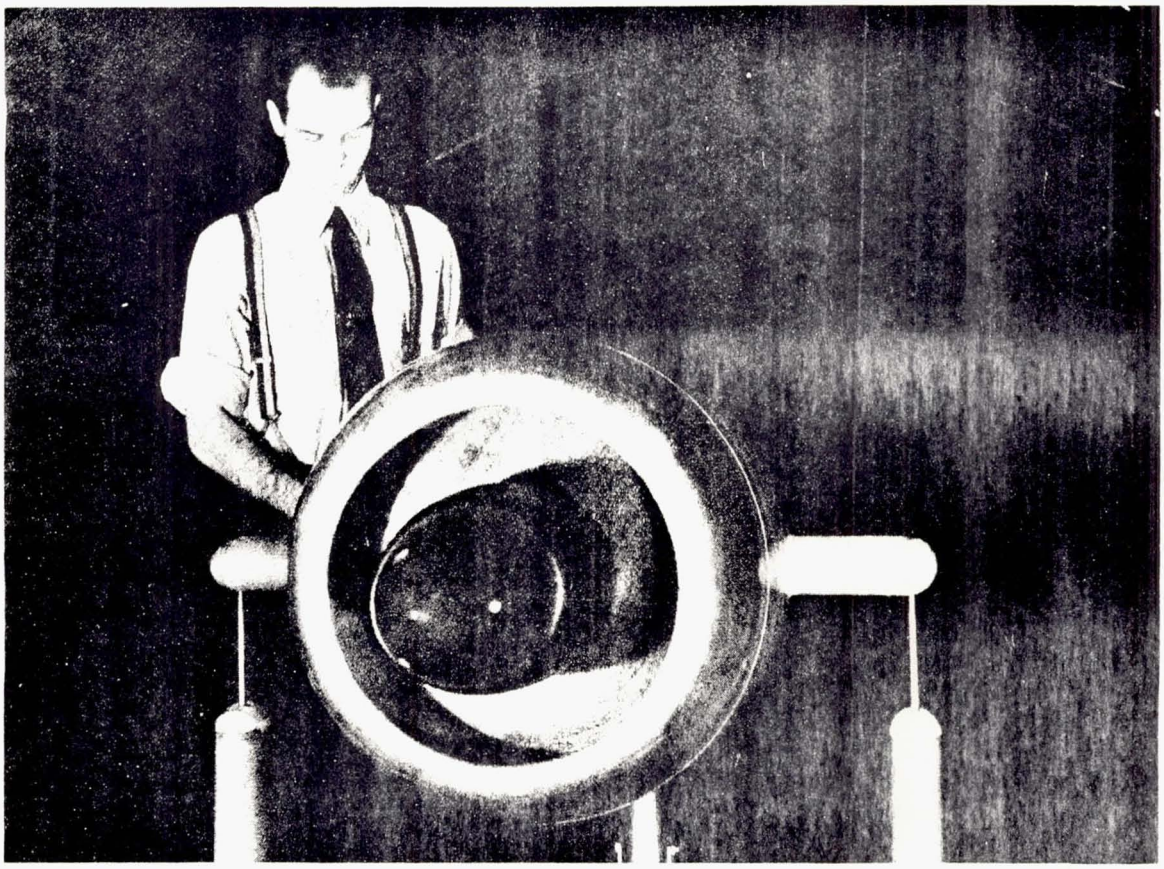

Figure 1.- Typical set-up in tunnel. No air flow through model.

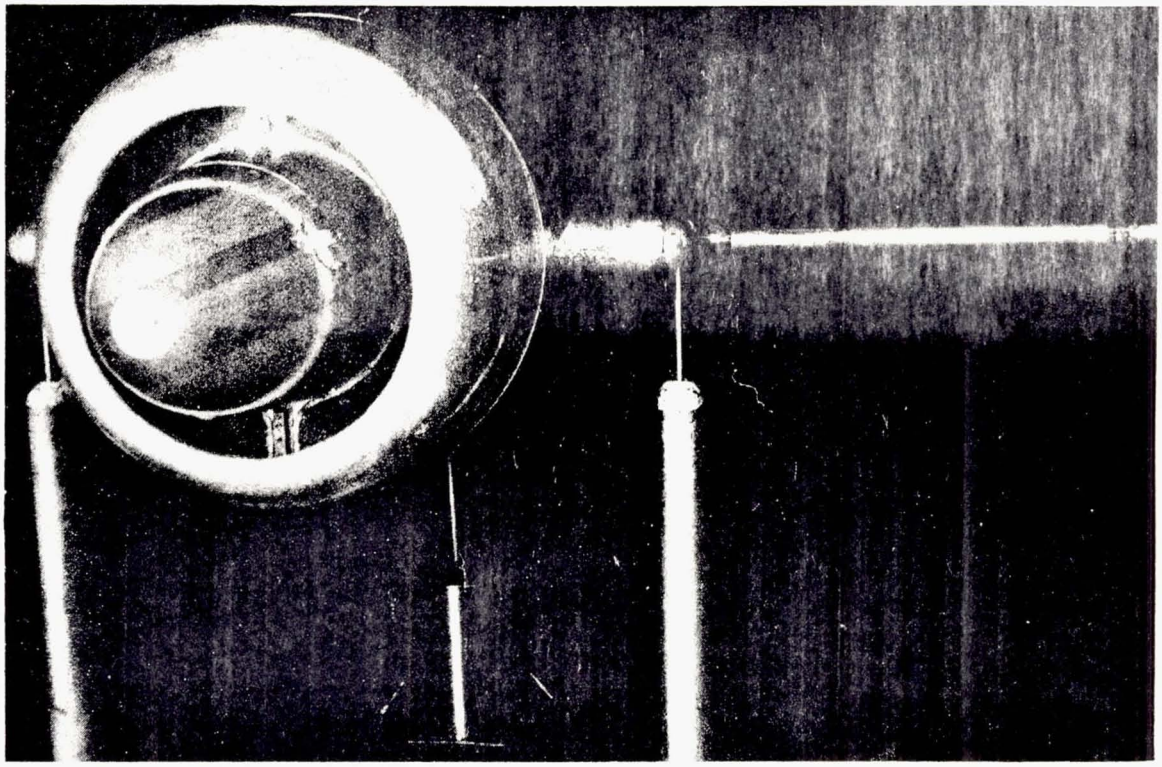

Figure 2.- Typical set-up in tunnel. Air flow through model.

THE GENERAL ARRANGEMENT OF TEST NACELLE
(MODEL SHOWN ON TUNNEL BALANCE SUPPORTS)

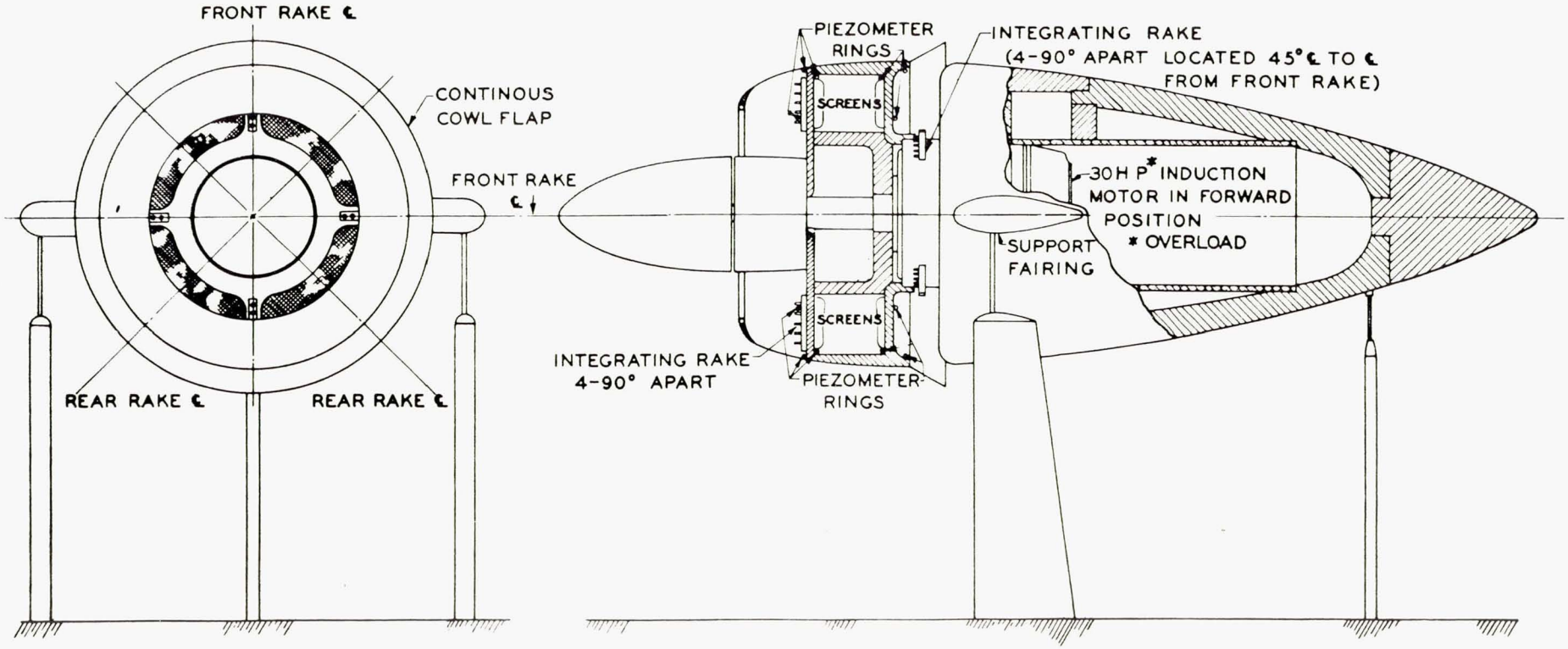

FIGURE 3

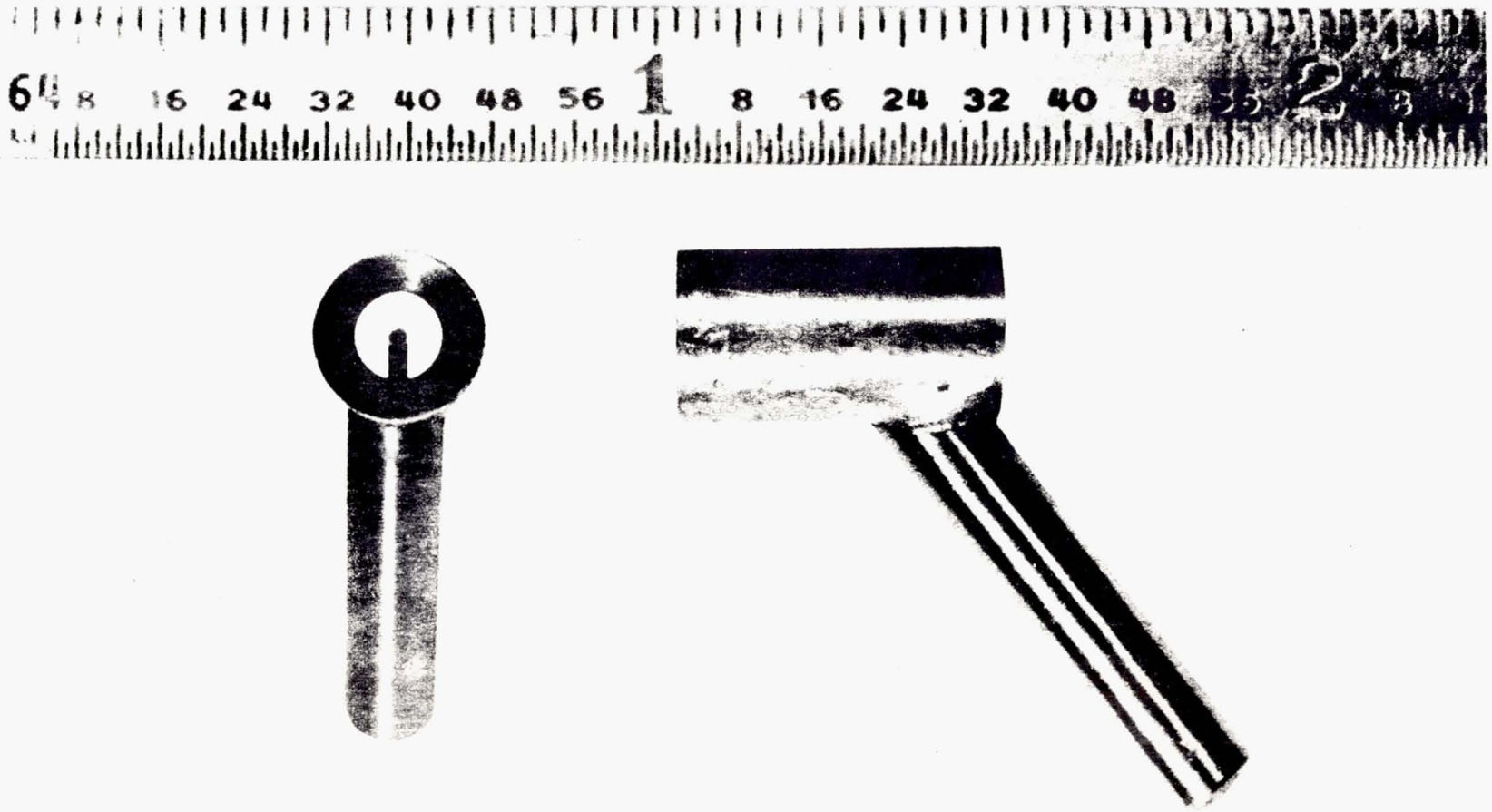

Figure 4.-Shielded total-head tube of Boeing design.

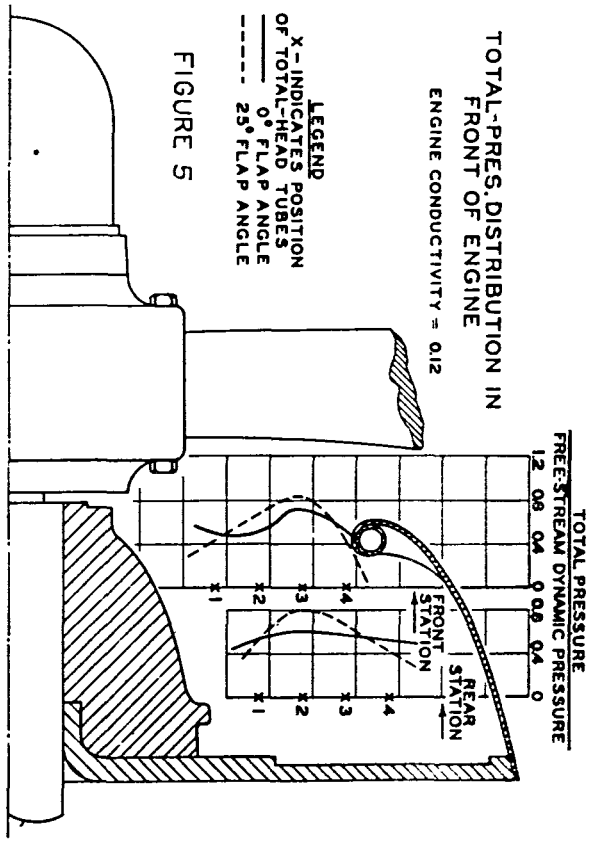

FIGURE 5

COMPARISON OF DRAG COEFFICIENTS IN THE TRANSITION FROM STREAMLINE BODY TO NACELLE WITH AIR FLOW

EFFECTIVE REYNOLDS NUMBER = 3×10^6
(BASED ON MAXIMUM DIAMETER)

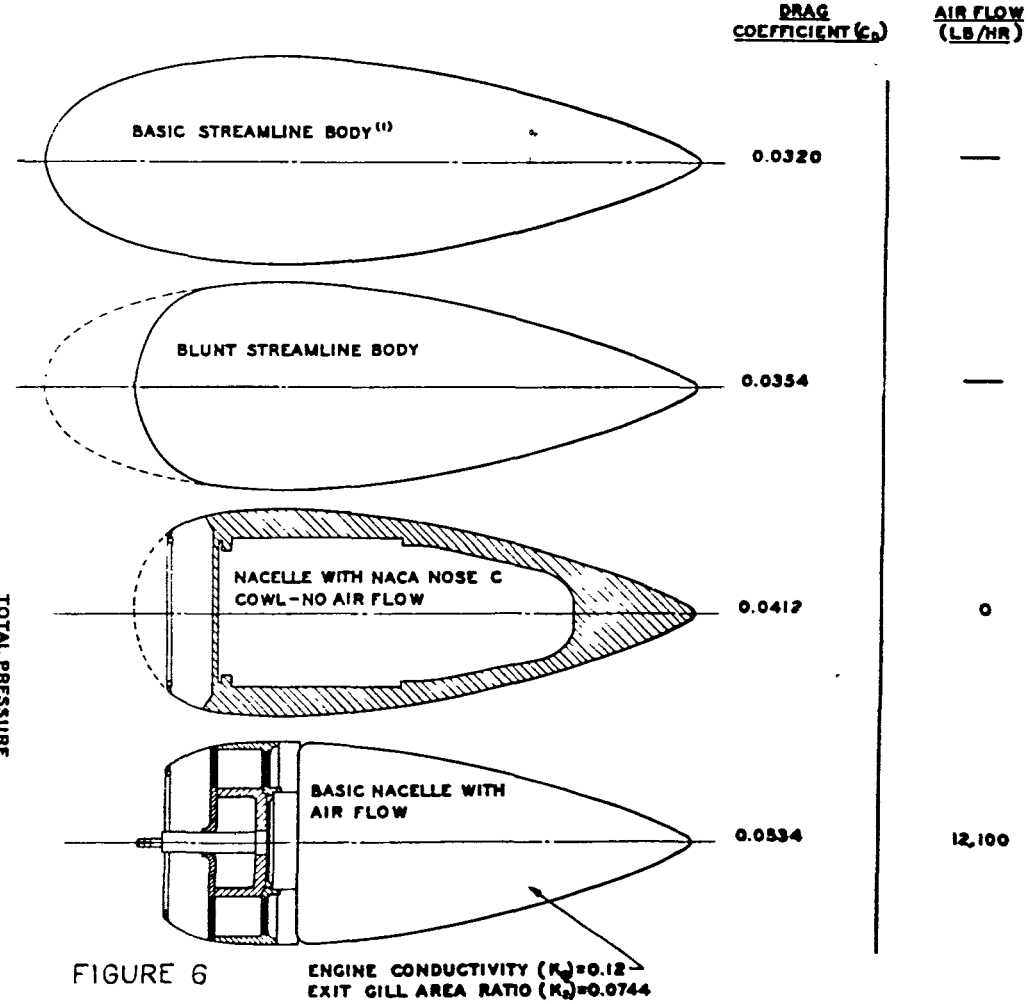

FIGURE 6

(1) EQUATION OF BASIC STREAMLINE BODY (F.R. = 3.25) IS $\pm y = \pm(3.9008x^{\frac{1}{2}} - .03715x^{\frac{3}{2}})$ BASED ON 105 PERCENT OF LENGTH. REAR 5% FAIRED TO ROUNDED TIP

Figure 7

THE EFFECT OF MASS FLOW AND CONDUCTIVITY ON NACELLE DRAG COEFFICIENT

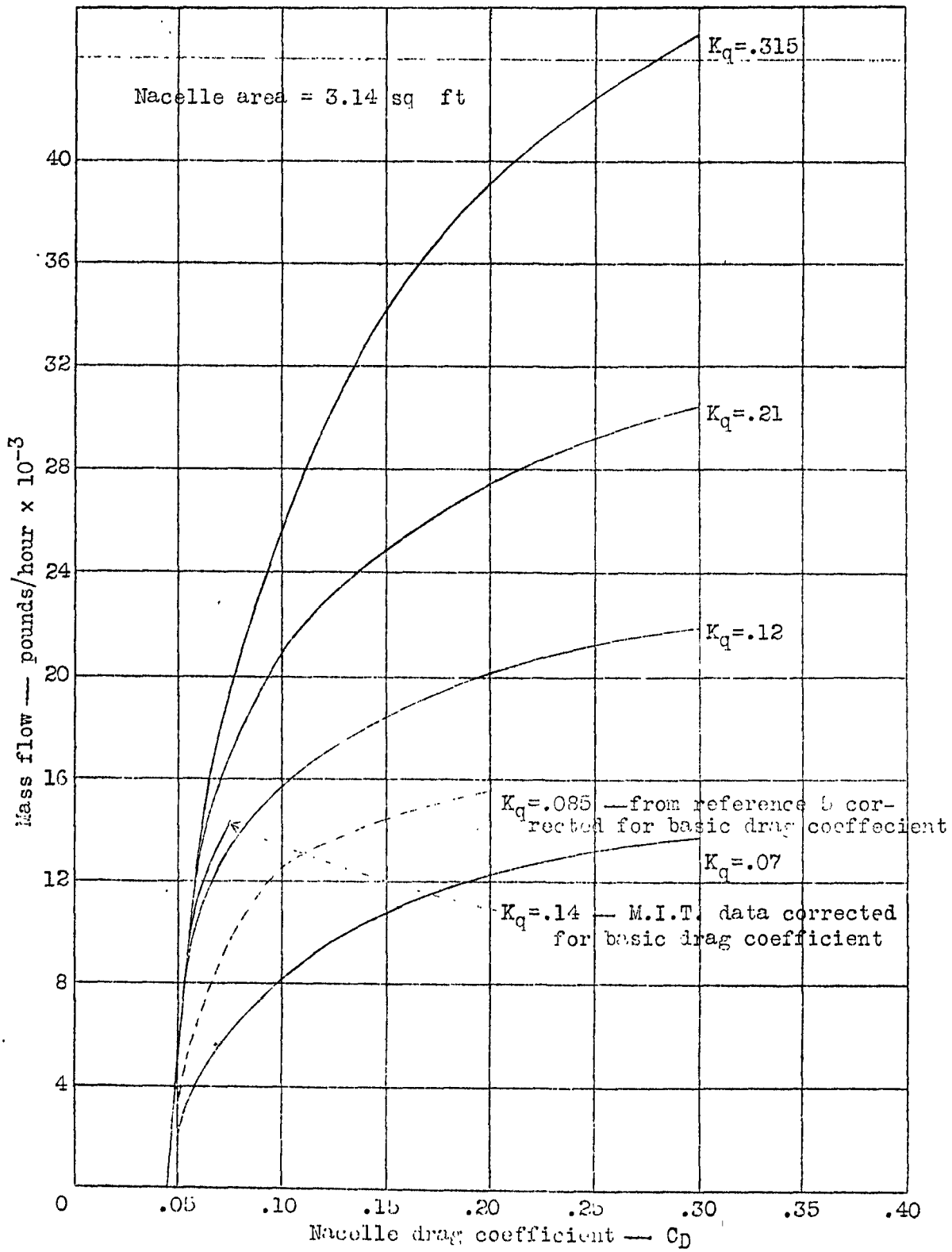

Figure 8
EFFECT OF CONTINUOUS COWL FLAPS ON ENGINE PRESSURE DROP
q=11.1 in. H_2O

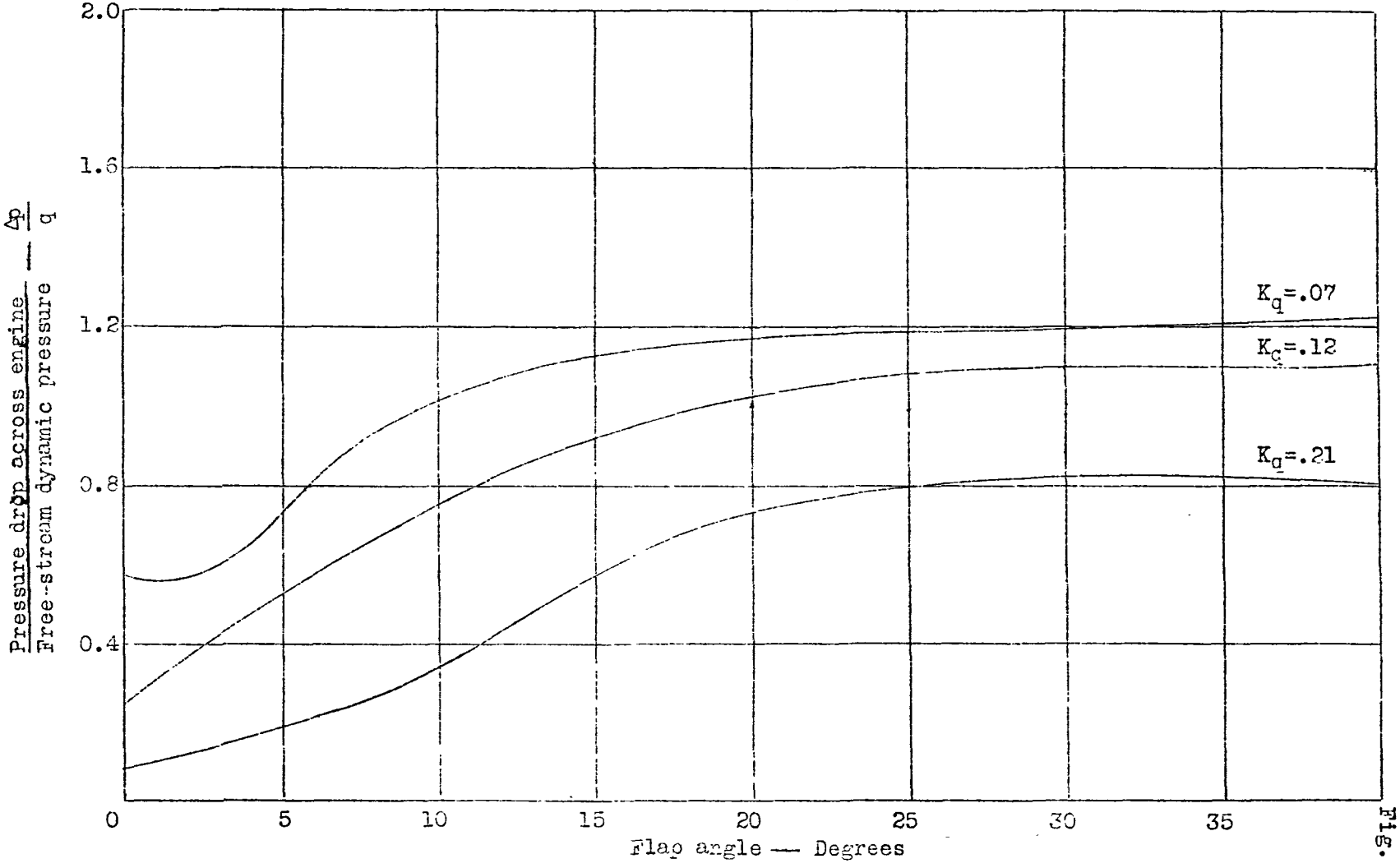

Figure 9

COMPARISON OF COWL FLAPS AND SHORTENED SKIRTS

Engine conductivity = 0.12
q = 11.1 in. H_2O

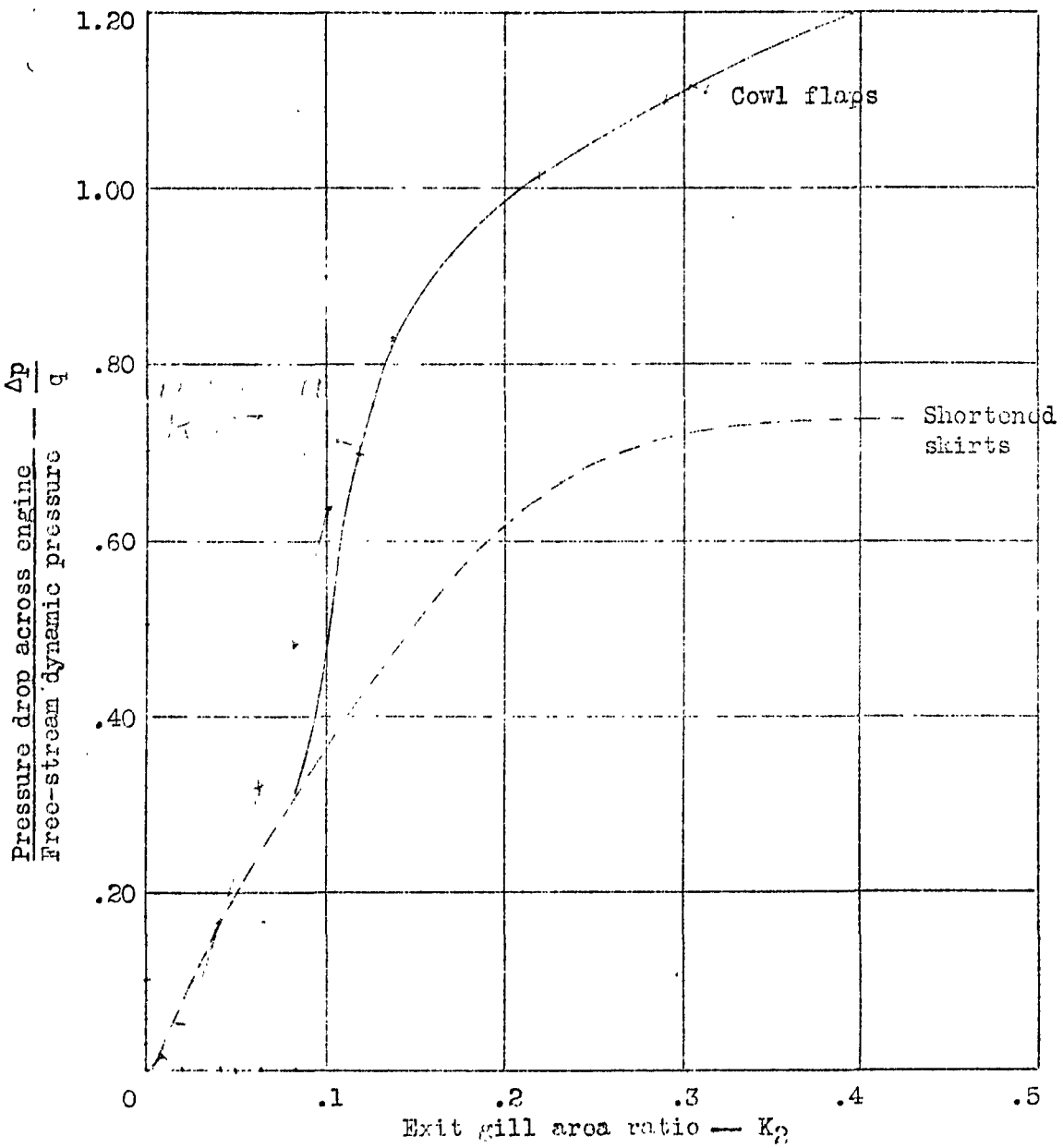

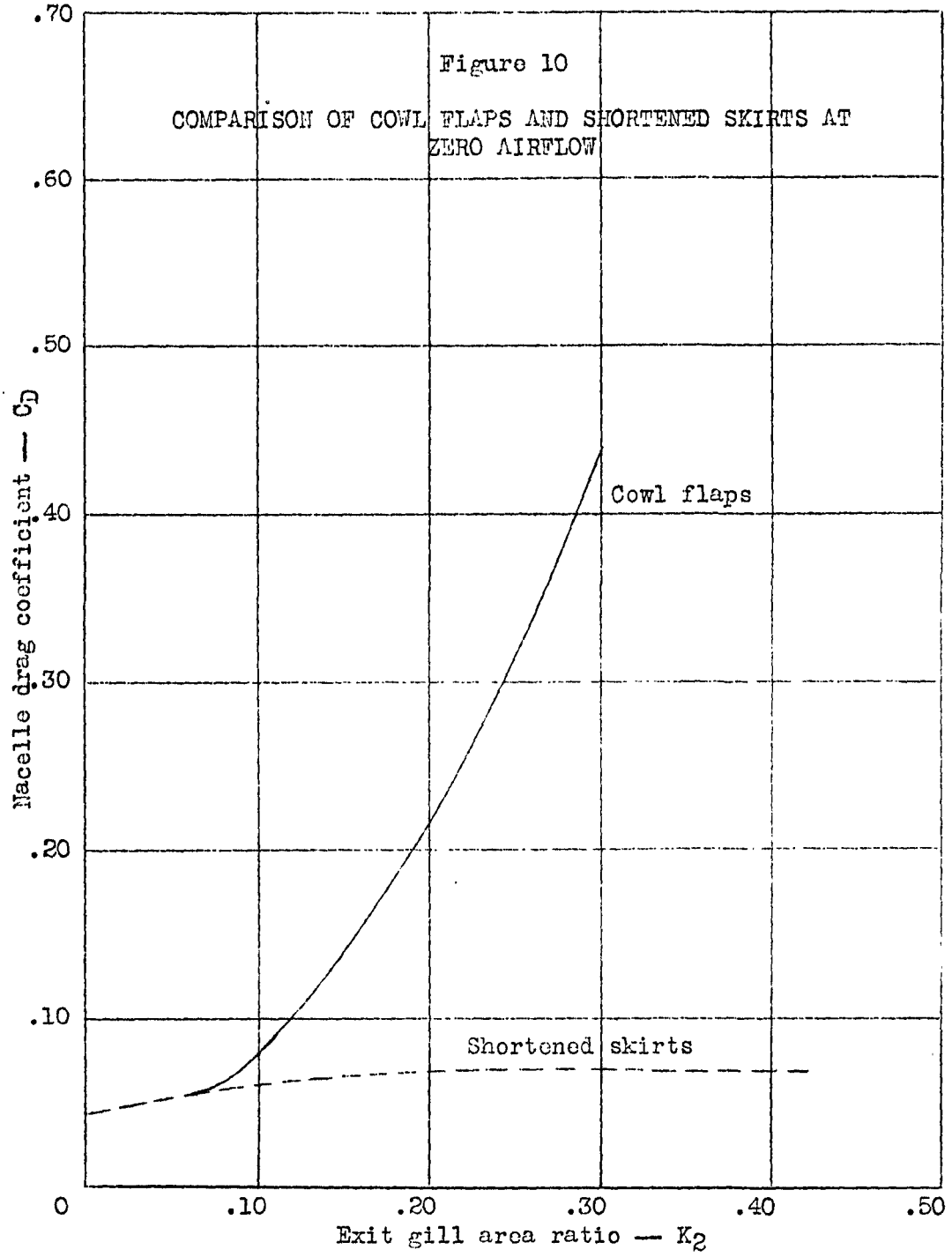
Figure 10
COMPARISON OF COWL FLAPS AND SHORTENED SKIRTS AT ZERO AIRFLOW
Cowl flaps
Shortened skirts
Nacelle drag coefficient — C_D
Exit gill area ratio — K_2
.70
.60
.50
.40
.30
.20
.10
0
.10
.20
.30
.40
.50

Figure 11 COMPARISON OF COWL FLAPS AND SHORTENED SKIRTS WITH AIRFLOW

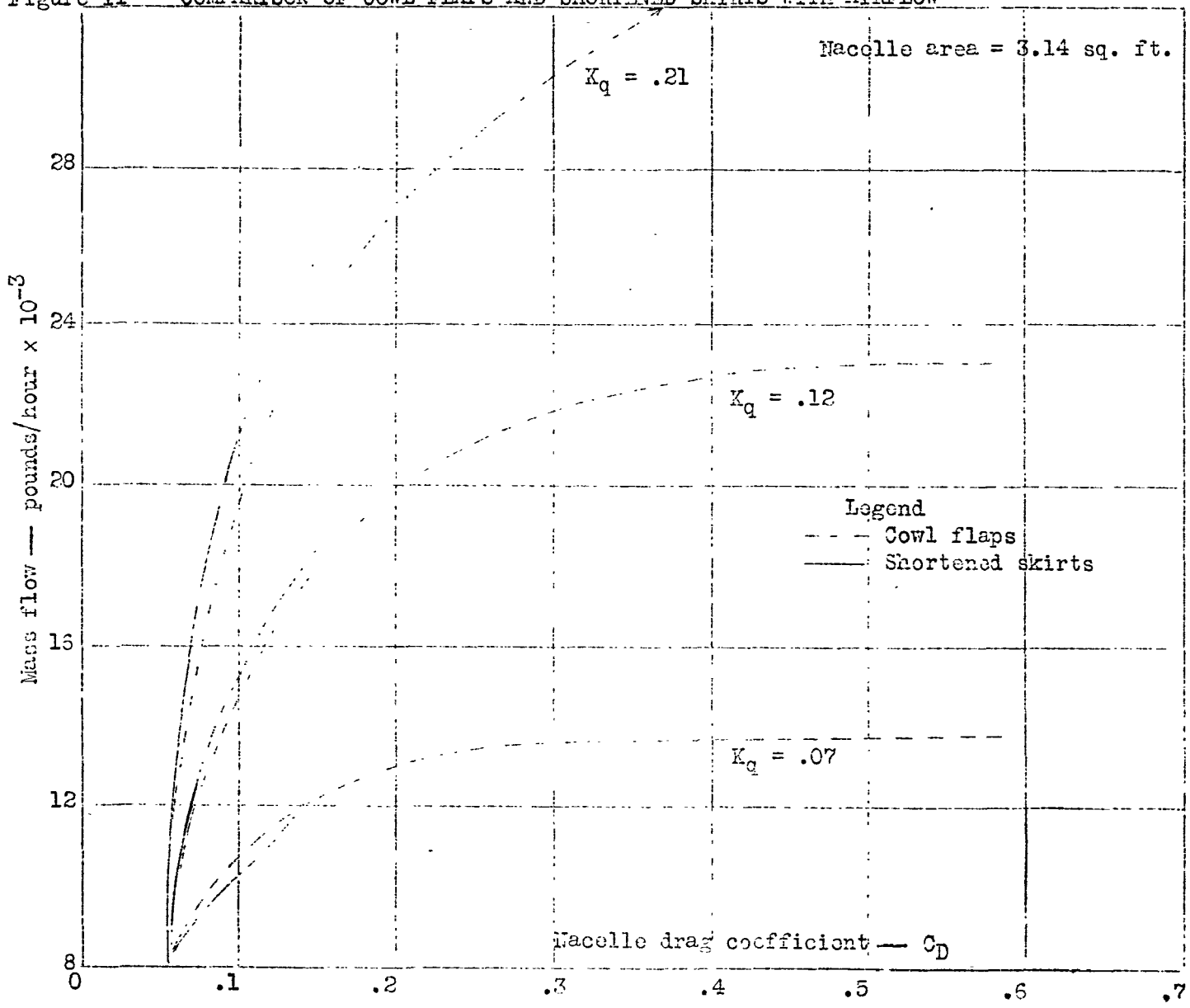

FLAP POSITIONS FOR BASIC NACELLE

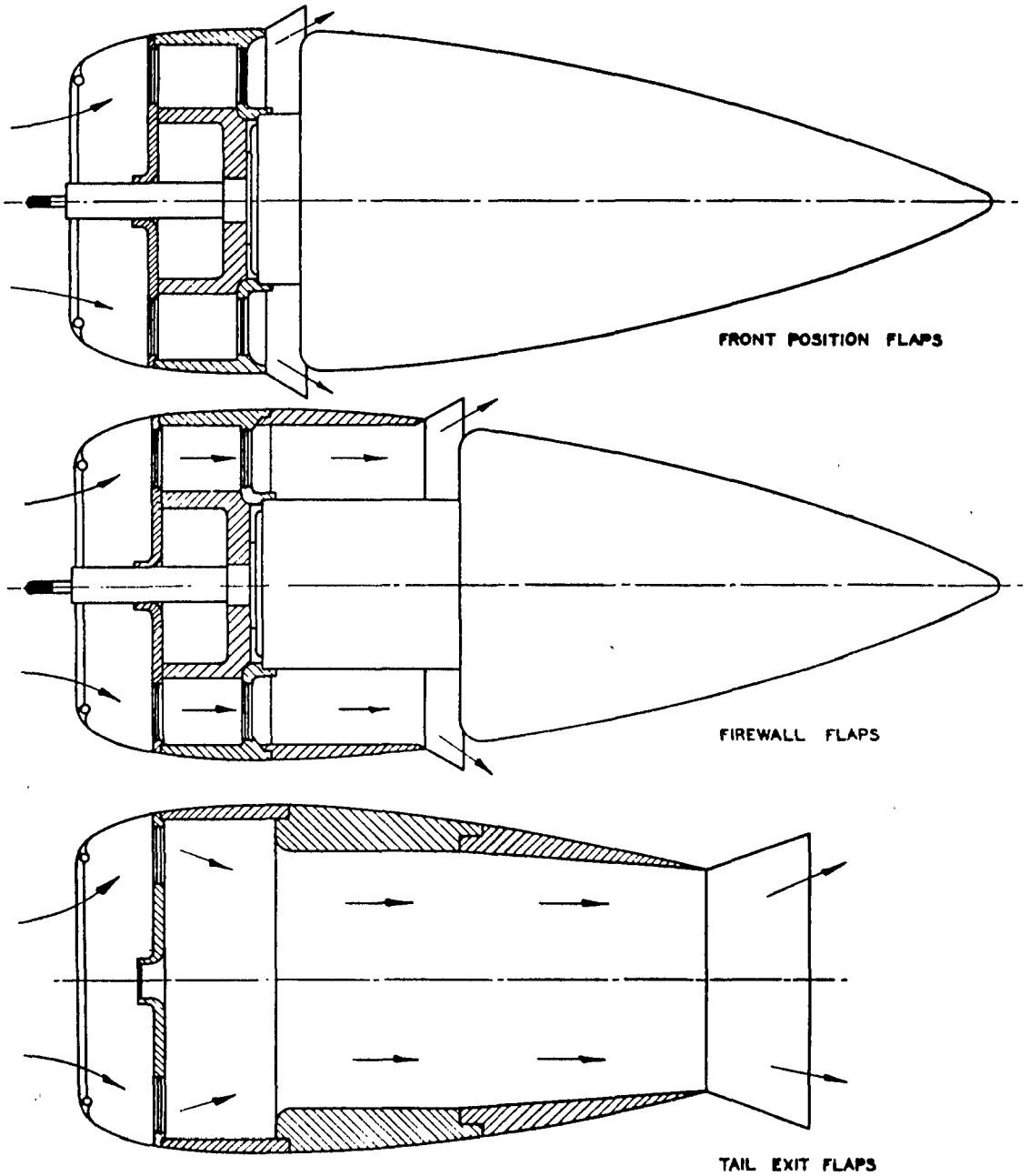

FIGURE 12

Figure 13

LOSS IN FLOW FOR TYPICAL NACELLE DUE TO REARWARD MOVEMENT OF HINGE POINT

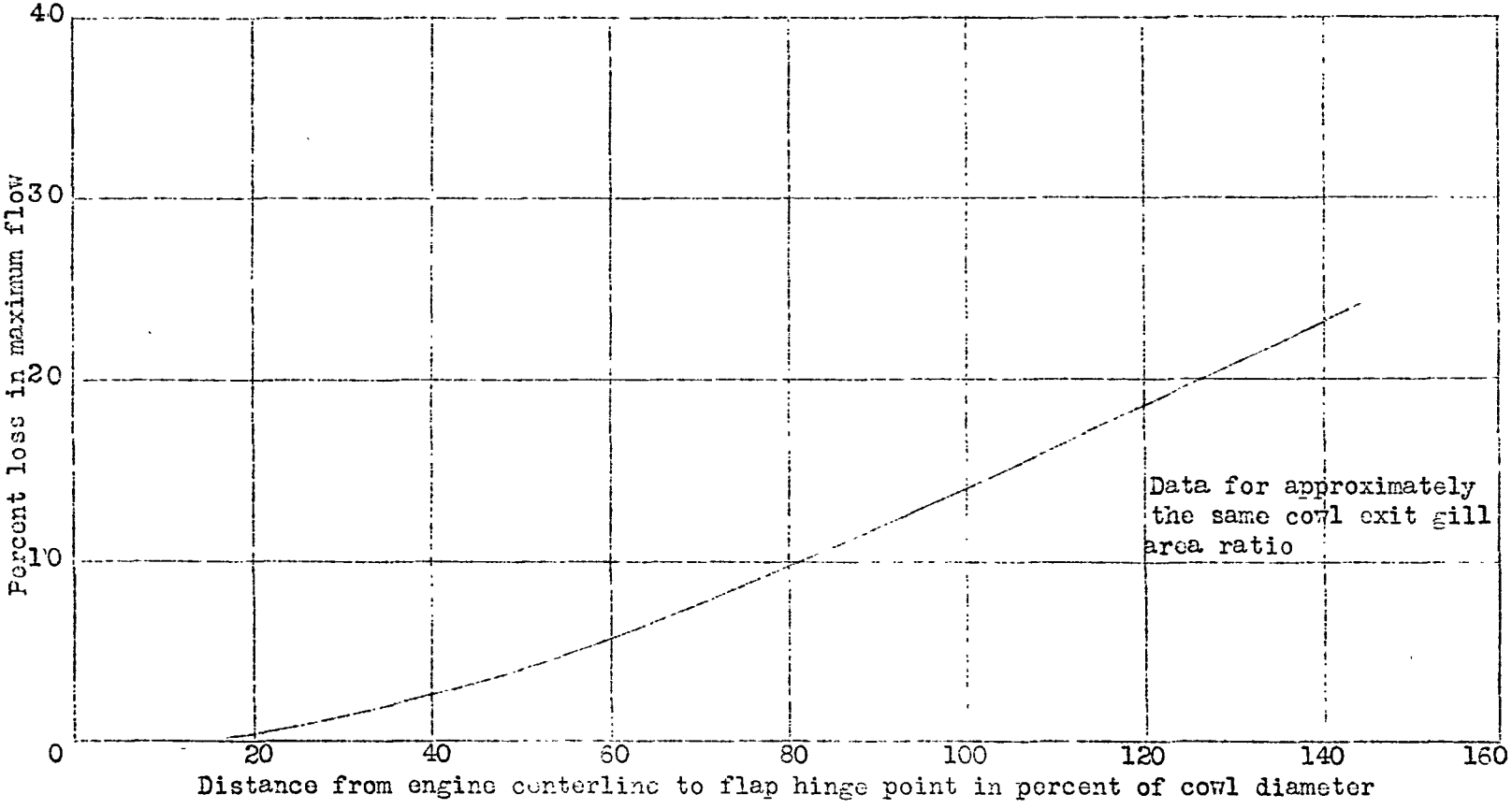

Figure 14

THE EFFECT OF FLAP POSITION ON MASS FLOW

Engine conductivity -- 0.07

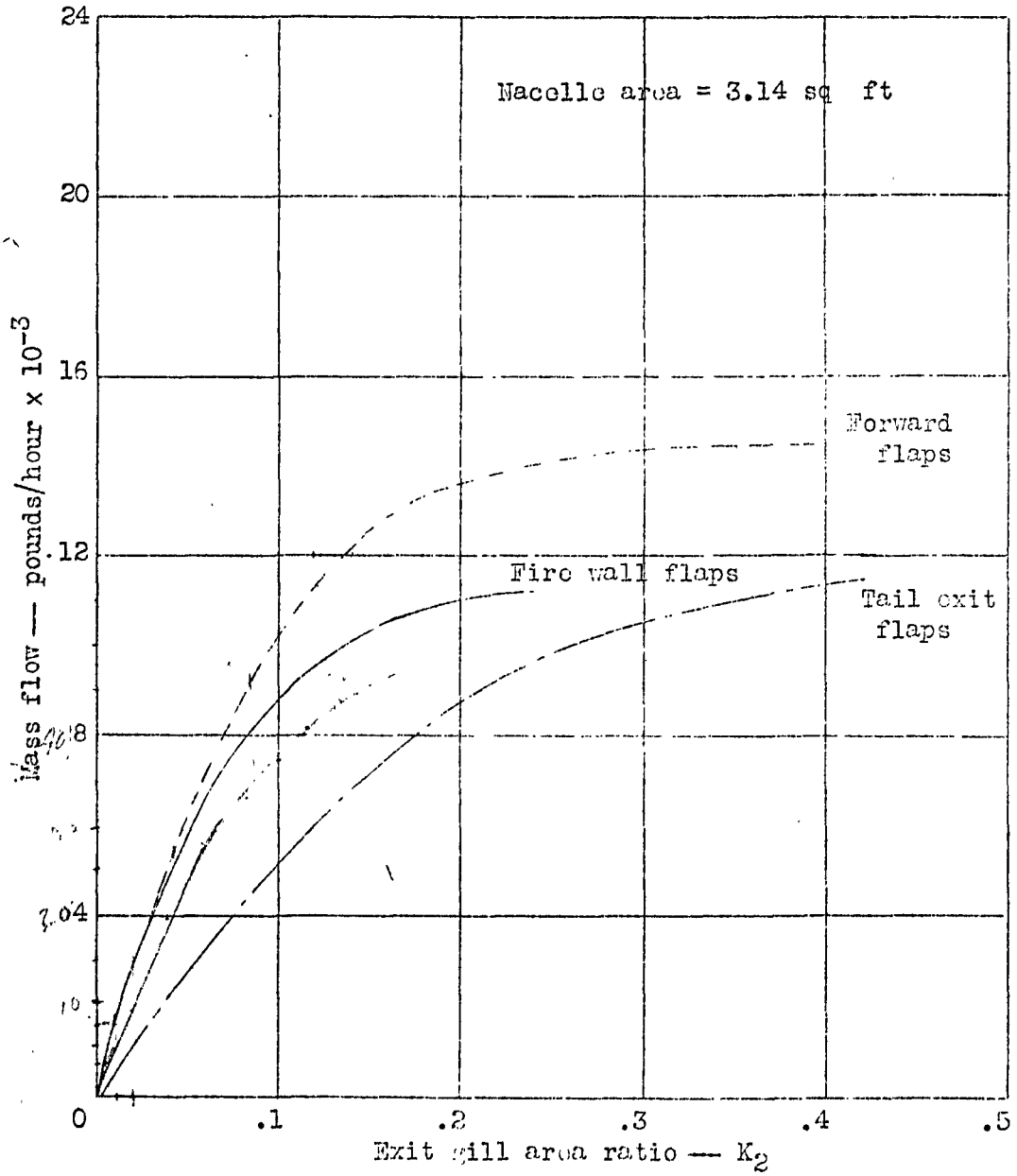

EFFECT OF FLAP POSITION ON NACELLE DRAG COEFFICIENT

(NOTE: DIRECT COMPARISON OF THESE TWO PLOTS SHOULD NOT BE MADE AS THEY ARE FOR TWO DIFFERENT CONFIGURATIONS)

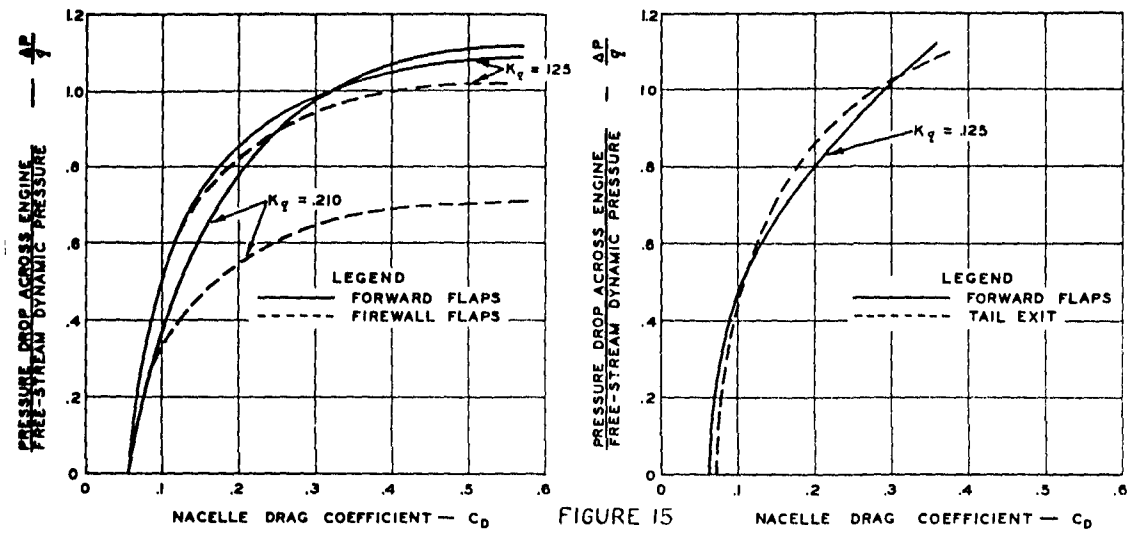

FIGURE 15

VARIATION OF PRESSURE RECOVERY WITH MASS FLOW AND ENGINE CONDUCTIVITY

BASED ON AIRSPEED OF 150 MPH

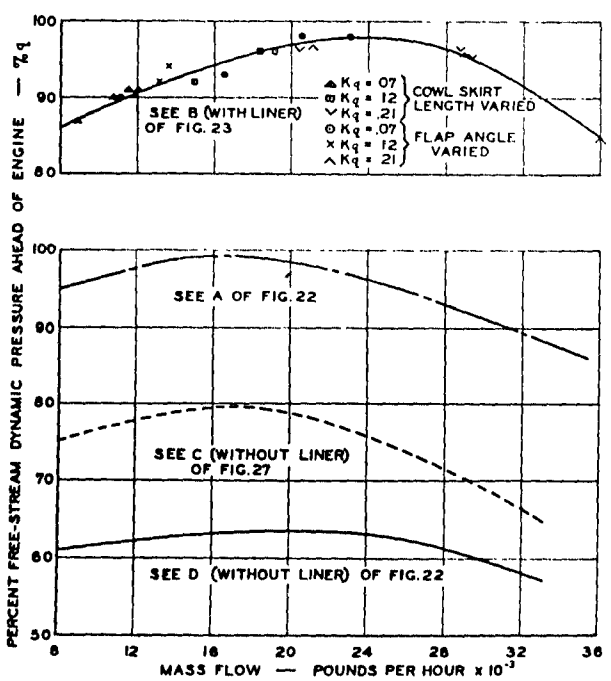

FIGURE 16a

VARIATION OF PRESSURE RECOVERY WITH COOLING AIRFLOW AND AIRSPEED

ANGLE OF ATTACK = 0 DEGREES

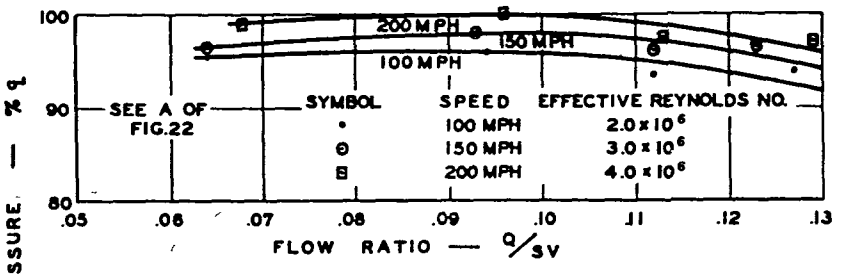

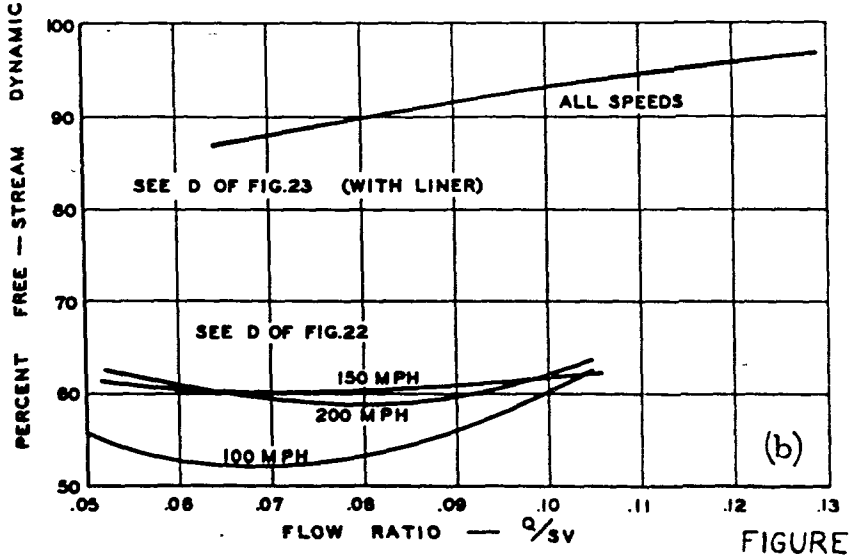

VARIATION OF PRESSURE RECOVERY WITH COOLING AIRFLOW AND AIRSPEED

ANGLE OF ATTACK = 4 DEGREES

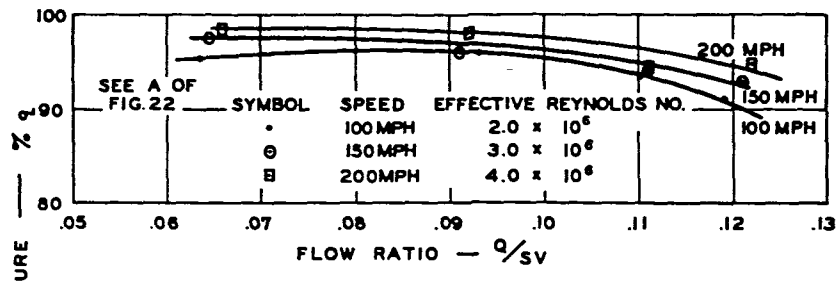

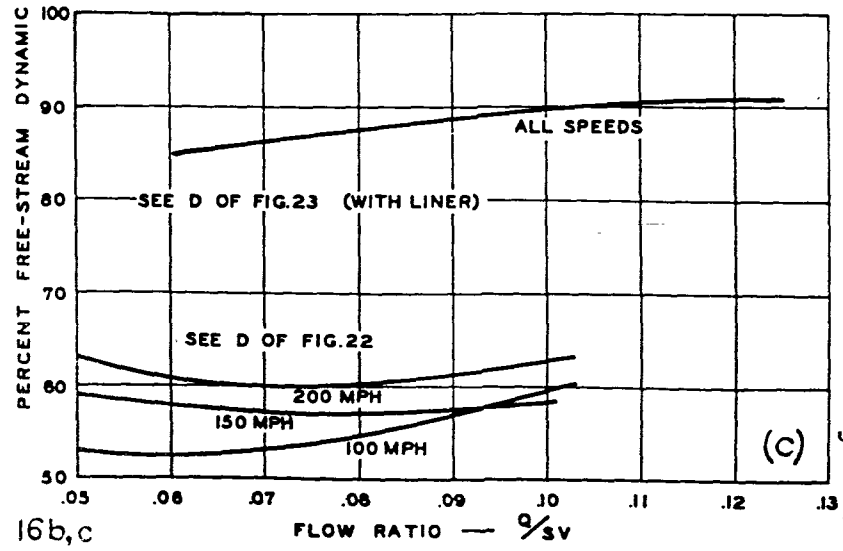

FIGURE 16b,c

Figure 17
COMPARISON OF PRESSURE RECOVERY IN FRONT OF TOP AND BOTTOM CYLINDERS WITH A CHANGE IN ANGLE OF ATTACK

Nacelle with spinner
Engine conductivity = 0.12
q = 11.1 in. H_2O

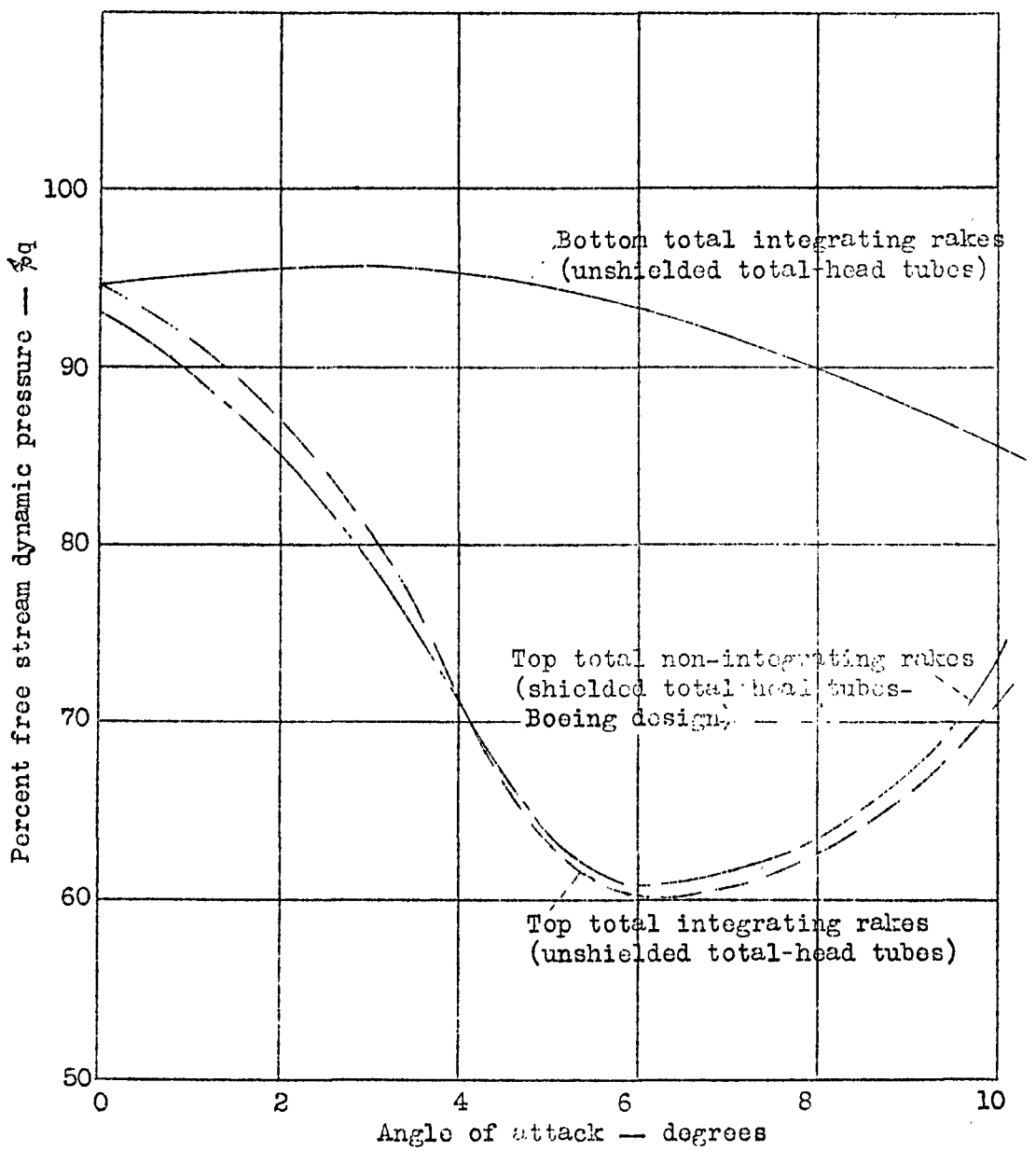

Figure 18

THE EFFECT OF PRESSURE RECOVERY ON NACELLE DRAG AT A GIVEN FLOW

Mass flow = 17,000 pounds/hour
Engine conductivity = 0.12
q = 57.6 lb /sq ft

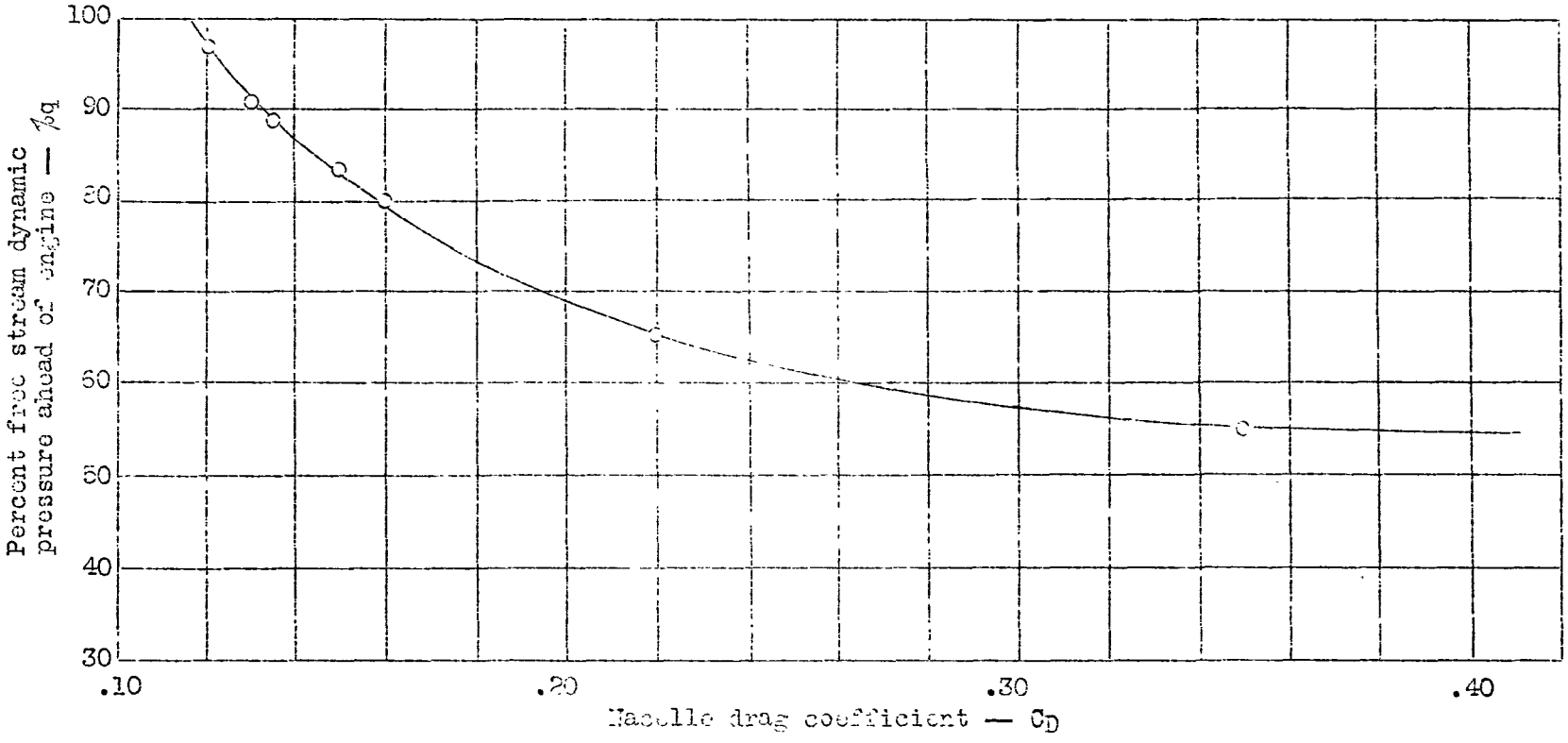

Figure 19

THE EFFECT OF PRESSURE RECOVERY ON NACELLE DRAG AT VARIOUS AIRFLOWS

Engine conductivity = 0.12
q = 57.6 lb /sq ft

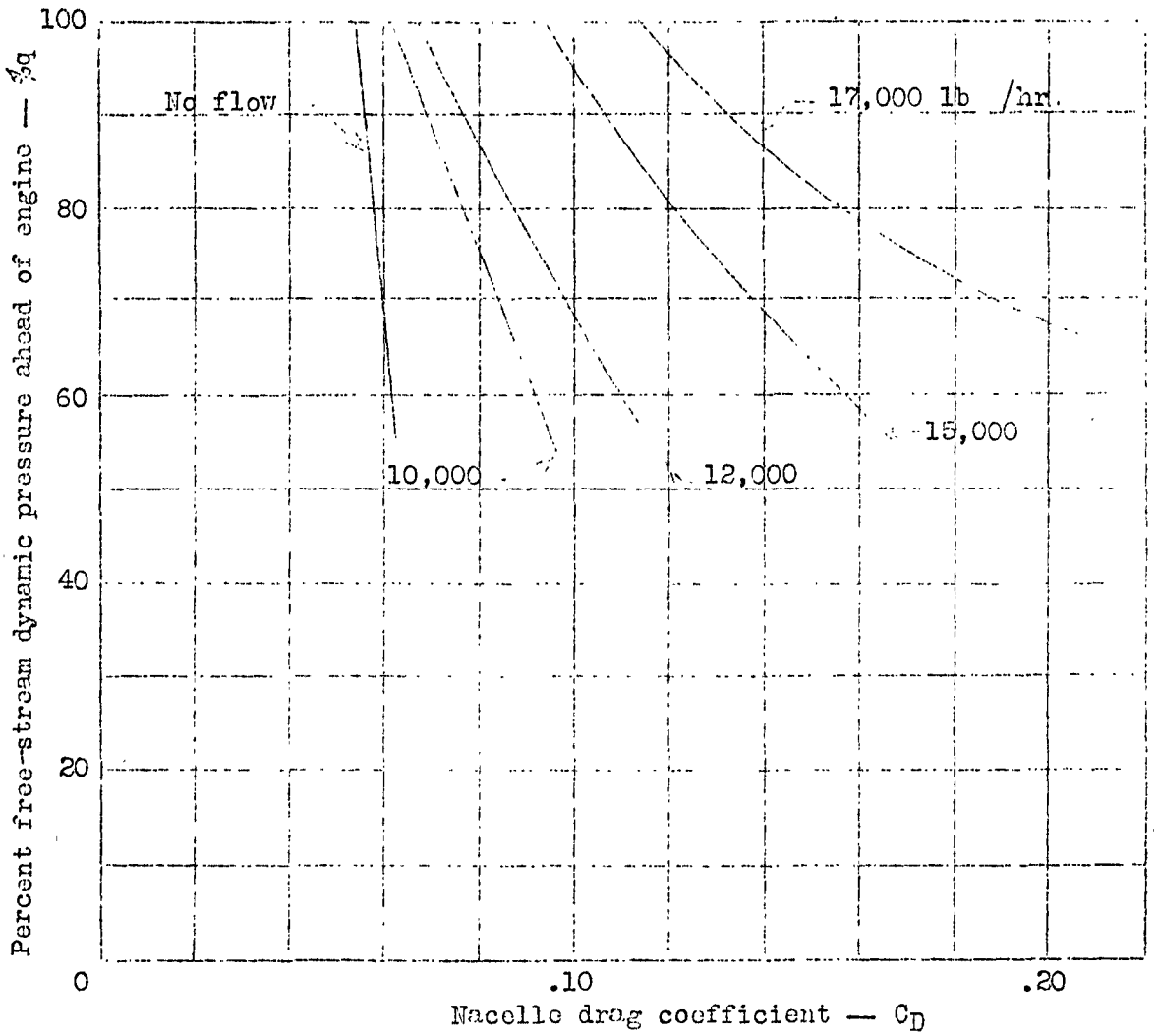

Figure 20

THE EFFECT OF PRESSURE RECOVERY AND CONDUCTIVITY ON NACELLE DRAG COEFFICIENT AT A GIVEN MASS FLOW

Mass flow = 12,000 pounds/hour

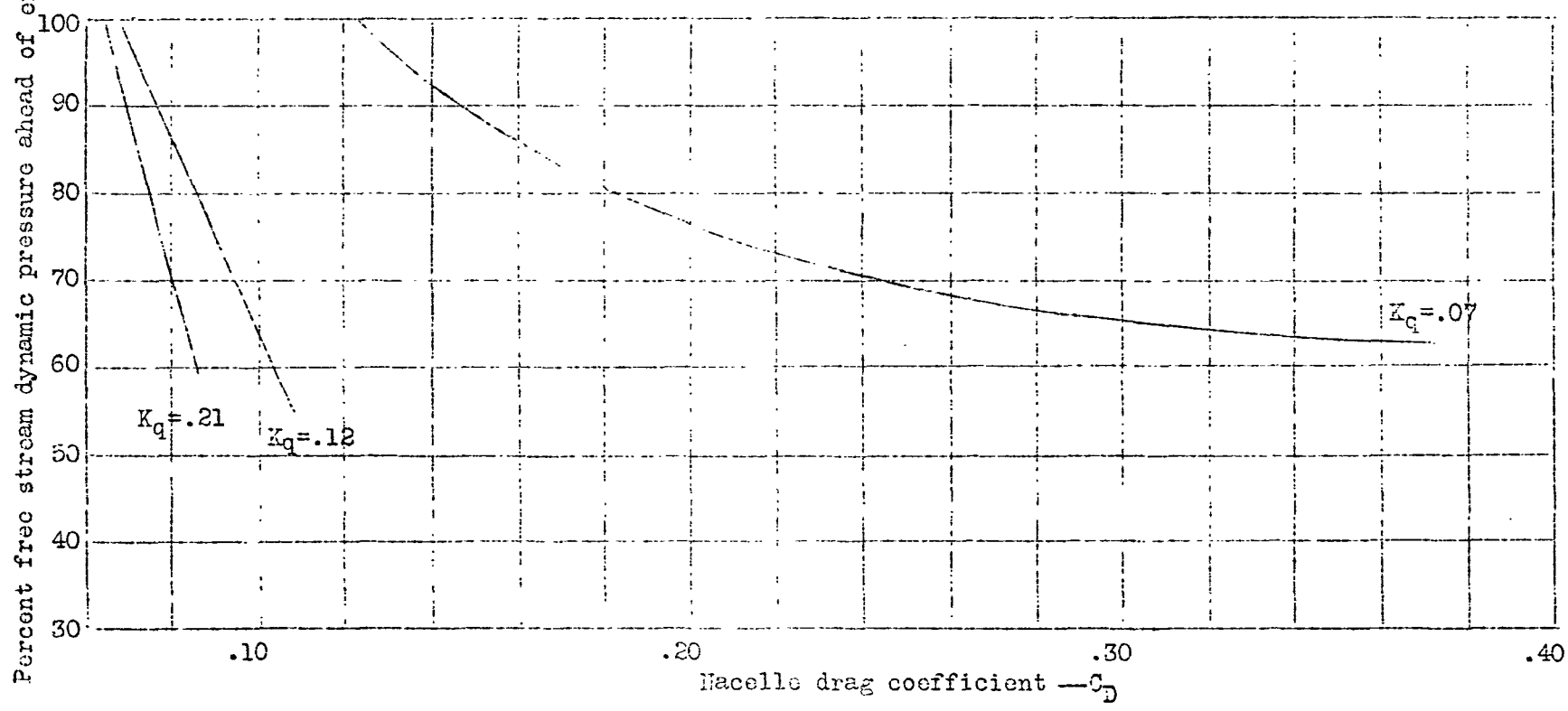

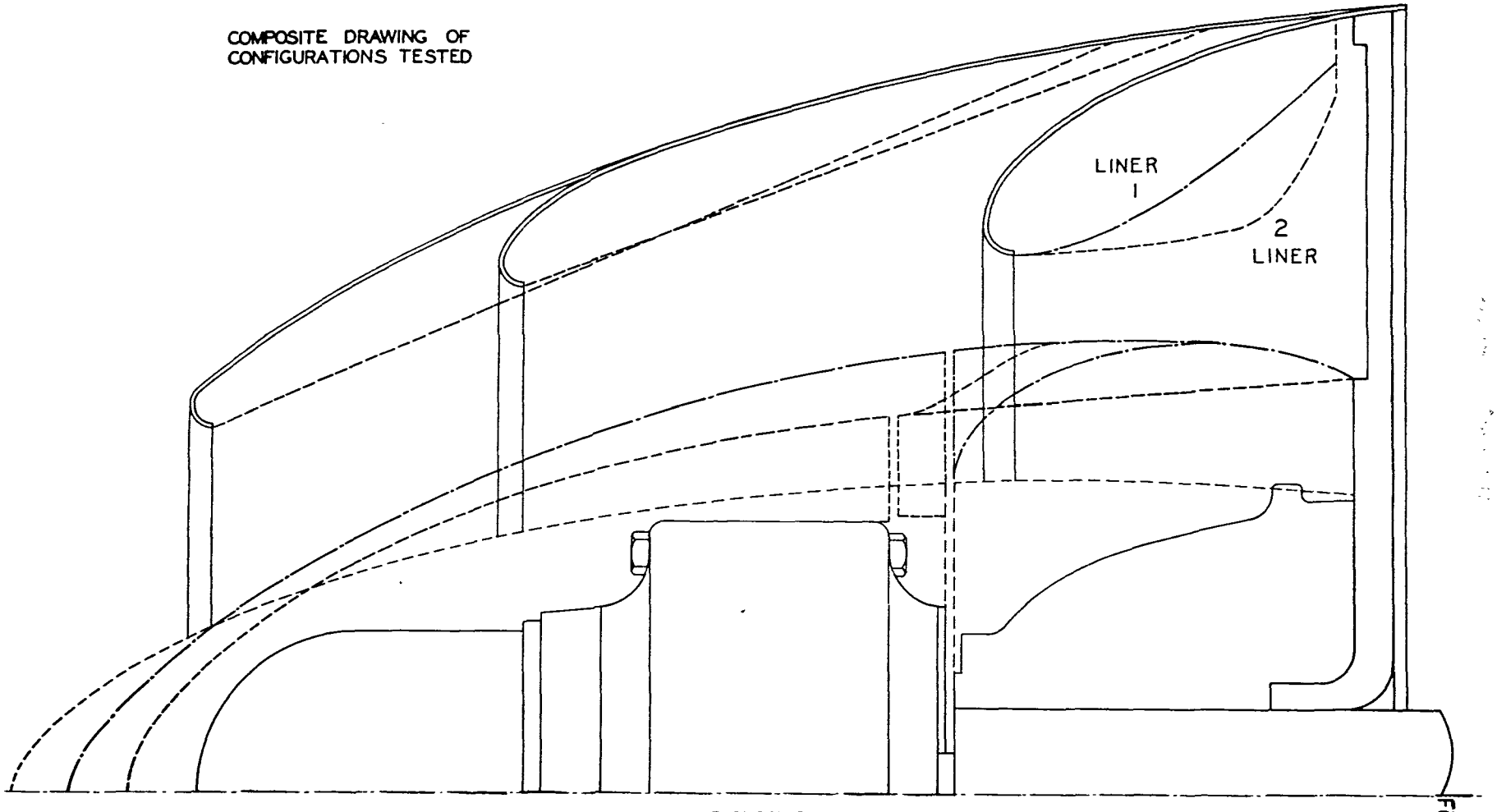
COMPOSITE DRAWING OF
CONFIGURATIONS TESTED
LINER
1
2
LINER

FIGURE 21

MEANS OF IMPROVING PRESSURE RECOVERY AND DRAG
—PROPELLER HUBS—

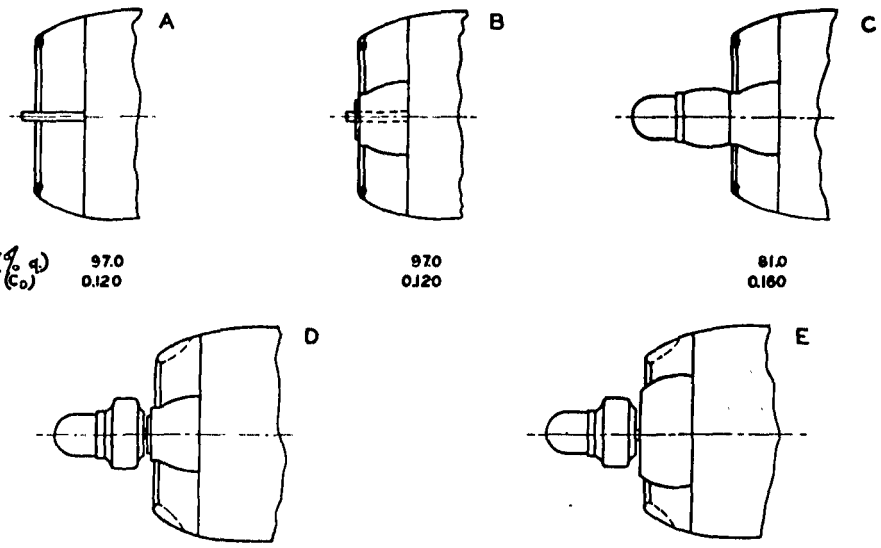

	A	B	C
PRESSURE RECOVERY (% q)	97.0	97.0	81.0
NACELLE DRAG COEFF. (C_D)	0.120	0.120	0.160

	D WITHOUT LINER	D WITH LINER	E WITHOUT LINER	E WITH LINER
PRESSURE RECOVERY (% q)	57.0	73.0	65.5	82.0
NACELLE DRAG COEFF. (C_D)	0.210	0.165	0.220	0.145

FIGURE 22

ALL DRAG COEFFICIENTS AND PERCENT FREE-STREAM DYNAMIC PRESSURES QUOTED AT FOLLOWING CONDITIONS:

ENGINE CONDUCTIVITY = 0.12 TUNNEL SPEED = 150 MPH
ANGLE OF ATTACK = 0 DEG FLAP ANGLE = 0 DEG
AIR FLOW = 17,000 LB/HR (FLAP SKIRT LENGTH VARIED)

MEANS OF IMPROVING PRESSURE RECOVERY AND DRAG
—PROPELLER SPINNERS—

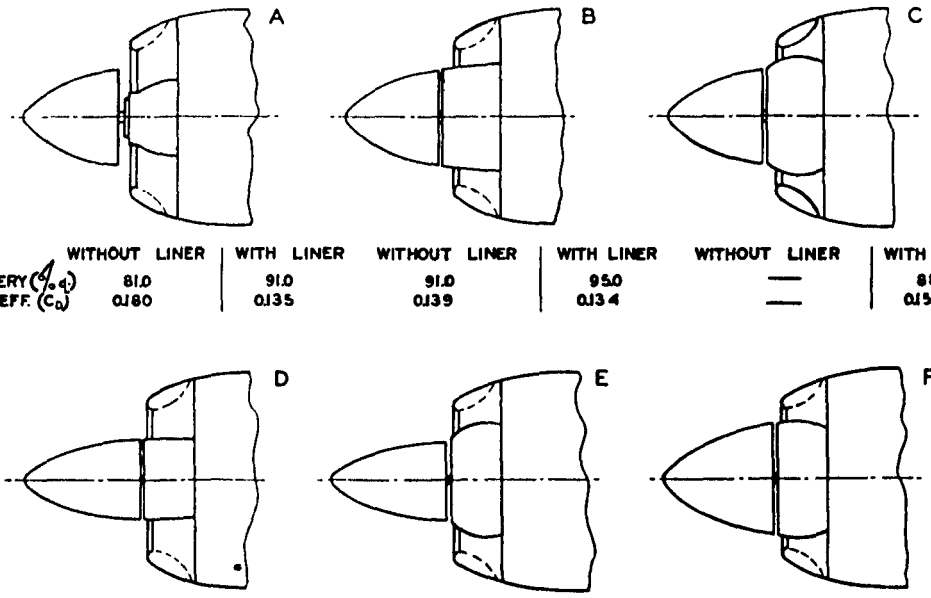

	A WITHOUT LINER	A WITH LINER	B WITHOUT LINER	B WITH LINER	C WITHOUT LINER	C WITH LINER
PRESSURE RECOVERY (% q)	81.0	91.0	91.0	95.0	—	88.0
NACELLE DRAG COEFF. (C_D)	0.180	0.135	0.139	0.134	—	0.150

	D WITHOUT LINER	D WITH LINER	E WITHOUT LINER	E WITH LINER	F WITHOUT LINER	F WITH LINER
PRESSURE RECOVERY (% q)	84.0	86.0	89.0	91.0	54.5	77.0
NACELLE DRAG COEFF. (C_D)	0.150	0.140	0.135	0.137	0.350	0.180

FIGURE 23

THE EFFECT OF OBJECTS PROTRUDING FROM THE COWL ENTRANCE ON PRESSURE RECOVERY AND DRAG COEFFICIENT

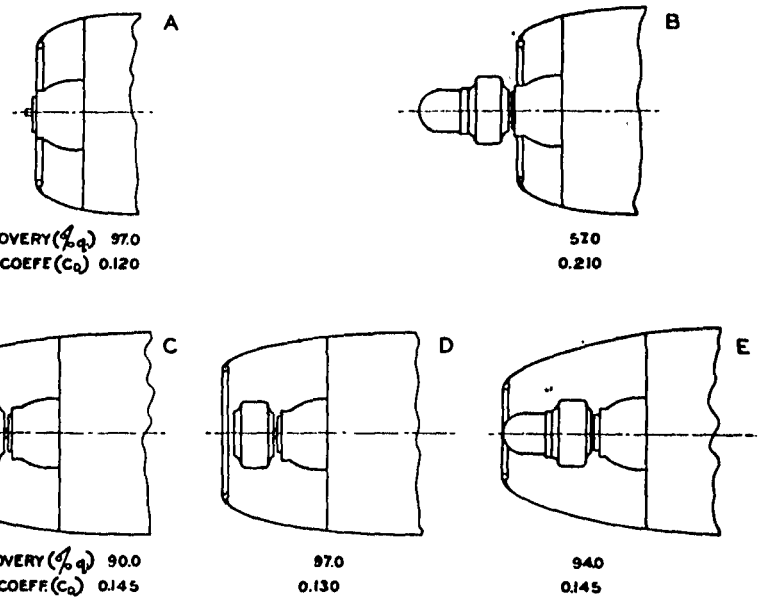

	A	B	C	D	E
PRESSURE RECOVERY ($\%q$)	97.0	57.0	90.0	97.0	94.0
NACELLE DRAG COEFF (C_D)	0.120	0.210	0.145	0.130	0.145

FIG. 24

TEST CONDITIONS

ENGINE CONDUCTIVITY = 0.12 TUNNEL SPEED = 150 MPH
ANGLE OF ATTACK = 0 DEG. FLAP ANGLE = 0 DEG
AIR FLOW = 17,000 LB/HR (FLAP SKIRT LENGTH VARIED)

EFFECT OF PROPELLER AND PROPELLER CUFFS ON PRESSURE RECOVERY
– HYDROMATIC HUBS AND SPINNERS –

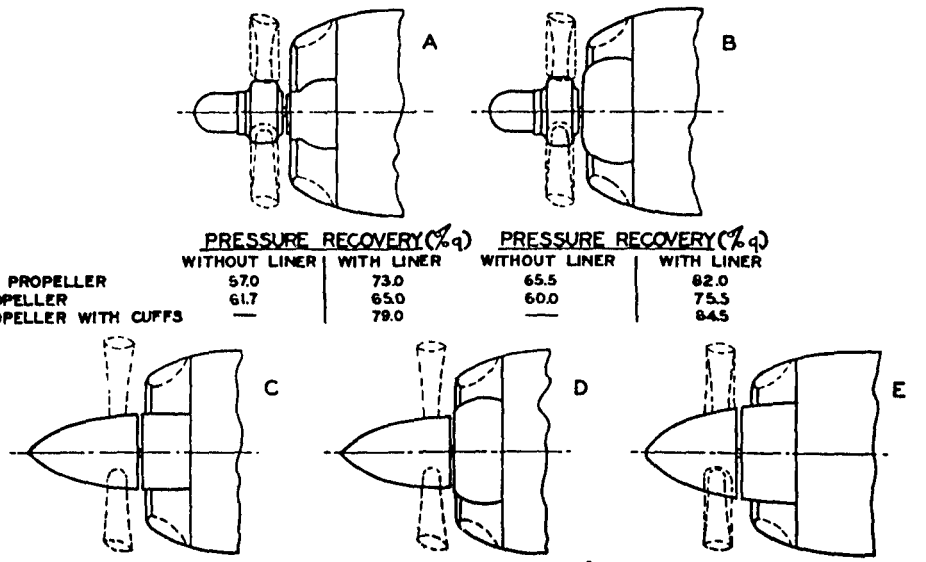

	A PRESSURE RECOVERY ($\%q$) WITHOUT LINER	A WITH LINER	B PRESSURE RECOVERY ($\%q$) WITHOUT LINER	B WITH LINER
NO PROPELLER	57.0	73.0	65.5	82.0
PROPELLER	61.7	65.0	60.0	75.5
PROPELLER WITH CUFFS	—	79.0	—	84.5

	C PRESSURE RECOVERY ($\%q$) WITHOUT LINER	C WITH LINER	D PRESSURE RECOVERY ($\%q$) WITHOUT LINER	D WITH LINER	E PRESSURE RECOVERY ($\%q$) WITHOUT LINER	E WITH LINER
NO PROPELLER	84.0	86.0	88.0	91.0	91.0	95.0
PROPELLER	77.5	79.0	—	81.0	—	89.5
PROP WITH CUFFS	—	—	—	—	—	83.0

FIG. 27

CONDITIONS OF TEST :– ENGINE CONDUCTIVITY = 0.12
TUNNEL SPEED = 150 MPH ANGLE OF ATTACK = 0 DEG
FLAP ANGLE = 0 DEG AIR FLOW = 17,000 LB/HR
(FLAP SKIRT LENGTH VARIED)

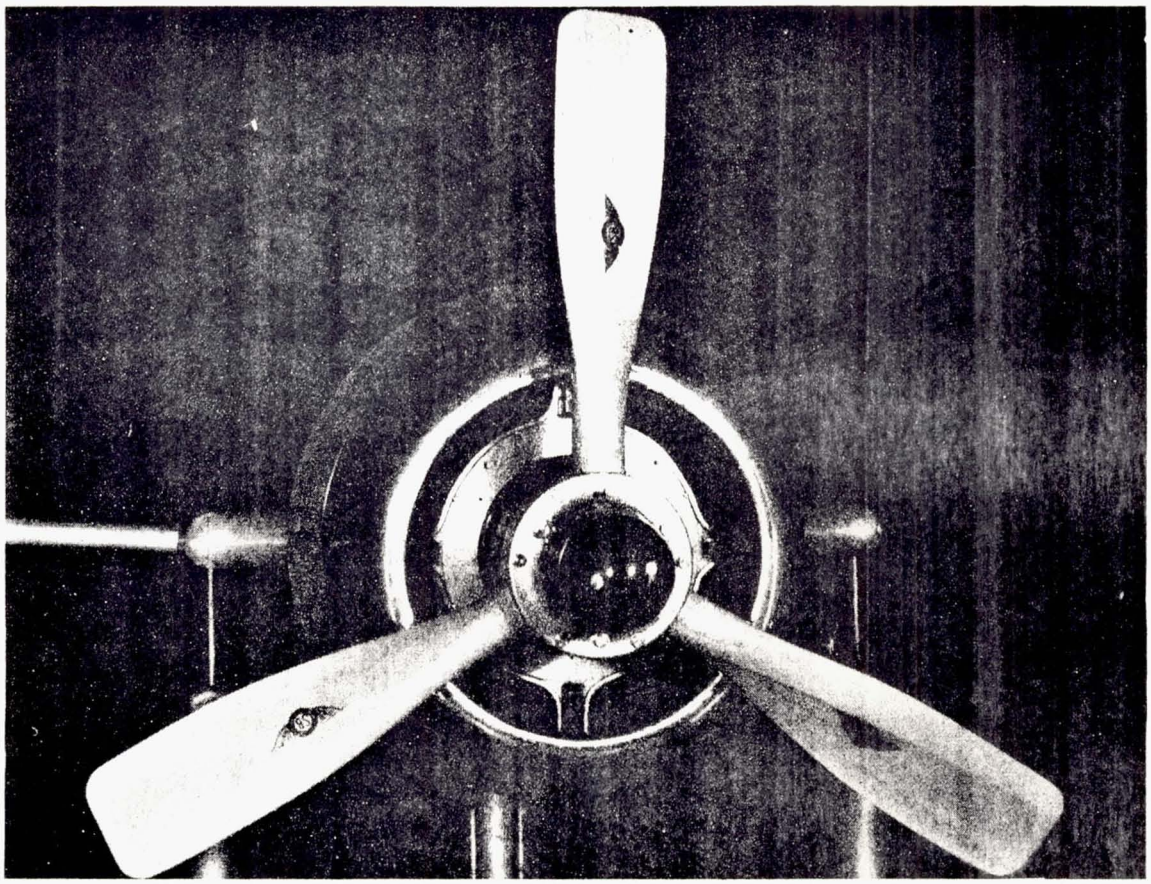

Figure 25.- Propeller-powered model in wind tunnel.

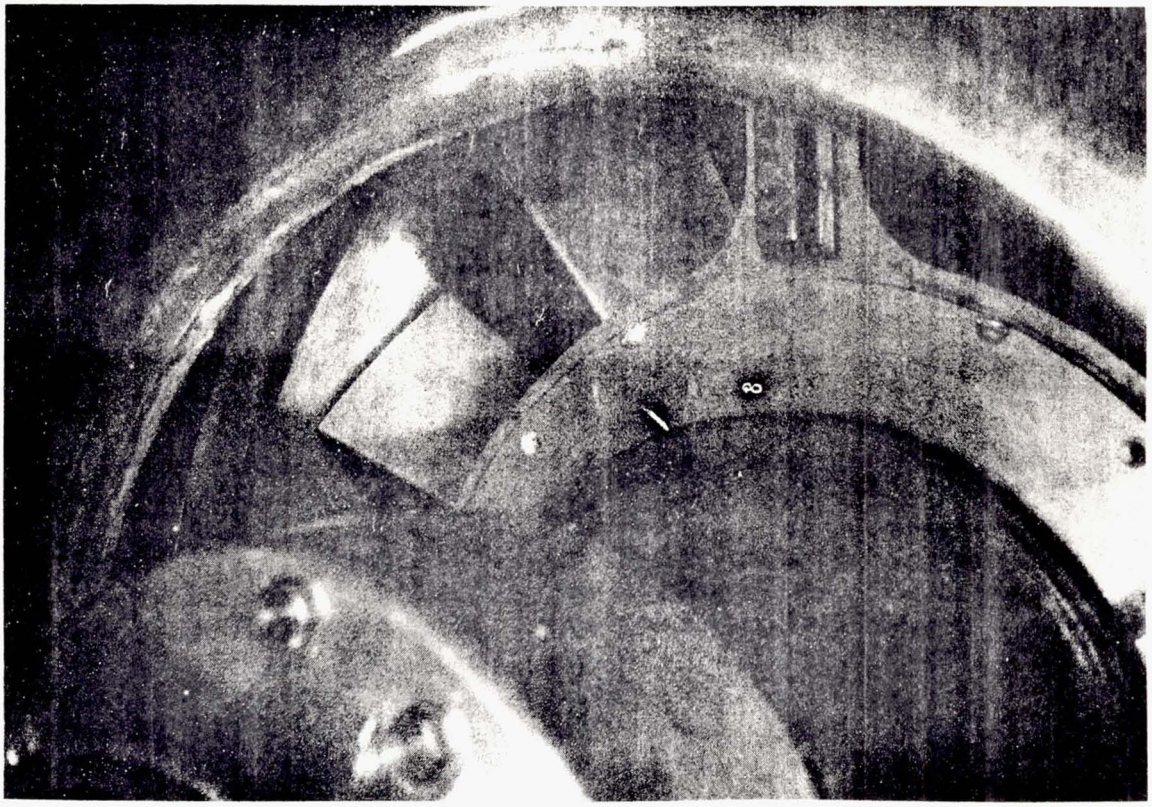

Figure 31.- Fan installation with front screens removed.

Figure 26

CHANGE IN PRESSURE RECOVERY AHEAD OF ENGINE CHARGEABLE TO PROPELLER

Engine conductivity = 0.12 Flap angle varied

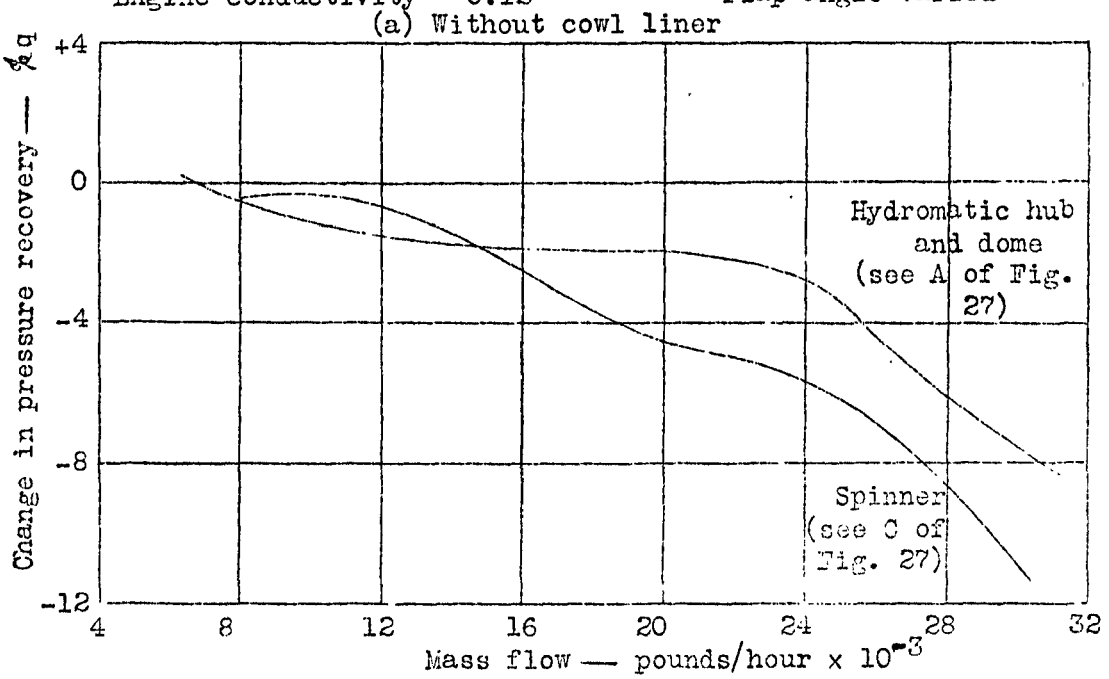

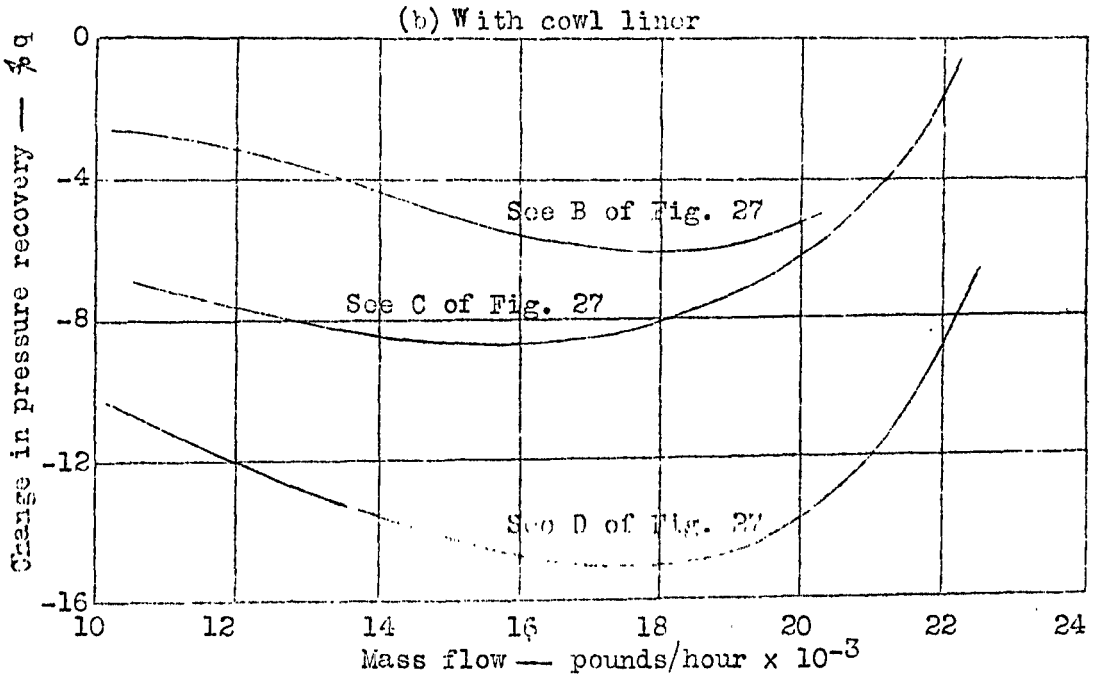

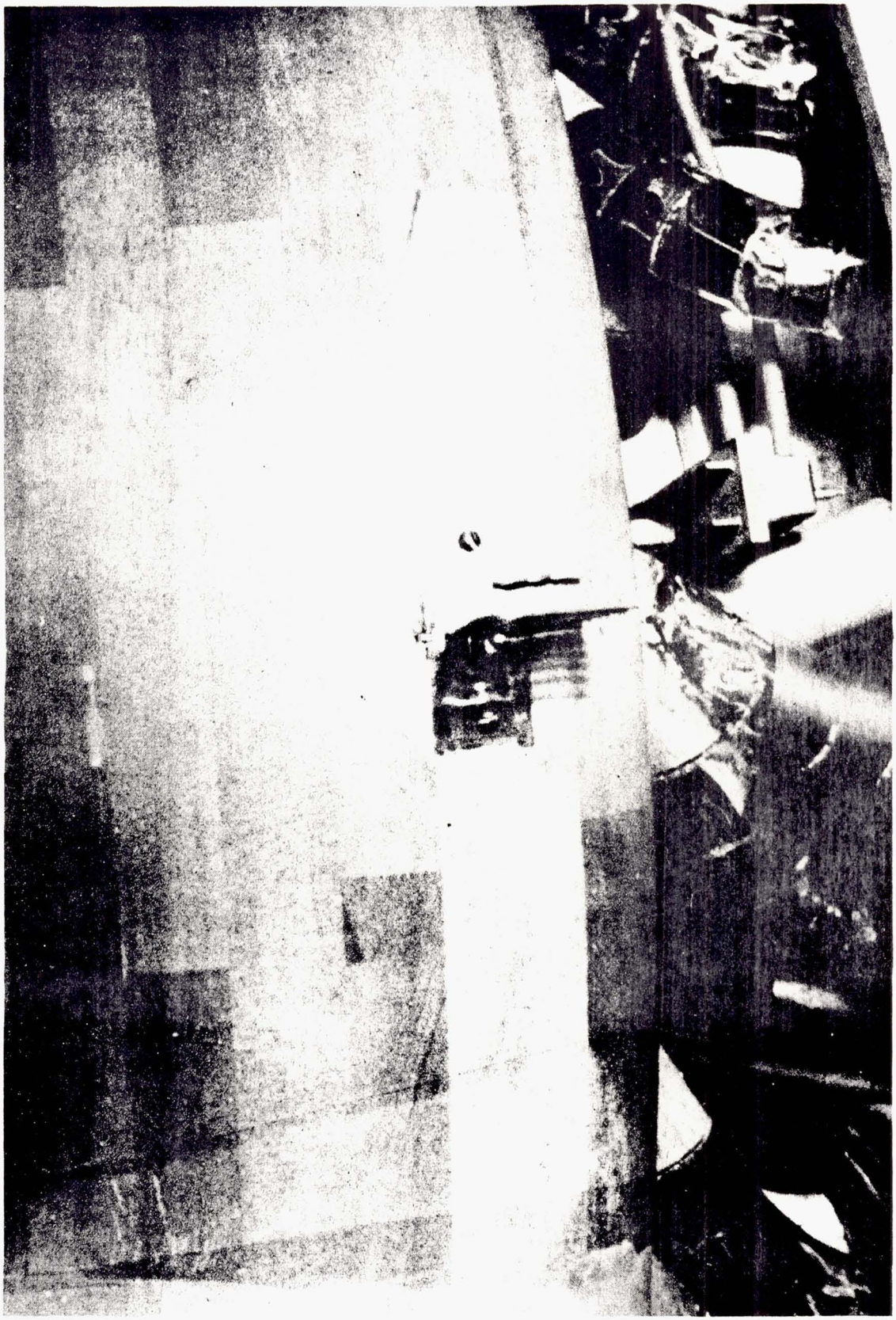

Figure 28.- Simulated intake and exhaust pipes, showing a pitot-static rake at cowl exit.

Figure 29

TYPICAL EFFECTS OF INTAKE AND EXHAUST PIPES ON PRESSURE DROP THROUGH ACCESSORY COMPARTMENT

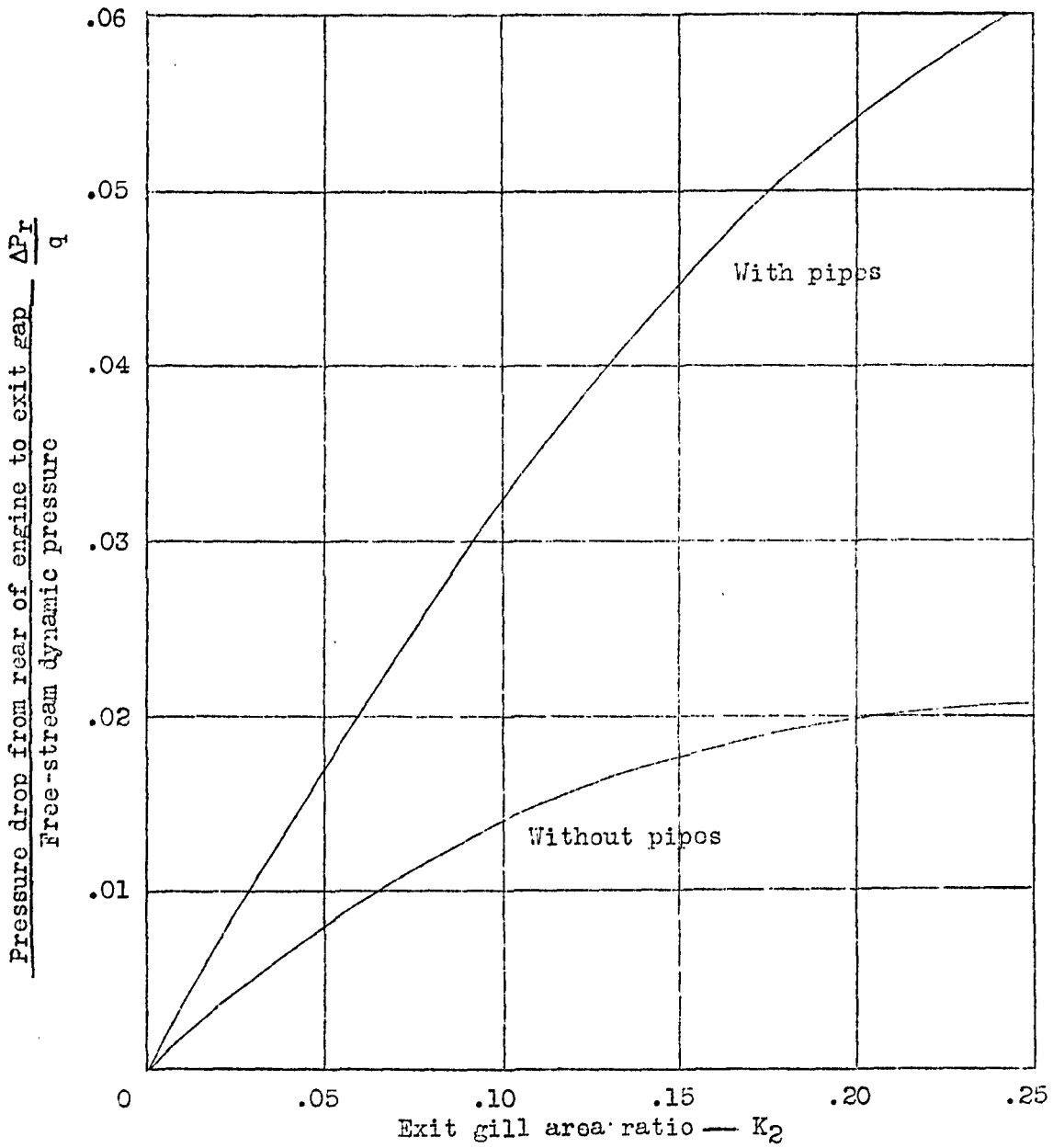

Figure 30

TYPICAL CONDUCTIVITY FOR INTAKE AND EXHAUST PIPES

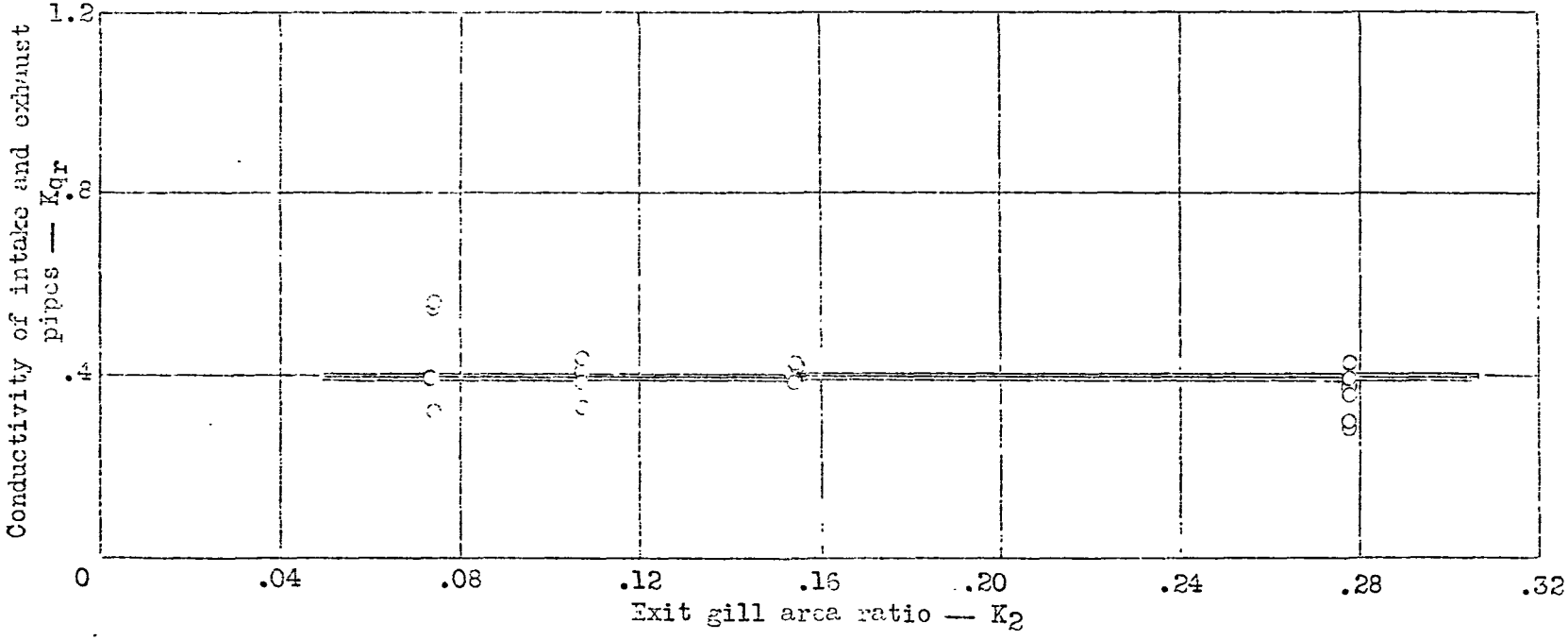

"Page missing from available version"

FIGURE 31

Figure 32

SAVING IN MODEL DRAG OBTAINED BY THE USE OF BLOWERS BEHIND ENGINE

Engine conductivity = 0.125 q = 11.1 in. H_2O

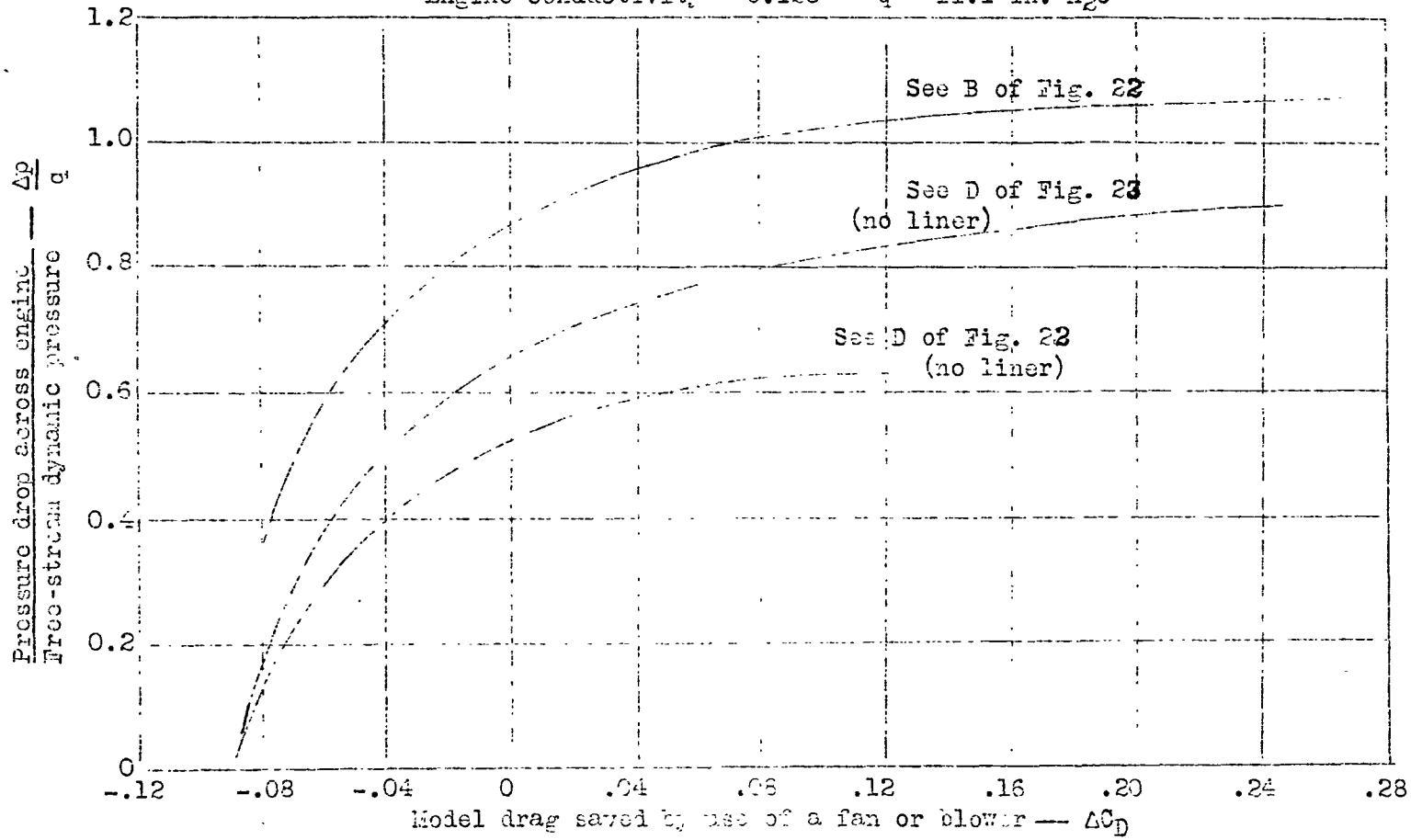

CRITICAL SPEEDS OF VARIOUS BODIES WITHOUT AIRFLOW

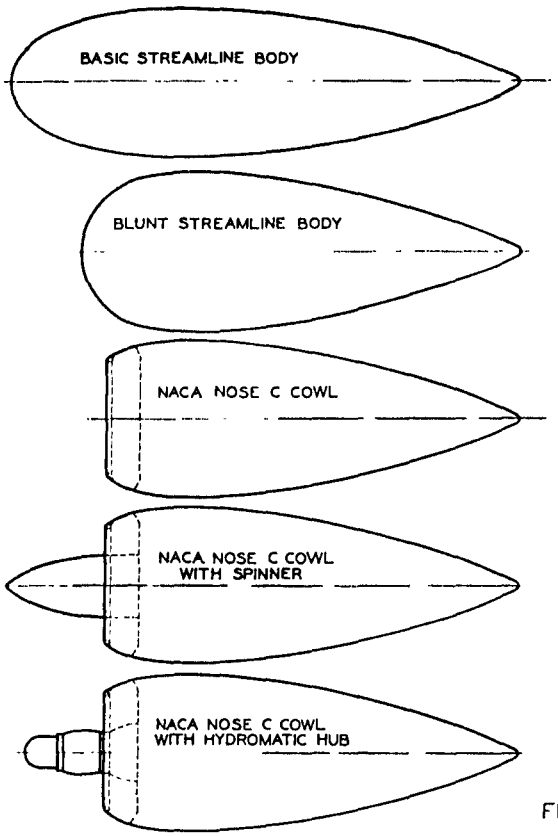

	CRITICAL SPEED AT 30,000 FT MPH	CRITICAL MACH NO M_c
BASIC STREAMLINE BODY	538	.790
BLUNT STREAMLINE BODY	445	.654
NACA NOSE C COWL	397	.585
NACA NOSE C COWL WITH SPINNER	435	.640
NACA NOSE C COWL WITH HYDROMATIC HUB	428	.630

FIGURE 33

EFFECT OF AIRFLOW ON CRITICAL SPEEDS OF NACELLES

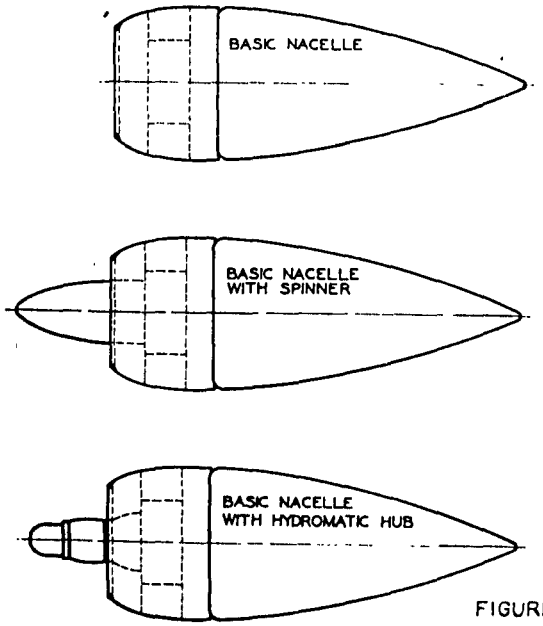

	CONDUCTIVITY K_q	MASS FLOW LB/HR	CRITICAL SPEED AT 30,000 FT-MPH	CRITICAL MACH NO M_c
BASIC NACELLE	0	0	397	.585
	.07	10,700	398	.587
	12	12,800	401	.590
	.21	13,470	404	.596
BASIC NACELLE WITH SPINNER	0	0	435	.640
	.07	8,530	397	.585
	.12	10,180	415	.610
	.21	9,680	427	.628
BASIC NACELLE WITH HYDROMATIC HUB	0	0	428	.630
	.07	7,730	435	.640
	.12	9,180	440	.647
	.21	8,880	445	.652

FIGURE 34

Figure 35

TYPICAL VARIATION OF NACELLE CRITICAL MACH NUMBER WITH FLAP ANGLE AND ANGLE OF ATTACK

Engine conductivity = .12

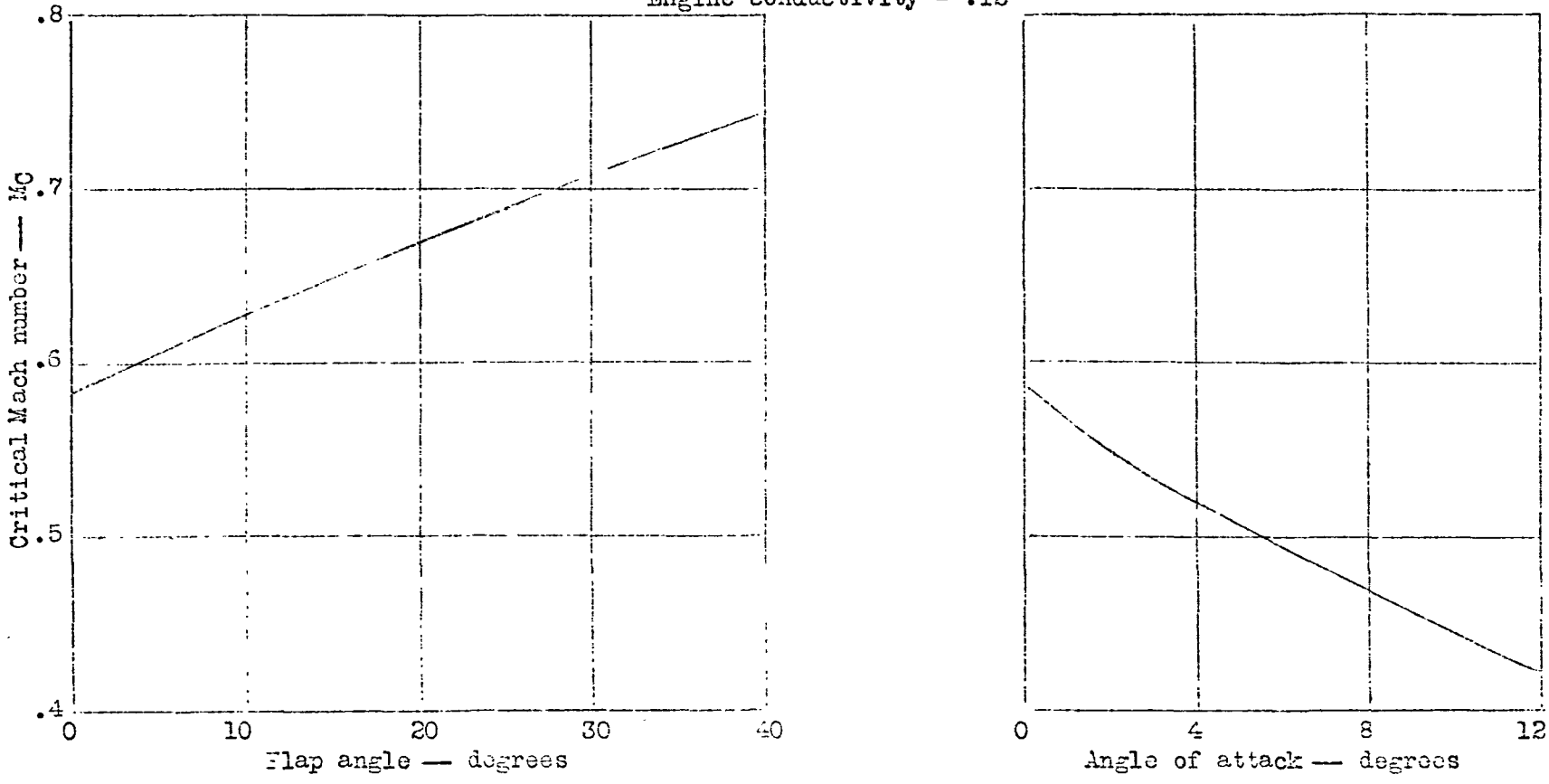

Figure 36 CHART FOR CALCULATION OF COOLING DRAG COEFFICIENT

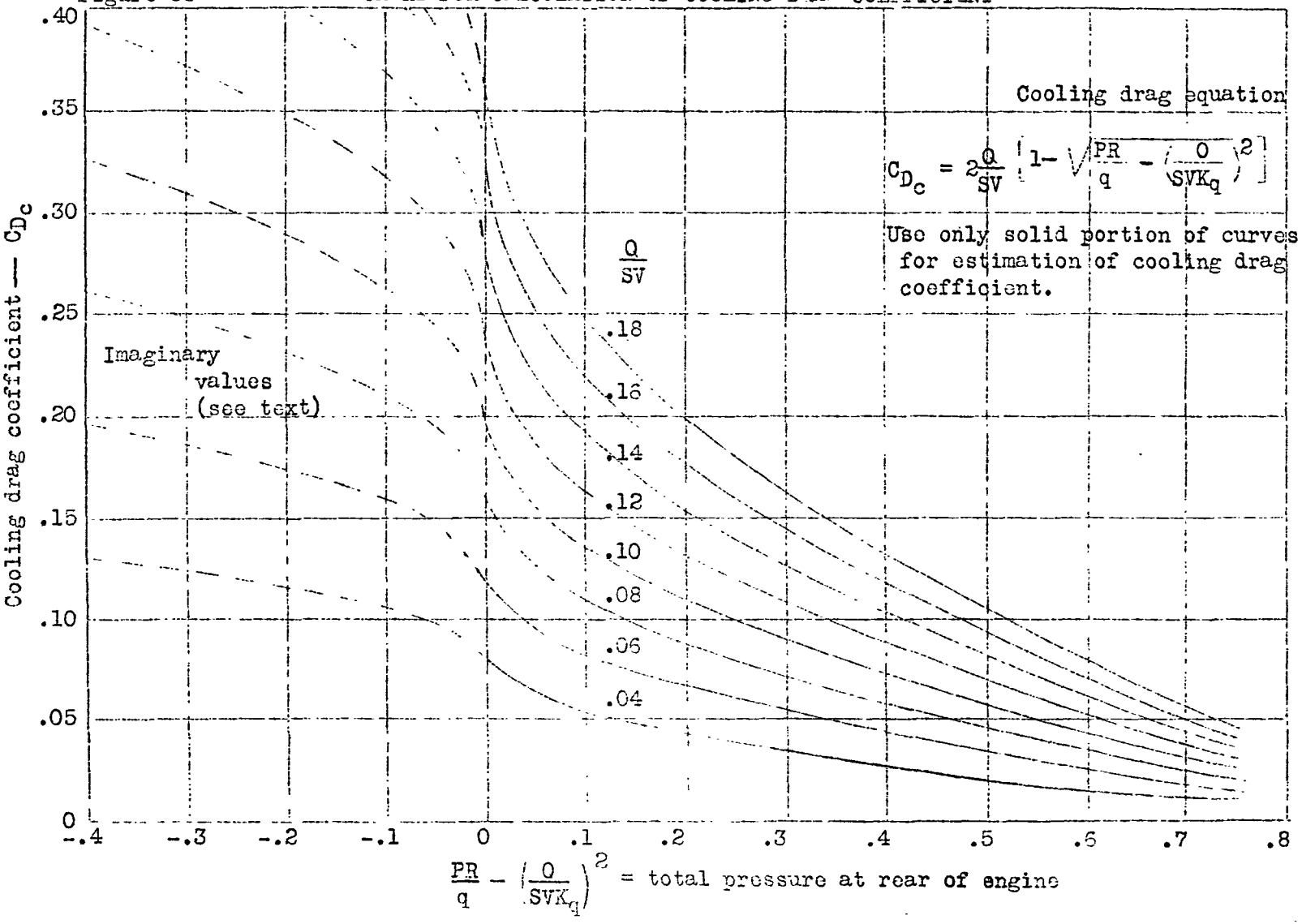

COOLING DRAG COEFFICIENT AS DETERMINED FROM THEORY AND TEST

TYPICAL VARIATION OF COMBINED COOLING AND FORM DRAG FOR NEGATIVE VALUES OF PRESSURE AT REAR OF ENGINE

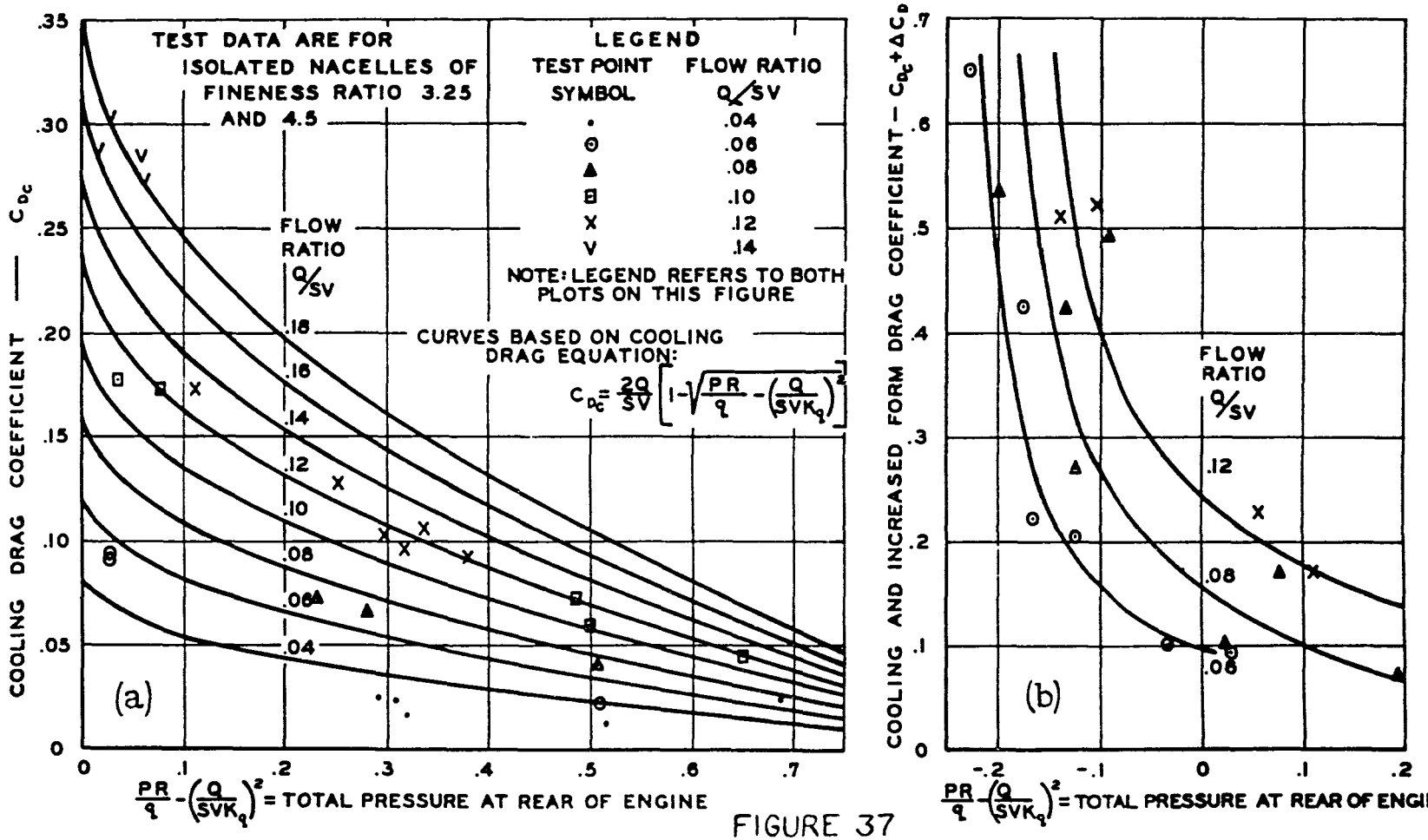

FIGURE 37

CHART FOR THE ESTIMATION OF PRESSURE RECOVERY FOR VARIOUS INSTALLATIONS WITH PROPELLERS

ANGLE OF ATTACK = 0 DEGREES

CURVE NO.	ENTRANCE AREA % MAX. NACELLE D.	DIFFUSER EXPANSION RATIO	DIFFUSER LENGTH RATIO	REFER TO FIG.	REFER TO SKETCH
1	17.1	3.48	2.55	27	B
2	17.1	3.48	2.55	27	B
3	36.3	—	—	27	A
4	21.0	2.82	2.38	27	E
5	29.2	2.46	1.52	27	C
6	29.2	—	—	27	C

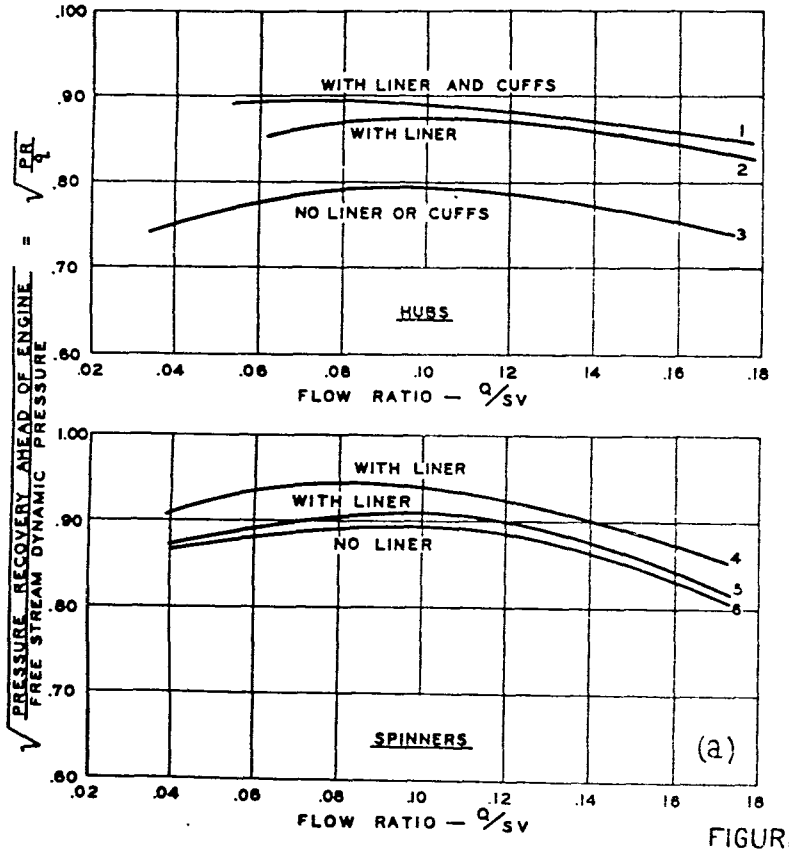

CHART FOR THE ESTIMATION OF PRESSURE RECOVERY FOR VARIOUS INSTALLATIONS WITH PROPELLERS

ANGLE OF ATTACK = 6 DEGREES

CURVE NO.	ENTRANCE AREA % MAX NACELLE D.	DIFFUSER EXPANSION RATIO	DIFFUSER LENGTH RATIO	REFER TO FIG.	REFER TO SKETCH
1	17.1	3.48	2.55	27	B
2	17.1	3.48	2.55	27	B
3	36.3	—	—	27	A
4	21.0	2.82	2.38	27	E
5	29.2	2.46	1.52	27	C
6	29.2	—	—	27	C

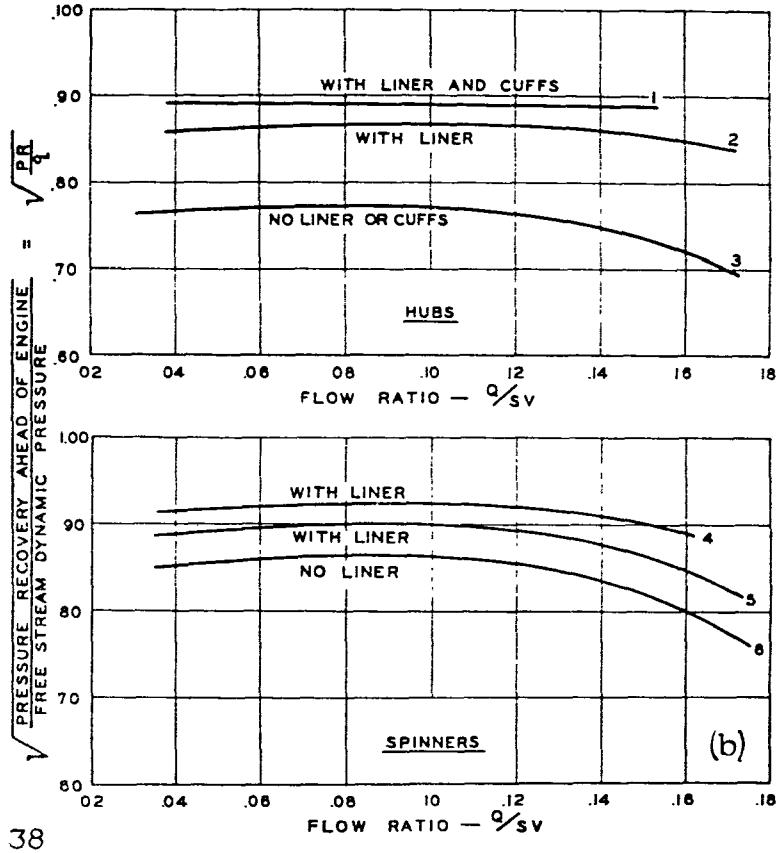

FIGURE 38

Figure 39

EXIT GILL AREA RATIO REQUIRED TO OBTAIN A GIVEN FLOW AT MAXIMUM SPEED

Continuous cowl flaps directly to rear of engine

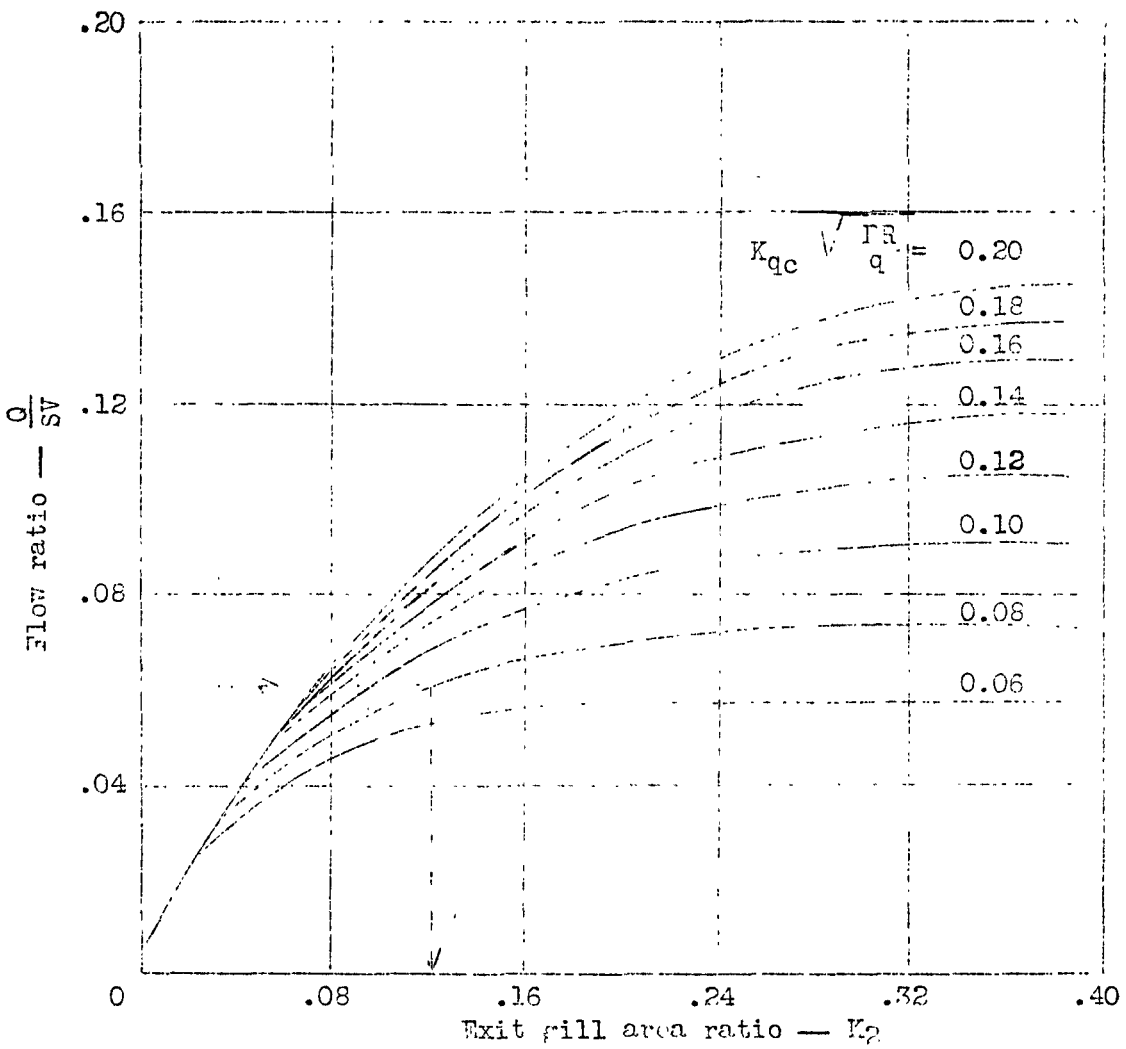

Note: $K_{q_c}\sqrt{\frac{\Gamma R}{q}} \cong K_{q_t}$

CHART FOR ESTIMATING GILL AREA RATIO FOR CONTINUOUS COWL FLAPS DIRECTLY TO REAR OF ENGINE

Fig. 40a VALUES OF $K_{q_c}\sqrt{PR/q}$ FROM 0.06 TO 0.12

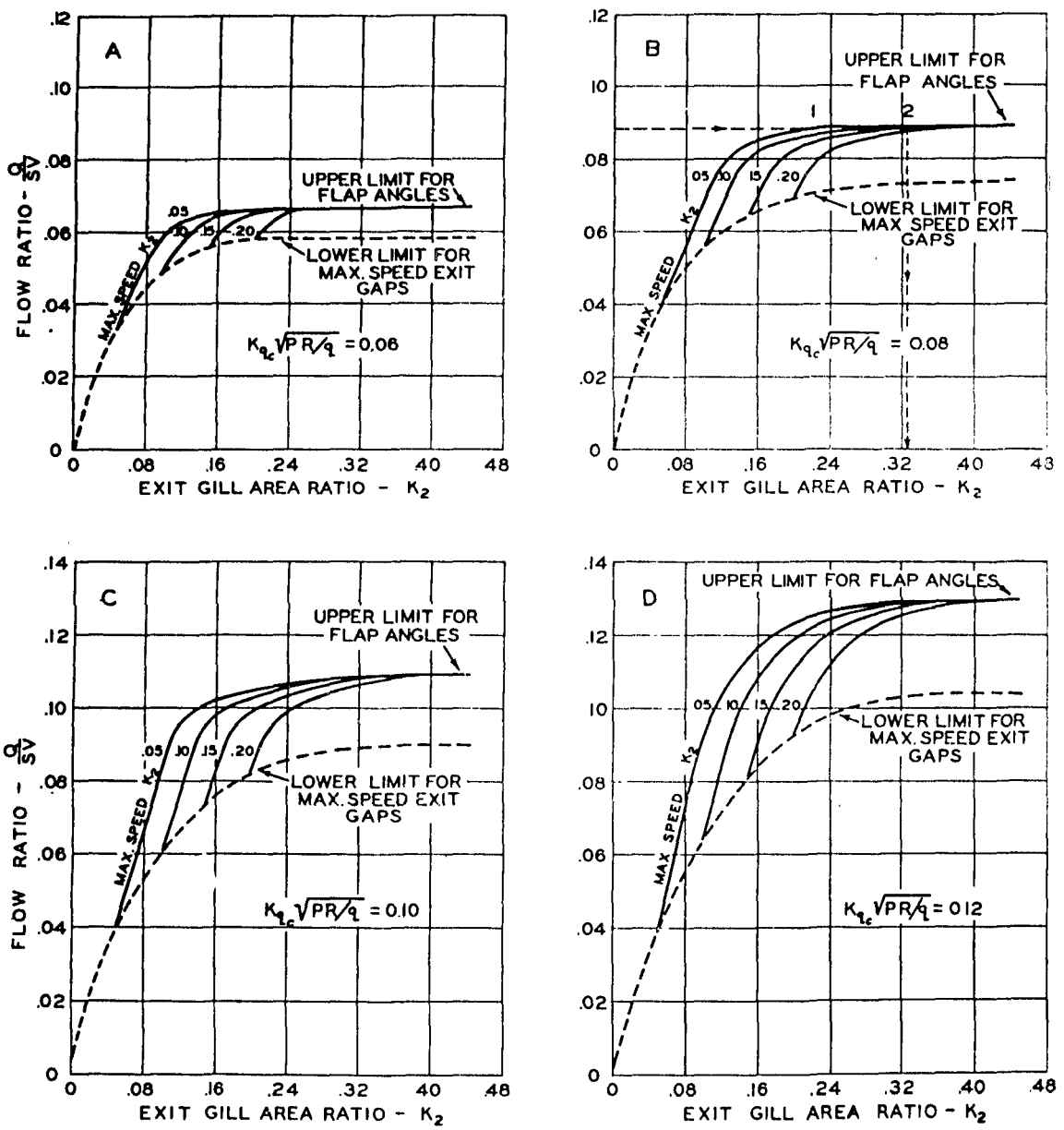

NOTE: $K_{q_c}\sqrt{\frac{PR}{q}} \cong K_{q_t}$

CHART FOR ESTIMATING GILL AREA RATIO FOR CONTINUOUS COWL FLAPS DIRECTLY TO REAR OF ENGINE

Fig. 40b

VALUES OF $K_{q_c}\sqrt{PR/q}$ FROM 0.14 TO 0.20

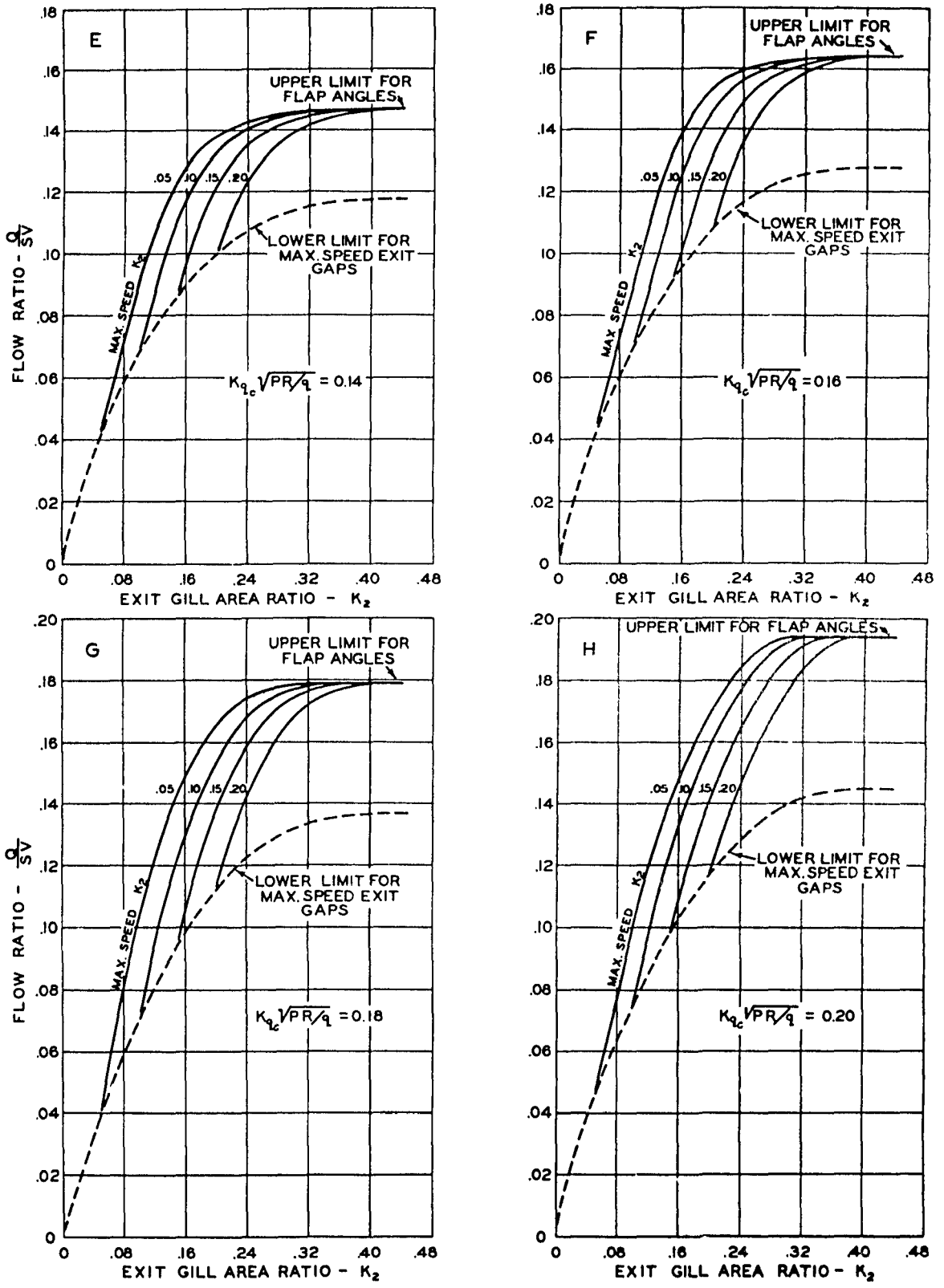

NOTE: $K_{q_c}\sqrt{\frac{PR}{q}} \cong K_{q_t}$

Figure 41

ESTIMATION OF MAXIMUM FLOW RATIO OBTAINABLE AT GIVEN VALUES OF CONDUCTIVITY AND PRESSURE RECOVERY

Continuous cowl flaps directly to rear of engine

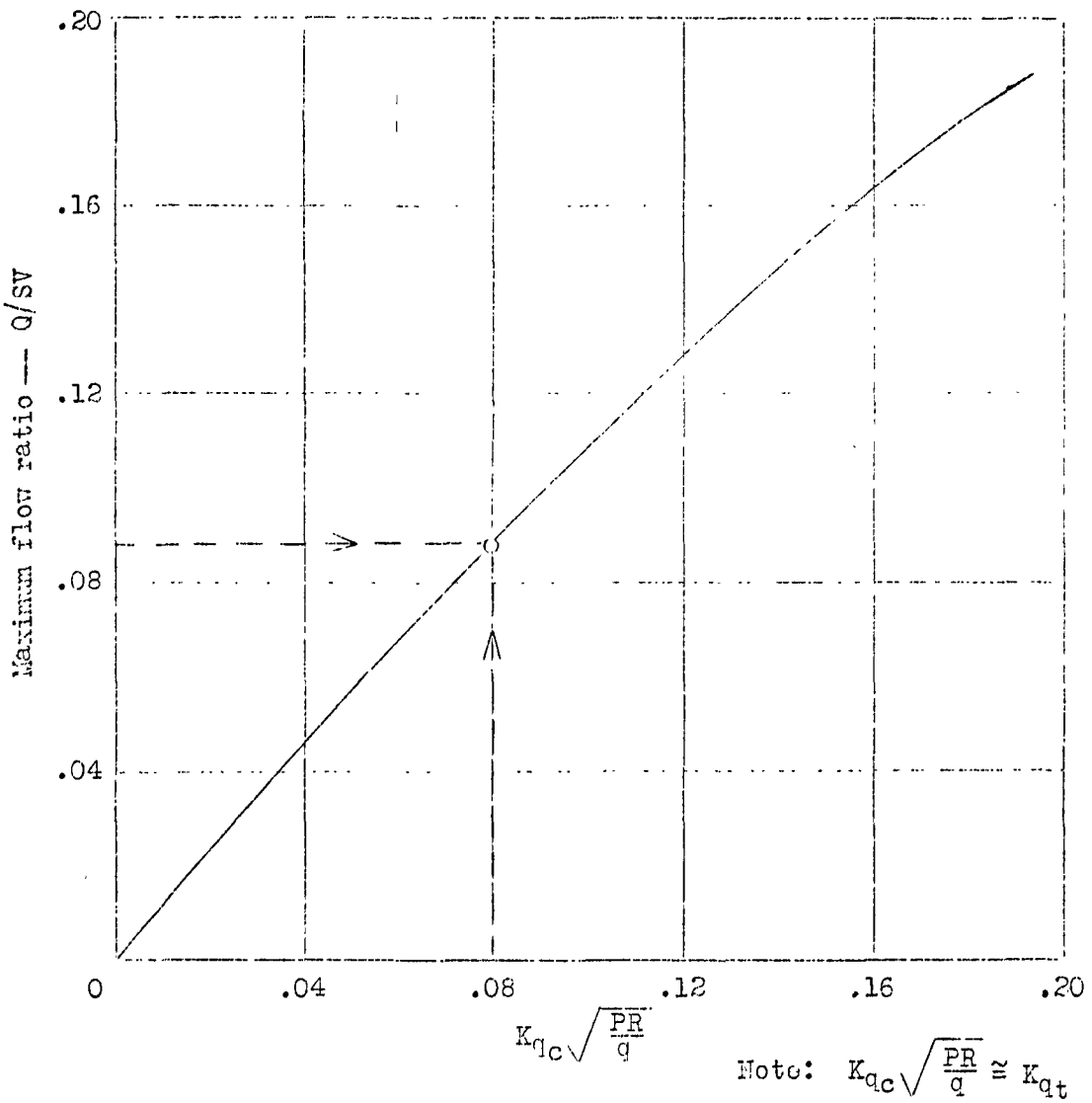

COMPARISON OF DATA ESTIMATED FROM CHARTS WITH FLIGHT TEST DATA

Fig. 42

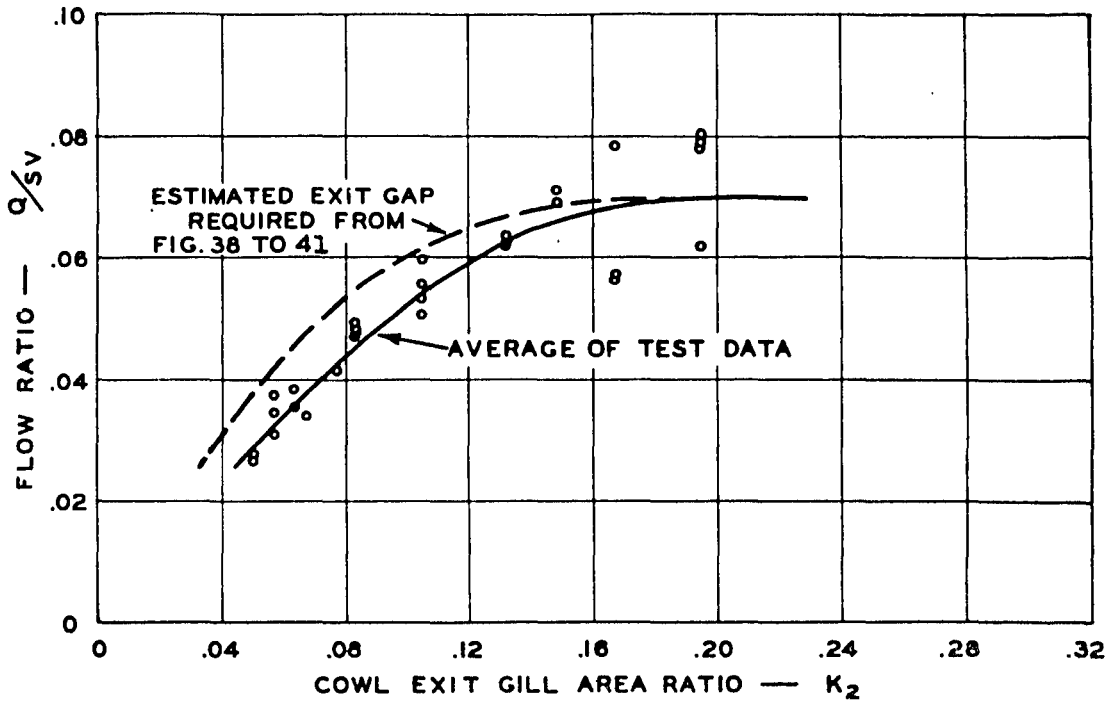

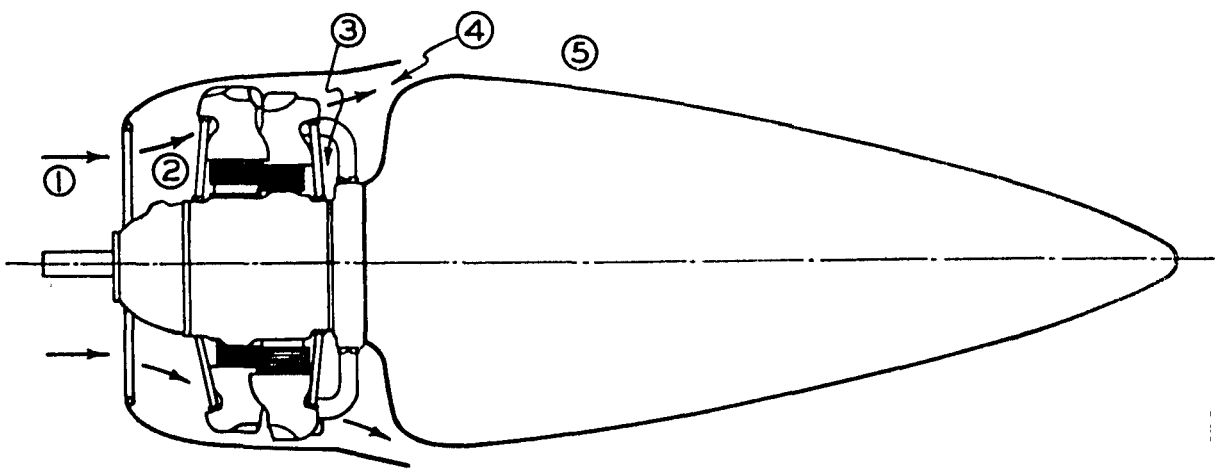

Fig.-43 Sketch to show stations used in derivation of equation (9).